AN INVESTIGATION OF SURGE WAVE PROFILES IN OPEN CHANNEL FLOW.

by

John Sandover B.Sc. A.C.G.I.
D.I.C. A.M.I.C.E.

A Thesis submitted to the University of Edinburgh for the Degree of Doctor of Philosophy, September 1956.

FOREWORD

This thesis was prepared whilst the author was an Assistant at the 'Sanderson Engineering Laboraties' of the University of Edinburgh, and he wishes to express his appreciation for all the facilities and assistance that he has received there, in particular, to his supervisors Professor R. N. Arnold D.Sc. and Dr. O. C. Zienkiewicz Ph.D. for all their encouragement, good advice, and practical help; to the clerical staff; and to the members of the technical staff of the Engineering Laboratories for their excellent work in the construction of the experimental apparatus.

INDEX.

SYNOPSIS.

When a sudden increase in the discharge occurs in an open channel, a surge wave is formed. This body of water appears to move along the initial surface. Depending on the discharge this surge can be undular, breaking undular, or steep fronted as the discharge increases.

A theoretical expression has been derived for the undular form, but no allowances have been made in the theory for the effect of forces that cause the waves to break. To simplify matters the surge was assumed to have been arrested, by superimposing on it a velocity equal and opposite to that of the mean velocity of the head of the surge. Then it appears as an undular hydraulic jump, with moving boundaries. The expression for the profile is derived for permanent flow, if solved alone, with no allowance for friction gives a solitary wave profile. Hence two further expressions have been derived for the changes in energy and momentum. After simplifying and assuming that the channel bed is horizontal and the channel cross section is rectangular, the resulting non dimensional equations are:-

$$\frac{1}{6}\left(\frac{dY}{dX}\right)^2 = EY^2 - \frac{Y^3}{2} + \frac{1}{2} - \not{S}Y \qquad (41)$$

$\frac{dY}{dX}$ is the slope of the water surface. E refers to energy, $\not{S}$ to momentum, and Y to depth. ($y = y_c Y$. y_c = critical depth).

$$\frac{d\not{S}}{dX} = \frac{g}{C^2}\left[\frac{1}{Y_o} - \frac{1}{Y}\right]^2\left[1 + \frac{2y}{\ell}\right] \qquad (71)$$

$$\frac{dE}{dX} = \frac{g}{YC^2}\left[\frac{1}{Y_o} - \frac{1}{Y}\right]^2\left[1 + \frac{2y}{\ell}\right] \qquad (72)$$

C - coefficient of friction.
suffix o - initial conditions.
ℓ - width of channel.
y - depth of water.

With the small channel used in the experiments, allowances had to be made for wall friction $\left(1 + \frac{2Y}{\ell}\right)$.

Benjamin and Lighthill show that this undular form of surge is not possible unless losses in energy and momentum occur.

The waves are termed 'cnoidal' waves because the profile can be represented, to a very close approximation by, the graph of the square of the Jacobean elliptic function cn x. The term 'cnoidal' was coined by Korteweg and de Vries.

The Equations 41, 71 and 72 were then obtained in a form suitable for computation, and a number of numerical examples were solved. The resulting profiles were checked by experiment, and the agreement between the results was considered to be good.

It is believed that if the calculations were made for greater initial depths then those possible in the model channel, that there would be greater agreement with recorded values. This is because of the uncertainty of the determination of the value of the coefficient of friction at low Reynolds numbers. At high values of R the friction coefficient can be determined more accurately. It is thought that probably the values derived from the Bazin, Manning, or Gauckler-Strickler formulae would then be suitable.

A considerable number of experimental determinations of wave profiles were made, and the results listed in graphical and tabular form. The curves show that until breaking occurs there is a definite dependence between wave length and amplitude of the waves.

Probably the most significant result of this study of the undular surge, is the realisation of the importance of the effect of friction on the shape of the waves constituting the surge. In a rough-sided channel for a given Y_o, the crest height is greater and increases more rapidly from wave to wave, and the wave length is shorter than in a channel with a smoother surface.

REFERENCES.

1. Airy G.B. - Encyclopaedia Metripolitana, London (1845).

2. Bazin H. - 'Recherches expérimentales':- 2nd part of 'Recherches hydrauliques' by Darcy et Bazin. Dunod, Paris (1865).

3. Benjamin & Lighthill - Proc. Roy. Soc. A. 224. 448. (1954).

4. Binnie & Orkney - Proc. Roy. Soc. A. 230. 225 (1955)

5. Boussinesq J. - Mem. div. Sav. L'Acad. Sci. Paris. 32. 56.(1891).

6. Favre H. - Étude Théorique et expérimentale des ondes de translation dans les canaux découvertes. Paris. Dunod (1935).

7. Goldstein S. - Modern Developments in Fluid Mechanics I. Oxford 1952.

8. Hunt J.N. - Proc. Roy. Soc. A. 231. 498 (1955).

9. Ippen A. T. - 'Damping Characteristics of the Solitary Wave' Technical Report 16. M.I.T. Dept. of Eng. (April 1955).

10. Iwasa Y. - Mem. Fac. Eng. Kyoto Univ. 17,264. Oct. 1955.

11. Keulegan & Patterson - J. Res. Nat. Bur. Standards. 21. 707 (1938) & 24. 47. (1940).

12. Korteweg & de Vries - Phil. Mag. 39. 422 (1895).

13. Lamb H. - Hydrodynamics. Cambs. Univ. Press.

14. Lémoine R. - La Houille Blanche. Mar. 1948. 183.

15. McCowan J. - Phil. Mag. 38. 351. (1894).

16. Michell A. - Phil. Mag. 36.430. (1893).

17. Prandtl L. - Fluid Dynamics. Blackie.London 1952.

18. Rayleigh, Lord.- Proc. Roy. Soc. 90 324 (1914): Phil Mag. 1 257 1876.

19. Rouse H. - Fluid Mechanics for Hydraulic Engineers. McGraw Hill, London (1938).

20 Russell J. Scott - Rep. Brit. Assoc. p.417 (1837). p.311 (1844).

21. Serre F. - Contribution to the study of Flowin Channels La Houille Blanche. June & Dec. 1953.

22. Stokes G. - Trans. Cambs. Phil. Soc. 8. 441 (1847) Papers 1 Cambs. Univ. Press (1880).

LIST OF DIAGRAMS

LIST OF PHOTOGRAPHS.

- NOTATION -

Suffix '0' denotes initial conditions

A	$(\frac{1}{Y_0} - \frac{1}{Y})^2$ or Area
a	wave amplitude
B	$\frac{(\Delta Y)^2(1 - Y_0^3)}{2Y_0^2}$
C	Coefficient of Friction
c	wave celerity
D	$\int_0^1 F'^2(\lambda)\, d\lambda$
E	H/y_c
F	function of z/y
f, f'', f''''	function of α, and 2nd and 4th differnlts.
G	$B(n+1)^2$
g	$2/\sqrt{1+1/k}$ or acceleration due to gravity
H	Energy per unit weight of fluid.
I	$\int_{-1}^{+1} \frac{du}{[(1-u^2)(1+ku)]^{1/2}}$
K	$\int_0^1 d\lambda \int_\lambda^\beta F'^2(\beta)\, d\beta$ or $\frac{y_1 - y_2}{y_1 + y_2 - \frac{2y_c^3}{y_1 y_2}}$
k	$\sqrt{\frac{2K}{K+1}}$
ℓ	width of channel
L	half wave length
M	Momentum flow rate per unit span ÷ g
m	Hydraulic mean radius
N	$\Sigma \Delta E (Y_{n+1})^2$
n	number of operations in calculations
P	$\Sigma \Delta \$ (Y_{n+1})$
p	intensity of pressure
Q & q	initial discharge, and Q/ℓ.
Q_r & Q_w	discharge at a given section, and equivalent discharge of hydraulic jump
R	H.g. (Benjamin and Lighthill)
R_N	Reynold's Number
r	flow number $= \frac{mQ_r}{y}$
S	M.g. (Benjamin & Lighthill)
\$	M/y_c^2
s	slope of channel bed.
T	$\frac{(\Delta Y)^3(n+1)^3}{2}$
U	mean horizontal velocity
u	point velocity in x direction or elliptic integral variable
V	mean velocity of head of surge
V_r	velocity of flow relative to boundaries.
w	velocity in z direction
ω	Specific weight of fluid.
W	$(1 + \frac{2y}{\ell})$
X & x.	x/y_c, and horizontal distance from coordinate centre
Y & y	y/y_c, and depth of flow.
y_c & y_s	critical depth, and mean depth of surge
y_{crest}	depth at wave crest.
y_1 & y_2	successive crest and valley depths (Elliptic integrals)
z	vertical coordinate axis
α & β	substitution functions
λ	$\frac{z}{y}$ substitution, or wave length.
ρ	fluid density
ψ	stream function
ϕ	velocity potential
φ	elliptic function $= \pi/2$
τ_0	friction force per unit boundary area.
ν	kinematic viscosity
η	$= y$ (Benjamin and Lighthill)
Δ	indicates an increment in the quantity.
Σ	indicates a summation.

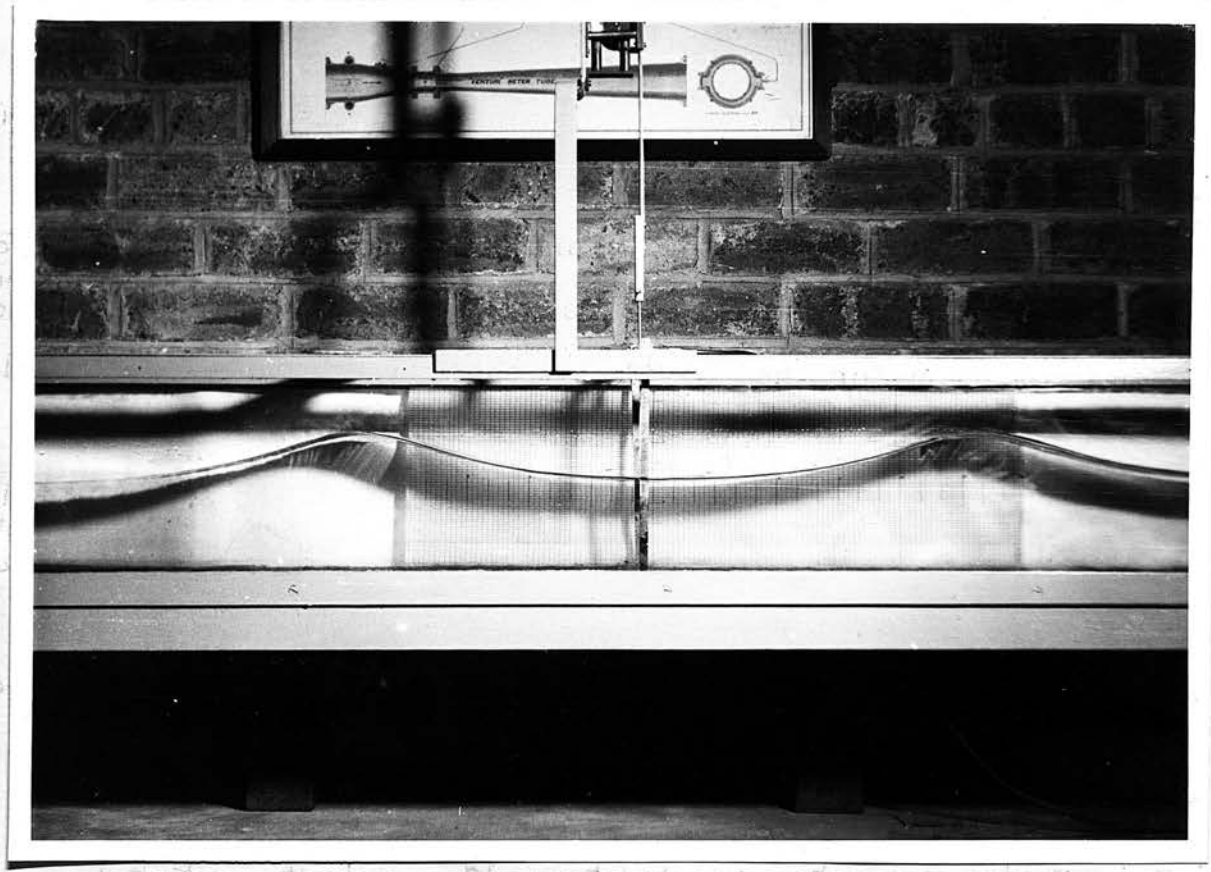

Plate 1. Head of an undular surge. y_o=4". gauge 5.

INTRODUCTION.

When a sudden discharge of water is released into a channel, or when the outlet to such a channel is suddenly closed, a 'Surge Wave' is formed. This has the form of a mass of water apparently moving along the initial water surface, and the shape of the profile of the surge depends upon the initial flow, the geometry of the channel, the roughness of the sides and bed, the bed slope, and the amount suddenly discharged. When the mean height of the surge is small compared with the original depth, it has an undular profile, and is then called an 'Undular Surge'. In this thesis an attempt is made to develop theoretically an expression for the profile of these undular surges, and to find the profiles in certain numerical examples. The accuracy of these calculations will then be checked by experiment.

In nature, surge waves occur as 'bores' or 'aegers' in tidal rivers. The inflowing tide is constricted by a 'bottle neck' in the river, and a bore is formed. This moves upstream, and decreases in height as it advances. Bores also occur moving upstream when a lock gate is suddenly closed, or downstream when the lock gate is suddenly opened. When a turbine is suddenly stopped or started, a surge is generated, either moving upstream in the supply channel, or downstream in the tailrace channel respectively. These are 'positive surges', and the surface level is always above that of the original water surface. 'Negative Surges' are formed when the flow is suddenly decreased but they move upstream, and the surface level is always below that of the original water level. In certain circumstances

there can exist 'negative undular surges'.

Three types of positive surges are formed as the additional discharge is increased; differentiated from each other by the shape of their surface profile. The undular surge is formed by small discharges, and as the discharge increases the amplitude of the undulations increases, whilst the wave lengths decrease. When the first undulation of the surge breaks, it is then recognised as the second type, or 'breaking undular surge'. Further increases in discharge lead eventually to the 'steep fronted surge' characterised by intense turbulence at its head. These three types are indicated in Figure 1.

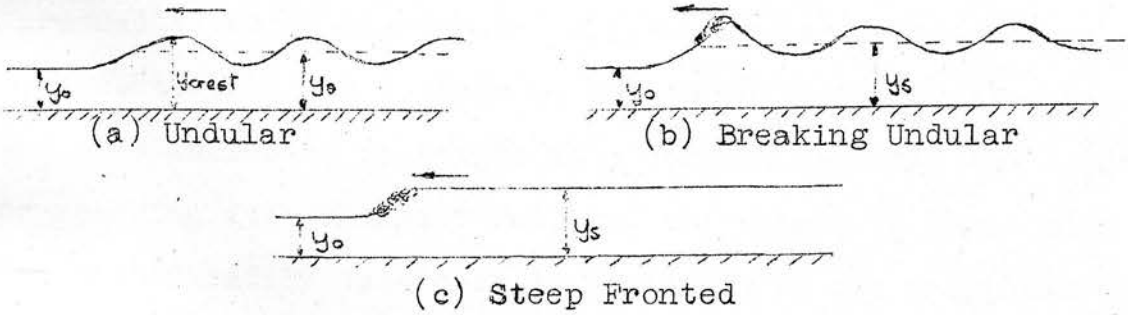

Fig. I. Surge Wave Profiles.

The equivalent stationary form of the positive surge is the hydraulic jump, and this also occurs in the three different forms listed above.

The undular surge with its train of waves has been the subject of considerable speculation and research. Considered as a series of progressive waves it has received the attention of many eminent mathematicians and physicists. More recently

considerable efforts have been directed to the solution of problems associated with the 'undular' surge, considering it as a particular case in the study of progressive waves. Apparently, however, very little has been accomplished towards the prediction of such a profile when the initial conditions are known. Usually friction has been ignored, and the results have indicated either a solitary wave, or a series of identical waves continuing to infinity upstream with a constant mean depth. In practice, however, it is found that the amplitude of the waves decreases towards the rear of the train, and that as the train advances the number of waves steadily increases, more being formed behind the surge. As can be observed the leading wave appears first, resembling a solitary wave, and a gradually increasing number of waves appear behind it, as it progresses, with the valleys of successive waves overlapping. Each wave increases in height to a certain maximum, the leading one reaching its maximum first, and the others in their turn. Then each steadily decreases in amplitude as the surge progresses. Eventually, and depending on the distance traversed, a number of waves will have reached an approximately permanent shape, although their size is continually decreasing.

The mean heights of these "permanent" waves are successively of a greater height above the channel bed as the observer moves towards the rear of the train. This is the result of the slope necessary to overcome friction effects along the length of the channel.

The initial formation of a wave shape is of some interest. As the discharge into the channel is suddenly increased, the surge front first appears in a form somewhat similar to that of the breaking surge. The initial rise of level is, however, insufficient to initiate breaking and the profile is evidently unstable forming the first wave almost immediately; as this wave grows, a train of similar waves develops behind it.

The maximum height that a wave can achieve before breaking, has been found experimentally to be approximately 1.75 times the initial depth but increasing slightly with increases in the initial depth, to about 1.80 times the initial depth.

Contrary to the usual method of approach, which considers the 'steep fronted surge' first, then examines the undular form, implying that the latter is a special case of the former, it would appear that the steep fronted surge is a special case of the undular surge. When the discharge has reached such a value that the leading wave in the surge breaks rapidly, this wave suddenly decreases in height, and hence moves at a lower velocity, the other waves trying to overrun it, and the valleys becoming filled. The surge then continues on its way as shown in Fig. 1(c). Eventually, however, should the discharge at the head of the surge decrease sufficiently it will revert to the undular form again. It can be observed that even, with very large discharges, there is a slight waviness in the profile. Further, at the inlet to the channel the first wave can always be seen to take shape, rapidly increase in height, break, the successive waves overrun the turbulent water, and the valleys

tend to fill.

As previously stated an attempt will be made to reach a general theoretical expression for the profile of the undular surge, and then certain numerical examples will be worked out. Owing, however, to the extreme tediousness of the calculations, two restrictions are made; that the bed slope, and the initial flow are zero. The calculated results will be checked by experiment, and it is hoped that the experimental results will yield data that is of practical use.

CHAPTER 2.

HISTORICAL SUMMARY

It would appear that ever since Euler and Lagrange stated their laws of fluid motion, the derivation of the equations of wave motion has been possible, but the great difficulty in solving the necessary equations has militated against this. Although much has been discovered about periodic wave trains, and a great number of approximate solutions have been derived, even for this relatively simple case an exact solution is not yet available. Friction is invariably neglected in these solutions, and other assumptions and approximations have to be made.

In his treatment of the problem of 'long waves' Lagrange derived what is probably one of the first equations governing wave motion:-

$$\frac{d^2y}{dt^2} = gy_o \left(\frac{d^2y}{dz^2} + \frac{d^2y}{dx^2}\right) \qquad (1).$$

Where y_o is the depth of the undisturbed liquid, y is the local depth, and z and x represent the respective co-ordinate axes. For waves of small magnitude, the above result can be solved to give an expression for the velocity of the wave 'c'.

$$c = \sqrt{gy_o} \qquad (2).$$

For waves of shorter length, one of the first great experimental works was that of Scott Russell (20)*, who obtained a great deal of experimental data on the solitary wave. He found empirically that the celerity of the wave was given to a very close approximation by the relationship

$$c = \sqrt{gy \text{ crest}} \qquad (3).$$

N.B.* Numbers in brackets ( ) refer to bibliography, when following a proper name.

He also made many observations on the formation of, and physical peculiarities of other forms of waves.

Scott Russell's work was, immediately complemented by the theoretical studies of Airy (1) in the 'Encyclopæ dia Metropolitana' on the subject of waves. For waves of small amplitude and assuming a sinusoidal profile, Airy derived the expression for the velocity of propagation of the wave.

$$c = \sqrt{\frac{g\lambda}{2\pi} \tanh \frac{2\pi y_s}{\lambda}} \qquad (4)$$

where λ is the wave length and y_s is the mean depth of the waves. If y_s becomes small, then Equation (4) reduces to Equation (2), alternatively if it is large, then

$$c = \sqrt{\frac{g\lambda}{2\pi}} \qquad (5)$$

These expressions give results that are in good agreement with practice for small waves.

Rayleigh (18) later derived an expression for the velocity of waves of finite amplitude in deep water, and a more exact form is due to Levi Cevita. Stokes (22) also extended Airy's method, but again, although of more general application, only held for waves of small magnitude.

The previously mentioned results, however, are not directly applicable to the problem in question, that is to a train of gravity waves behind a surge in an open channel. A great deal of work has been accomplished on the problem of gravity waves in open channels, including the allied phenomena of the 'Solitary Wave'. The most important early results were those obtained by Boussinesq (5) and Rayleigh from the theoretical point of view, and the work of Bazin (2), the great French experimentalist.

He constructed a large channel, over 600m. long, and conducted what were probably the first accurate measurements on the profiles of undular surges. Another great experimentalist of this epoch was Scott Russell, but most of his work was concerned with the solitary wave.

In 1895 Korteweg and de Vries (13) using a method similar to that of Rayleigh - (i.e.) assuming that the vertical and horizontal velocities could be represented by a rapidly converging periodic series, obtained an expression for the profile of long waves of finite amplitude in an open channel. If σ is a constant, depending on the physical properties of the fluid in the channel, c_1 and c_2 are constants of integration, and α is some arbitary constant, then their equation takes the form:-

$$\sigma\left(\frac{dy}{dx}\right)^2 = 2\alpha y^2 - y^3 + c_1 - c_2 y \qquad (6)$$

an equation for the profile of a permanent wave. This can be rewritten as

$$y = h\,cn^2 x\sqrt{\frac{h+b}{\sigma}} \quad \left(Mod.k = \sqrt{\frac{h}{h+b}}\right) \qquad (7)$$

which represents the graph of the square of the Jacobean elliptic function cn.x, with modulus k. h and b are the roots of the quadratic

$$y^2 + 2\alpha y + C_2 = 0. \qquad (8)$$

In analogy with the term sinusoidal, Konteweg and de Vries applied the term 'cnoidal' to the wave profiles represented by Equation (7). When k = 0 the waves are sinusoidal, and as k tends to become=1 the waves tend to the solitary wave form.

Very little attention was then paid to the specific problem of the undular surge until Favre (6) in 1935 conducted some experiments into the shape of the profiles of these surges. His main pre-occupation was with the change in shape of the surge itself, regarding it as steep fronted, as it progressed down the channel, and his theoretical work deals solely with this aspect. Part of the experimental work, however, was to determine a number of the undular profiles, and this was accomplished in a novel and ingenious manner. Two cameras were suspended above the channel, with the line joining them, at right angles to the axis of the channel. Simultaneous photographs of the oncoming surge were taken, and the results were plotted using the methods employed in photogrammetry. These results are discussed later.

An ingenious theoretical approach to this problem was later proposed by Lémoine (14) to account for the dissipation of energy in an undular surge. He suggested that the waves were formed in an effort to dissipate the energy, which was radiated through the wave train. This energy is expended in turbulence at or near the head of the steep fronted surge, but no such turbulence occurs with the undular surge. Lémoine's theory was based on the sinusoidal method used by Airy, and his results are strongly criticised by Benjamin and Lighthill (3) who show to a very good approximation, that the waves in an undular surge are cnoidal waves. They also obtain an expression for the profile of the waves, which is similar to that of Korteweg and de Vries, but the rather ambiguous constants of integration of the latter are replaced by terms that are subject to physical evaluation:,

(i.e.) $\frac{1}{2}Q^2 \left(\frac{dy}{dx}\right)^2 = 2Ry^2 - gy^3 + Q^2 - 2Sy.$ (9).

where R and S are energy and momentum functions respectively. Whilst showing that cnoidal waves cannot exist unless effects of friction are taken into account Benjamin and Lighthill do not show how this can be accomplished in practice.

A very useful theoretical approach to the problem of gradually varied flow in open channels, and one adaptable with certain approximations to the problem of undular surges is presented in the extremely interesting treatise by Serre (21). Although he does not specifically treat the matter of undular hydraulic jumps, or surges, the method is easily adapted to these problems. A more detailed account of an adaption of his method is included in this thesis, and it is proposed to show that it yields results of considerable significance, although it departs in general from the classical approach of Rayleigh, Korteweg and de Vries, etc. It is very interesting to note, however, that the form of his final equations is, subject to suitable transformations, identical with that obtained by Benjamin and Lighthill. The reason for this similarity is given later.

Keulegan and Patterson (11) have gathered together a great deal of information on the subject of these waves, very little of it original, but they checked their solutions with the experimental results of Bazin and Favre.

Binney and Orkney (4) conducted some very interesting experiments, and showed among other results that the breaking of the first wave of the undular surge occurs at approximately

a Froude number = 1.26. This corresponds in the present notation to a limit of approximately $y_o/y_c = 0.83$. This is at considerable variance with Serre's theoretical value of 0.57.

Hunt (8) used an approximation for the velocity distribution:-

$$V(y) = V\ (y\ \text{surface}) \times \left(\frac{y}{y\ \text{surface}}\right)^{\frac{1}{7}} \qquad (10)$$

in the sinusoidal theory and obtained an expression for c, the celerity of a gravity wave in an open channel. The remainder of his work, however, is mainly a recapitulation of that of Korteweg and de Vries, leading to the standard cnoidal wave form.

Yoshiaki Iwasa (10) develops Serre's equations including terms due to vertical accelerations, but when the same approximations are made, as in Serre's work, in order that the equations may be solved his results are exactly the same as Serre's, but unfortunately without any mention of the effects of friction.

The theoretical part of this thesis is based on Serre's method, for the solution of problems in gradually varied flow, and an attempt is made, using the relationships that are evolved to predict the profile of certain surges in practice. The results are checked by experiments in a small channel.

CHAPTER III.

Theoretical considerations leading to the approximate equations for the profile of an undular surge.

General Equations. Method of Elliptic Integrals.

(1). GENERAL EQUATIONS.

In order that the expressions obtained may not be too cumbersome, it is assumed that:-

(1). The fluid motion is two dimensional.

(2). A rectangular channel section is used of width 'l'.

(3). The bed slope.. is sufficiently small for

$$\cos s \equiv 1 \text{ and } \sin s \equiv S$$

(4). The co-ordinate centre is at the outlet of the channel with the z axis being vertical and the x axis being the longitudinal centre line of the channel.

(5). The flow is considered as being permanent, and hence terms involving differentiation with respect to time can be ignored. To accomplish this for the problem of a surge on originally still water, a velocity equal and opposite to the surge is generally applied. This brings the surge to rest, and it appears as a hydraulic jump, but with moving boundaries (Fig. 2).

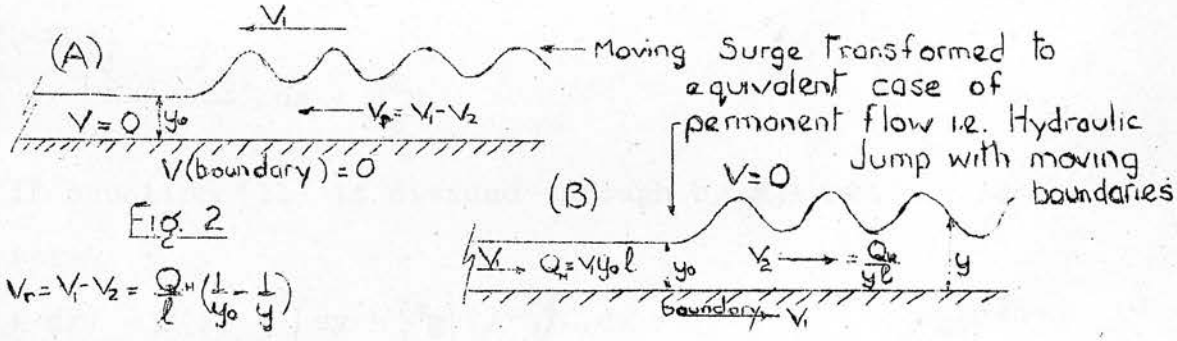

Fig. 2

$$V_r = V_1 - V_2 = \frac{Q}{l}\left(\frac{1}{y_0} - \frac{1}{y}\right)$$

(6). The velocity distribution is uniform and equal to U, across any section . Hence u = U = Q/l.y. (Fig. 3).

If two sections A and B are considered at distances x and (x + dx) from the origin.

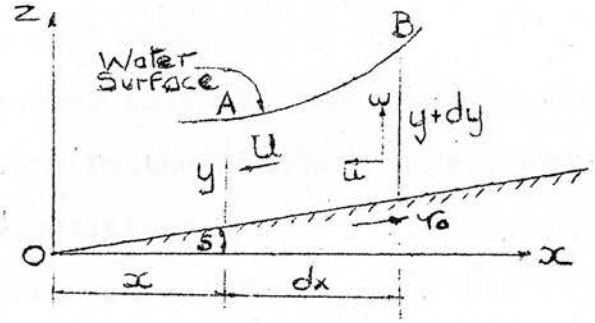

Fig. 3 Flow details at Sections A and B

Then from the momentum relationship

$$\rho Q(U_B - U_A) = \int_A pdA - \int_B pdA - \tau_0 dx\,(l + 2y) + \rho g l y s dx$$

or rewritten (11).

$$\int_B p\,dA + \rho Q U_B - \int_A pdA - \rho Q U_A = \rho g l y s dx - \tau_0 dx(l+2y).$$

where Q is the discharge

ρ is the fluid density

U is the mean velocity

u & w are the local components of velocity

τ_0 is the friction force per unit area

If now M represent a momentum function per unit width of channel

$$M(x) = \int_0^y \frac{p(z,\,x)}{\rho g}\,.\,dz + \frac{U^2 y}{g} \qquad (12).$$

and if equation (11) is divided through by $\rho g l$, it can be rewritten

$$M(x + dx) - M(x) = \left[sy - \frac{\tau_0}{\rho g}\right]\left(1+\frac{2y}{l}\right).\,dx \qquad (13)$$

and therefore $$\frac{dM}{dx} = \left(sy - \frac{\tau_0}{\rho g}\right)\left(1+\frac{2y}{l}\right) \qquad (14).$$

Similarly if H is the energy per unit weight of fluid

$$H(x) = \frac{\ell}{y} \int_0^y \left(\frac{p}{w} + z + \frac{u^2 + w^2}{2g}\right) dz \qquad (15).$$

and we have that

$$\int_B \left(\frac{p}{w} + z + \frac{u^2 + w^2}{2g}\right) udA - \int_A \left(\frac{p}{w} + z + \frac{u^2 + w^2}{2g}\right) udA = \frac{\tau_0}{w} u(\ell + 2y)dx \qquad (16)$$

whence $\frac{dH}{dx} = s - \frac{\tau_0}{wy}\left(1 + \frac{2y}{\ell}\right)$ (17)

It is assumed that all the momentum and energy losses occur through friction in the boundary layer, and that outside this limit the flow is Irrotational.

Owing to the curvature of the fluid filaments the pressures cannot be taken as the equivalent hydrostatic pressures. The pressure distribution is given by

$$\frac{1}{\rho g}\frac{\partial p}{\partial z} = -1 - \frac{u}{g}\frac{\partial w}{\partial x} - \frac{w}{g}\frac{\partial w}{\partial z} \qquad (18)$$

from continuity considerations

$$\frac{du}{dx} = -\frac{dw}{dz} \qquad (19)$$

but $u = U = \frac{Q}{\ell y}$

$$\therefore \frac{du}{dx} = -\frac{Q}{\ell y^2}\frac{dy}{dx} \quad \& \quad \frac{dw}{dz} = +\frac{Q}{\ell y^2}\frac{dy}{dx} \qquad (20)$$

Integrating Equation (20)

$$w = \frac{Q}{\ell y^2}\frac{dy}{dx}z + c \qquad (21)$$

at the bottom $w = 0$ and $z = 0$ $\therefore$ $c = 0$

$$\therefore w = \frac{Q}{\ell y^2}\frac{dy}{dx}z \qquad (22)$$

Substituting these values into Equation (18)

$$\frac{1}{\rho g}\frac{\partial p}{\partial z} = -1 - \frac{Qz}{g\ell y}\left[-\frac{2Q}{\ell y^3}\left(\frac{dy}{dx}\right)^2 + \frac{Q}{\ell y^2}\frac{d^2y}{dx^2}\right] - \frac{Q}{g\ell y^2}\left(\frac{dy}{dx}\right)^2 z \left(\frac{Q}{\ell y^2}\right) \qquad (23)$$

$$= -1 + z\left[\frac{Q^2}{g\ell^2 y^4}\cdot\left(\frac{dy}{dx}\right)^2 - \frac{Q^2}{g\ell^2 y^3}\frac{d^2y}{dx^2}\right] \qquad (24)$$

Integrating and knowing that $p = 0$ when $z = y$

$$\frac{p}{\rho g} = y - z + \frac{(y^2 - z^2)}{2}\left[\frac{Q^2}{g\ell^2 y^3}\cdot\frac{d^2y}{dx^2} - \frac{Q^2}{g\ell^2 y^4}\left(\frac{dy}{dx}\right)^2\right] \qquad (25)$$

From this result, Equation (12) on integrating and simplifying becomes

$$M(x) = \frac{y^2}{2} + \frac{Q^2}{3g\ell^2}\frac{d^2y}{dx^2} - \frac{Q^2}{3g\ell^2 y}\cdot\left(\frac{dy}{dx}\right)^2 + \frac{Q^2}{g\ell^2 y} \qquad (26)$$

and Equation (15) becomes

$$H(x) = y + \frac{Q^2}{3g\ell^2 y}\frac{d^2y}{dx^2} - \frac{Q^2}{6g\ell^2 y^2}\left(\frac{dy}{dx}\right)^2 + \frac{Q^2}{2g\ell^2 y^2} \qquad (27)$$

Equations (14), (17), (26) and (27) form the basis of the ensuing treatment of the problem .

As they stand at the moment, these equations are rather cumbersome, and the following simplification is adopted.

Equation (27) can be rewritten

$$\frac{Q^2}{3g\ell^2 y}\left[\frac{d^2y}{dx^2} - \frac{1}{2y}\left(\frac{dy}{dx}\right)^2\right] = H - y - \frac{Q^2}{2g\ell^2 y^2} \qquad (28)$$

and this is equivalent to

$$\frac{Q}{6g\ell^2}\frac{d}{dy}\left[\frac{1}{y}\left(\frac{dy}{dx}\right)^2\right] = H - y - \frac{Q^2}{2g\ell^2 y^2} \qquad (29)$$

Then if for the moment H is regarded as constant then Equation (29) can be immediately integrated to give after multiplying through by y

$$\frac{Q}{6g\ell^2}\left(\frac{dy}{dx}\right)^2 = Hy^2 - \frac{y^3}{2} + \frac{Q^2}{2g\ell^2} + Cy \qquad (30)$$

If C were known, then theoretically the profile of the gradually varied flow could be computed, if H and Q were known. The only function other than H and Q, needed to determine the profile, however, is M, and if this were found, then C could be evaluated.

Rewriting Equation (26)

$$\frac{Q^2}{3g\ell^2}\left[\frac{d^2y}{dx^2} - \frac{1}{y}\left(\frac{dy}{dx}\right)^2\right] = M - \frac{y^2}{2} - \frac{Q^2}{g\ell^2 y} \qquad (31)$$

If $z(y)$ is put equal to $\left(\frac{dy}{dx}\right)^2$, then Equation (31) becomes

$$\frac{Q^2}{6g\ell^2}\left[\frac{dz}{dy} - \frac{2z}{y}\right] = M - \frac{y^2}{2} - \frac{Q^2}{gy\ell^2} \qquad (32)$$

On dividing through by y^2 Equation (32) can be put in the form

$$\frac{Q^2}{6gl^2}\frac{d}{dy}\left[\frac{z}{y^2}\right] = \frac{M}{y^2} - \frac{1}{2} - \frac{Q^2}{gy^3\ell^2} \qquad (33)$$

Then assuming for the moment that M is constant Equation (33) can be integrated to give, after multiplying through by y^2

$$\frac{Q^2}{6gl^2}\left(\frac{dy}{dx}\right)^2 = -My - \frac{y^3}{2} + \frac{Q^2}{2g\ell^2} + C\,y^2 \qquad (34)$$

Then it is apparent from inspection of Equations (30) and (34) that the following relationship between H, M, and Q, y, and x will hold

$$\frac{Q^2}{6g\ell^2}\left(\frac{dy}{dx}\right)^2 = Hy^2 - \frac{y^3}{2} + \frac{Q^2}{2g\ell^2} - My \qquad (35)$$

To make this of more general application, it would be preferable to have it in dimensionless form, and hence, if y_c is the critical depth, let

$$y = y_c\,Y \qquad (36)$$

$$x = y_c\,X \qquad (37)$$

and we also have $y_c^3 = \frac{Q^2}{g\ell^2}$ (38)

substituting these values in Equation (35) the resulting equation is:-

$$\frac{1}{6}\left(\frac{dY}{dX}\right)^2 = \left(\frac{H}{y_c}\right)Y^2 - \frac{Y^3}{2} + \frac{1}{2} - \left(\frac{M}{y_c^2}\right)Y \qquad (39)$$

Let $\frac{H}{y_c} = E$ and $\frac{M}{y_c^2} = \phi$ (40)

then

$$\boxed{\frac{1}{6}\left(\frac{dY}{dX}\right)^2 = EY^2 - \frac{Y^3}{2} + \frac{1}{2} - \phi Y} \qquad (41)$$

If Equation (41) is solved for a numerical example, a solitary wave profile is obtained. This is as would be expected, since the effects of friction are neglected. Therefore, it is necessary that in any practical case, the effects of friction

should be included, and this can be accomplished using equations (14) and (17) in addition. Once again, however, it is preferable that they should be derived in a simplified form, and therefore using the following relationships

$\tau_0 = f\rho\frac{U^2}{2}$ where f is a friction coefficient (42)

$C^2 = \frac{2g}{f}$ where C is Chezy's friction coefficient (43)

and remembering that $U = \frac{Q}{A_y}$, Equations (14) and (17) can be rewritten. In the following, the working will be given only for Equation (14), as Equation (17) is very similar. Therefore we have that:-

$$\frac{dM}{dx} = sy - \frac{Q^2}{C^2 A_y^2}\left(1 + \frac{2y}{\ell}\right) \tag{44}$$

and using the notation of Equation (40)

$$\frac{d\mathcal{S}}{dX} = \frac{d\,M/y^2}{dX} = \frac{1}{y_c^2}\frac{dM}{dX} = \frac{1}{yc}\frac{dM}{dx} \tag{45}$$

and therefore Equation (44) becomes,

$$\frac{d\mathcal{S}}{dX} = sY - \frac{g}{C^2 A_Y^2}\left(1 + \frac{2y}{\ell}\right) \tag{46}$$

This, however, as stated earlier only applies to the problem of permanent flow, which from the point of view of this thesis is the Hydraulic jump. The value of the variation of $\mathcal{S}$ and E are required, however, for the moving surge. The value of Q in these two cases is different. Fig. 2A, represents the velocities in the undular surge, whilst Fig. 2B, represents the velocities when the surge has been reduced to the equivalent case of permanent flow.

It is convenient here to refer back to Equation 44 which can be rewritten

$$\frac{dM}{dx} = sy - \frac{V^2}{C^2} \tag{47}$$

and at any section in Fig.2 B V_r is the velocity of the fluid relative to the boundary,

and therefore $V_r = -(V_2 - V_1) = -\left(\frac{Q_u}{y\ell} - V_1\right)$ (48)

but $V_1 = \frac{Q_u}{y_o \ell}$

and therefore $V_r = \frac{Q_u}{\ell}\left(\frac{1}{y_o} - \frac{1}{y}\right)$ (49)

and from this Equation, (47) becomes

$$\frac{dM}{dx} = -sy + \frac{Q^2}{c^2 \ell^2}\left(\frac{1}{y_o} - \frac{1}{y}\right)^2 \left(1 + \frac{2y}{\ell}\right) \quad (50)$$

the rate of change of Momentum of a Surge.

Using the notation of Equation (40)

$$\frac{d\not{S}}{dx} = -sY = \frac{g}{c^2}\left[\frac{1}{Y_o} - \frac{1}{Y}\right]^2 \left[1 + \frac{2y}{\ell}\right] \quad (51)$$

and similarly

$$\frac{dE}{dX} = -s + \frac{g}{Yc^2}\left[\frac{1}{Y_o} - \frac{1}{Y}\right]^2 \left[1 + \frac{2y}{\ell}\right] \quad (52)$$

In equations (51) and (52) the changes of $\not{S}$ and E are seen to be positive. That this must be so, will be realised by inspection of Fig.2B. Under the waves the boundary moves more rapidly than the fluid and hence, in the positive 'x' direction the surge gains in energy and momentum. In reality this is stating that at the head of the surge the energy and momentum are at a minimum value. Hence the signs in the relevant equations are now changed.

This result shows that unless the channel is 'semi infinitely' wide, the result is not general, (i.e.) that having determined the flow profile for one particular channel, it will not hold for another channel with the same ratio for $\frac{y_o}{y_c}$, unless $\frac{y_o}{\ell}$ and C are the same for both channels.

Equations (41), (51) and (52) are then the equations to be used in the prediction of the profiles of undular surges in rectangular open channels.

(2). METHOD OF ELLIPTIC INTEGRALS.

It is interesting to note that some checks on the calculations are available, by what is described in this thesis as the method 'of elliptic integrals'. It has already, been stated that the waves in the train of an undular surge have been shown to approximate very closely to cnoidal waves. That is, the profile of the waves approximates to the graph of the square of Jacobean elliptic function cn x, with different moduli k.

If Y_1 and Y_2 represent the heights of a successive crest and valley respectively, and if these values are substituted in Equation (41), noting that $\frac{dY}{dX}$ in each case is zero, then by substitution,

$$E = \frac{Y_1 + Y_2}{2} + \frac{1}{2Y_1Y_2} \qquad (53)$$

and $$S = \frac{Y_1Y_2}{2} + \frac{Y_2 + Y_1}{2Y_1Y_2} \qquad (54)$$

Replacing these values in Equation (41)

$$\frac{1}{3}\left(\frac{dY}{dX}\right)^2 = (Y - Y_1)(Y - Y_2)\left(\frac{1}{Y_1Y_2} - Y\right) \qquad (55)$$

and then the half wave length

$$L = \frac{1}{\sqrt{3}} \int_{Y_1}^{Y_2} \frac{dY}{\sqrt{(Y - Y_1)(Y - Y_2)\left(\frac{1}{Y_1Y_2} - Y\right)}} \qquad (56)$$

and then using the change of variable

$$Y = \frac{Y_1 + Y_2}{2} + \frac{Y_1 - Y_2}{2}u \qquad (57)$$

$$L = \frac{1}{\sqrt{3\left(\frac{Y_1 + Y_2}{2} - \frac{1}{Y_1Y_2}\right)}} \cdot \int_{-1}^{+1} \frac{du}{\sqrt{(1 - u^2)(1 + Ku)}}$$

where $K = \dfrac{Y_1 - Y_2}{Y_1 + Y_2 - \dfrac{2}{Y_1 Y_2}}$ (58)

which represents a uniformly convergent elliptic integral of standard form for $-1 < K < +1$

Alternatively with the original notation,

$$L = \frac{Q}{\ell\sqrt{3g\left(\dfrac{y_1 + y_2}{2} - \dfrac{y_c^3}{y_1 y_2}\right)}} \cdot \int_{-1}^{+1} \frac{du}{\sqrt{(1 - u^2)(1 + Ku)}} \qquad (59)$$

where $K = \dfrac{y_1 - y_2}{y_1 + y_2 - \dfrac{2y_c^3}{y_1 y_2}}$ (60)

$y_1 y_2$ and $\dfrac{y_c^3}{y_1 y_2}$ are the three roots of equation (35) when $dy/dx = 0$.

From these expressions it is possible to obtain a check on the heights of the crests and valleys, and on the wave lengths. The method will be indicated later.

In the following Chapter, the methods of applying the relationships already obtained will be given. Various other matters are also dealt with later, such as the value of the Chezy coefficient C.

CHAPTER IV

THE APPLICATION OF THE RELATIONSHIPS DERIVED IN CHAPTER III.

Method used to determine the flow profile.

Rearrangement of formulae to simplify calculations.

Methods in calculations. Elliptic Integrals.

List of Calculations. Determination of the friction coefficient (C).

(1) Method used to determine the flow profile.

To facilitate the calculations the following assumptions were made;- that the bed slope of the channel, and the initial flow were zero. Hence our surge wave moves in water that originally is stationary. Then the preliminary steps in the calculations are as follows:-

The values of E_o and $\mathcal{S}_o$ are first obtained, where the suffices 'o' refer to conditions at the foot of the leading wave of the surge (i.e.) still water conditions.

$$M_o = \frac{y_o^2}{2} + \frac{Q^2}{g\ell^2 y_o} \qquad (61)$$

$$\text{and } H_o = y_o + \frac{Q^2}{2g\ell^2 y_o^2} \qquad (62)$$

which employing Equation (40) give

$$\mathcal{S}_o = \frac{Y_o^2}{2} + \frac{1}{Y_o} \qquad (63)$$

$$\text{and } E_o = Y_o + \frac{1}{2Y_o^2} \qquad (64)$$

Hence Q_o and y_o must be known to calculate $\mathcal{S}_o$ and E_o.

It is then presumed that since the changes in S and E are small compared with the change in Y, that for a small change in Y, $(= \Delta Y)$ $\mathcal{S}$ and E can be assumed to remain constant and equal to

ϕ_o and E_o respectively. Hence if these values of ϕ and E are put in equation (41) together with $Y = Y_o + \Delta Y$, then a value for $\frac{dY}{dX}$ will be obtained at this value of Y. Assuming that ΔY is small, then ΔX is $\Delta Y/(dY/dX)$. The smaller ΔY, the greater is the accuracy. This value of ΔX is then used in equations (51) and (52) to give the change in ϕ and E, if the value of C be known. For greater accuracy these values could be replaced in the original equation, and eventually new values of ϕ and E obtained. This by a process of reiteration would give an answer very close to the truth, but usually the first approximation is sufficient. The process is then repeated for further increments in Y, continuing as far as is required, and thus the wave profile can be plotted as the calculations proceed.

If ΔY at the start of the calculations is infinitely small, then ΔX is infinitely large, and as predicted theoretically by Serre, the wave front never reaches the initial level. In practice the distance ΔX is reasonably short, but in the calculations it is very difficult to know how much to allow, when the results are to be compared with experiment. Usually the first value of $\Delta Y = 0.01$, and this gives a slightly shorter front to the wave than is indicated in practice.

As previously stated, in the case of the undular surge, the increments in ϕ and E have to be added to ϕ_o and E_o. Referring to Figure 2, it can be seen that under the waves the boundary is moving faster than the fluid, and hence the fluid must be gaining in energy. Looked at in reality this shows that the head of the surge is a position of minimum energy and momentum, and that the farther one proceeds towards the rear of the surge, the greater these values become. In the hydraulic

jump these values will of course decrease as the observer moves towards the rear of the jump.

When the profile has been determined to the first crest, the sign of $\frac{dY}{dX}$ has to be reversed. This is because X is a continuous function of Y, and we know from physical considerations that the depth of the water must decrease again.

(2). Rearrangement of formulae to simplify calculations.

Whilst the profile of a surge could be determined directly by the method of Section I of this chapter, it would be a long and laborious process, hence the following relationships have been evolved. Using Equation (41) as explained in the first section of this chapter

$$\frac{1}{6}\left(\frac{dY}{dX}\right)_0^2 = E_0\left(Y_0 + \Delta Y\right)^2 - \frac{\left(Y_0 + \Delta Y\right)^3}{2} + \frac{1}{2} - \phi_0 \cdot \left(Y_0 + \Delta Y\right) \qquad (65)$$

where $\left(\frac{dY}{dX}\right)_0$ is the slope of the profile at $Y = Y_0 + \Delta Y$

Then $$\Delta X = \frac{\Delta Y}{\left(\frac{dY}{dX}\right)_0} \qquad (66)$$

Hence from Equations (51) and (52) the values of ΔE_0 and $\Delta \phi_0$ can be obtained and:-

$$\frac{1}{6}\left(\frac{dY}{dX}\right)_1^2 = \left(E_0 + \Delta E_0\right)\left(Y_0 + 2\Delta Y\right)^2 - \frac{\left(Y_0 + 2\Delta Y\right)^3}{2} + \frac{1}{2} - \left(\phi_0 + \Delta \phi_0\right)\left(Y_0 + 2\Delta Y\right) \qquad (67)$$

and by inference

$$\frac{1}{6}\left(\frac{dY}{dX}\right)_n^2 = \left(E_0 + \Delta E_0 + \Delta E_1 + \cdots + \Delta E_{n-1}\right)\left(Y_0 + (n+1)\Delta Y\right)^2 - \frac{\left(Y_0 + (n+1)\Delta Y\right)^3}{2} + \tfrac{1}{2} - \left(\phi_0 + \Delta \phi_0 + \Delta \phi_1 + \cdots + (\Delta \phi)_{n-1}\right)\left(Y + (n+1)Y\right) \qquad (68)$$

Then using the values of E_0 and ϕ_0 (Equations (63) and (64) with this last equation; expanding and then eliminating like terms, and putting —

$$(\Delta E_0 + \Delta E_1 + \cdots + \Delta E_{n-1}) = \sum \Delta E \quad \text{and}$$

$$(\Delta \phi_0 + \Delta \phi_1 + \cdots + \Delta \phi_{n-1}) = \sum \Delta \phi \qquad (69)$$

$$Y_0 + (n+1)\Delta Y = Yn$$

The following expression is obtained which greatly reduces the labour in the calculations:-

$$\frac{1}{6}\left(\frac{dY}{dX}\right)_n = \frac{(n+1)^2(\Delta Y)^2(1 - Y_0^3)}{2Y_0^2} - \frac{(n+1)^3(\Delta Y)^3}{2} + (\sum \Delta E).(Y_n)^2 - (\sum \Delta \phi)(Y_n) \qquad (70)$$

and the equations relating changes in energy and momentum to depth became

$$\frac{d\phi}{dX} = \frac{g}{C^2}\left[\frac{1}{Y_0} - \frac{1}{Y}\right]^2\left[1 + \frac{2y}{\ell}\right] \qquad (71)$$

$$\frac{dE}{dX} = \frac{g}{C^2}\left[\frac{1}{Y_0} - \frac{1}{Y}\right]^2\left[1 + \frac{2y}{\ell}\right] \qquad (72)$$

From these three equations, knowing the discharge at the point in the length of the channel where the wave profile is to be calculated, the original depth, and C; then for a particular channel the profile of the undular surge may be determined, if the bed slope is zero.

(3) Methods in Calculation.

If the known quantities at the entry of the channel are Q, C, y , and the channel cross section, then the procedure in calculating the wave profile at a known distance from the entry is as follows:-

(a) Knowing the above quantities the discharge at the given position can be found using any of the normal calculation procedure (i.e. that due to Favre) or by model experiments. If the initial value of Q is used then the profile obtained will give the height of the highest wave that will result in the channel.

(b) Knowing the value of Q at the position required, and if y_s represents the mean height of the surge, to a good approximation the velocity of the surge $V = \frac{Q}{\ell (y_s - y_o)}$ (73)

Let Q_H be the discharge for the equivalent hydraulic jump

$= V\, y_s \ell$

$\therefore\ Q_H = y_c^{3/2} \ell\, g^{1/2} = \frac{Q y_o}{y_s - y_o}$ (74)

further $y_s = \frac{y_o}{2}\left[-1 + \sqrt{1 + 8\left(\frac{y_c}{y_o}\right)^3}\right]$ for a rectangular channel (75)

and therefore y_c can be obtained by a rapid process of trial and error from

$$\left(\frac{Q}{-\frac{3}{2} + \frac{1}{2}\left(1 + 8\left(\frac{y_c}{y_o}\right)^3\right)^{1/2}}\right) = y_c^{3/2} \ell \cdot g^{1/2} \quad (76)$$

Alternatively y_s and V can be obtained directly from Bavres calculations. (See Appendix for numerical example).

Knowing y_c and y_o, Y_o can be determined, and using Equations (70) (71) and (72) the profile of the surge can be calculated, if the value for the coefficient of friction is known.

(4) Procedure in calculations using the Method of Elliptic Integrals.

Having calculated the profile of the undular surge, the wave lengths can be checked by the method of elliptic integrals.

In equation (59) there occurs the integral

$$I = \int_{-1}^{+1} \frac{du}{\sqrt{(1 - u^2)\,(1 + Ku)}} = \int_{-1}^{+1} \frac{du}{\sqrt{(1 - u)\,(1 + u)\,(1 + Ku)}}$$

$$= \frac{1}{\sqrt{K}} \int_{-1}^{+1} \frac{du}{\sqrt{(1 - u)\left(u - (-1)\right)\left(u - \left(-\frac{1}{K}\right)\right)}} \quad (77)$$

This corresponds to the standard elliptic integral—

$$\int_b^y \frac{dt}{\sqrt{(a-t)(t-b)(t-c)}} \qquad \text{where} \quad \begin{aligned} a &= 1 \\ b &= -1 \\ c &= -1/K \end{aligned} \qquad (78)$$

and $a > y > b > c$ which holds as $-1 < K < +1$

The solution is of the form $g\,sn^{-1}(\sin\varphi, k)$

where $g = \frac{2}{\sqrt{a-c}} = \frac{2}{\sqrt{1+1/K}}$ and $\varphi = \sin^{-1}\sqrt{\frac{(a-c)(y-b)}{(a-b)(y-c)}}$ $\qquad (79)$

$= \sin^{-1} 1$

$= \frac{\pi}{2}$

and $k^2 = \frac{a-b}{a-c} = \frac{2K}{K+1}$.

and therefore

$$I = \frac{2}{\sqrt{K+1}}\, sn^{-1}\left(\sin\frac{\pi}{2}, \sqrt{\frac{2K}{K+1}}\right) \qquad (80)$$

If this is introduced into Equation (59) the half wave length L can be determined. Alternatively Equation (59) can be simplified for waves of small amplitude.

$$L = \frac{\pi y_c^{3/2}}{\sqrt{3\left(\frac{y_1 + y_2}{2} - \frac{y_c^3}{y_1 y_2}\right)}} \left(1 + \frac{3K^2}{16}\right) \qquad (81)$$

This method involving the use of elliptic integrals can also be extended to give the values of L, y_1 and y_2 for successive indulations. The method is necessarily approximate, but is quite useful to provide some answers without the work involved in the full calculation of the profile.

In equation (41) if $\frac{dy}{dx} = 0$,

$$EY^2 - \frac{Y^3}{2} + \frac{1}{2} - \phi Y = 0 \qquad (82)$$

If E and ϕ are given the values E_o and ϕ_o (Equation (63) and (64)) then (82) can be solved for Y. This will yield three values of Y, and the equivalent values of y_1 and y_2 can be calculated. Then using Equation (81) an approximate value is obtained for L. Putting $L = \Delta X$ an approximate value of $\Delta\phi$ and ΔE can be obtained to the crest of the first wave. Alternatively E and ϕ

can be obtained directly from Equations (53) and (54). Putting these values back into Equation (82) further and more accurate values of Y may be obtained. These are then substituted in Equation (57) to obtain L more accurately. This is then repeated if greater accuracy is required.

The process is repeated for subsequent valleys and crests, and thus a series of values of Y_1, Y_2 and L are obtained for each wave. These can either be used as checks on the main calculations, or for a rapid determination of the three quantities Y_1, Y_2 and L for each undulation.

(5) List of Calculations.

From the experiments undertaken, it was quickly realised that the maximum height of the leading wave is reached - i.e. breaking occurs for approximately $Y_0 = 0.83$. Purely for interest's sake, however, two profiles were calculated for several waves at $Y_0 = 0.80$ with two extreme values of C in an infinitely wide channel. In the first $\frac{g}{C^2} = 0.002$ which represents an extremely smooth channel, and for the second $\frac{g}{C^2} = 0.08$ representing an extremely rough surface. These two profiles are shown in Fig.25 The results are discussed later, but it is of great interest to note the differences in the two profiles.

A profile is also obtained for $Y_0 = 0.9$ when $y_0 = 2"$, and the effects of friction are neglected (i.e.) $C = \infty$. This as would be expected has the form of a solitary wave

Finally profiles were calculated for; $Y_0 = 0.9$ with $y_0 =$ 2", 3" and 4"; and $Y_0 = 0.87$, and 0.95 with $y_0 = 2"$. These were calculated with values of C appropriate to a smooth glass channel, and then repeated for $Y_0 = 0.9$ and $y_0 = 2"$ 3" and 4", using 'C' values appropriate to the channel lined with netting.

6. Determination of the friction coefficient (C).

To solve equations (70) to (72) requires a knowledge of the coefficient of friction, or rather of the variation in the value of this coefficient. The other terms are known or can be calculated, but the value of 'C' still has to be determined. From calculations and from observation it was soon evident that the profiles of the surges do depend very largely upon the losses of energy and momentum in the surge. These losses are due not only to friction between the fluid and its boundaries, but also losses in the fluid itself. It has been assumed, however, that the losses are confined to the boundary layer and hence are proportional to the boundary surface area. In a wide channel the friction effects of the sides could be neglected, but not in the small channel used in these experiments.

The use of the name Chezy coefficient for 'C' is rather misleading, since it gives the impression that once the Chezy constant for the particular surface, and the depth are known then the friction coefficient is known. This, however, has been found to give much lower values of friction than occur in practice, unless the velocity of flow is reasonably high, the boundary surface is rough, and the initial depth is more than just a few inches.

It was found that in the channel used in the experiments the velocity of flow (and hence the Reynolds number) was too low for the empirical value of C to be even approximately accurate. This was true even when the channel surface was lined with netting. Hence a more analytical approach was tried, using the well known relationship for laminar flow

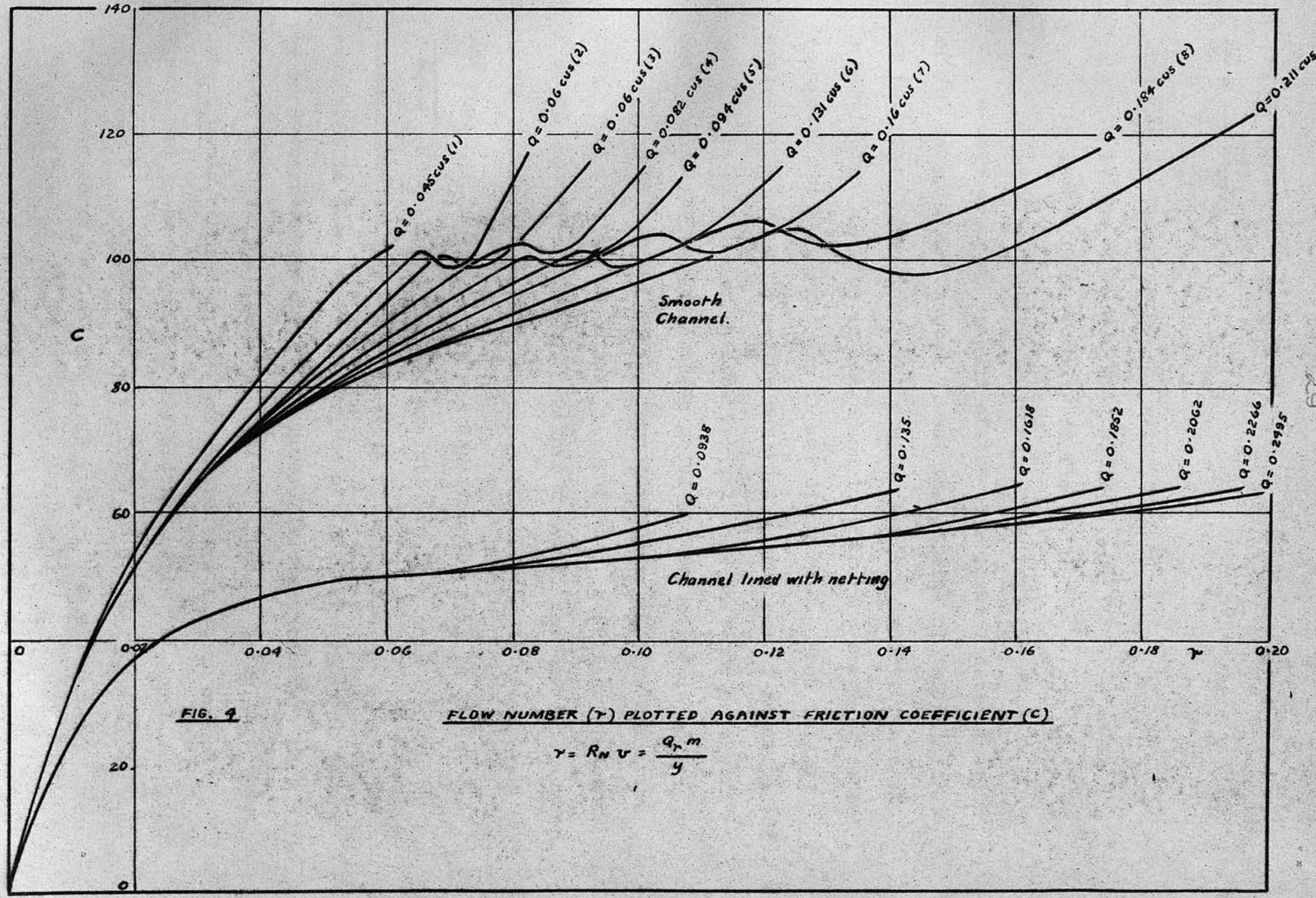

FIG. 9

FLOW NUMBER (γ) PLOTTED AGAINST FRICTION COEFFICIENT (C)

$$\gamma = R_N v = \frac{q_\gamma m}{y}$$

$$\frac{dy}{dx} = \frac{\frac{U^2}{C^2 m}}{1 - \frac{U^2}{gy}} \qquad (83)$$

where $\frac{dy}{dx}$ is the slope of the water surface

m is the Hydraulic Mean Radius

U is the mean velocity of flow

y is the depth of flow.

A more detailed account of the experimental determination of 'C' is given in Chapter 7, but the outline of the method is as follows. The slope of the water surface is determined at a particular position in the channel, where the surge is to be recorded; for different depths and discharges. From this a series of values of 'C' can be obtained by the use of Equation (83).

It is well known in experimental work that one of the criteria of similarity between model and prototype in work similar to this, is that the Reynolds number (R_N) be equal in each. It is also known that the friction coefficient (whether f or C) does vary with R_N. Rather than use the Reynolds number, it was thought preferable to use a flow number 'r' ($= V_r m = \frac{Q_r m}{\ell y} = \frac{Q_m m}{\ell} \cdot \left(\frac{1}{y_o} - \frac{1}{y}\right)$, Fig. 2 and Equation 49) this is of course $= R_N$. Hence C was plotted against 'r', for both the smooth channel and the channel lined with netting, Fig. 4. It can be seen that in both cases, the value of 'C' does appear to tend to an average value when 'r' $>$ 0.08. It does, however, vary about a mean as the discharge varies. Then in order that these curves could be used in the calculations, a further set of curves had to be calculated and plotted, with 'Y' graphed against 'r', Fig. 5. These curves were for Y_o = 0.9 and y_o = 2, 3, and 4 ins. and for Y_o = 0.87 and 0.95 with y_o = 2 ins alone.

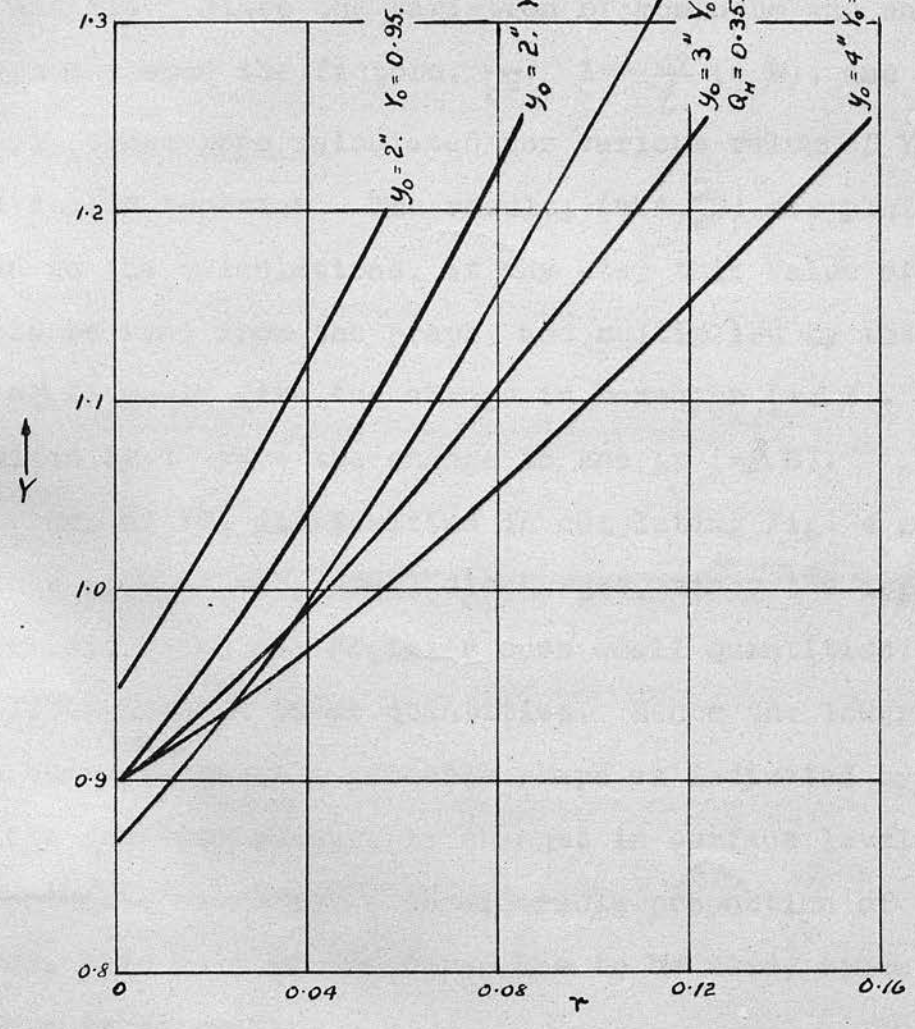

FIG. 5 DEPTH FUNCTION (Y) PLOTTED AGAINST FLOW NUMBER r

$Y = y/y_c$. $r = R_N v = \frac{Q_N m}{l}\left(\frac{1}{y_0} - \frac{1}{y}\right)$

Therefore at any point in the calculations if Y were known, 'r' could be found, and then from the 'r' to 'C' graph , 'C' could be found.

To facilitate the calculations even further, a final curve was calculated and plotted in each of the above combinations of y_o and Y_o. Since the variation of momentum and energy are dependent upon the factors, $\frac{g}{c^2}$; $1 + \frac{2y}{\ell}$ (= W); and $(\frac{1}{Y_o} - \frac{1}{Y})^2$ (=A); these were calculated for various values of Y, and then multiplied together. The result, $(W.A.\frac{g}{c^2})$ was plotted against Y. Then in the calculations, at any step this value of $W.A.\frac{g}{c^2}$, could be read from the graph, and multiplied by the change in X (=Δ X) would give the change in momentum (=Δ M). This in turn divided by Y gave the change in energy (=Δ E).

One of the difficulties in completing Fig. 4 was obtaining values of 'C' at very small discharges, since the apparatus available would not register such small quantities, or such small changes in these quantities. Hence the lower part of the curve is given a probable shape as indicated by the results at the smallest measurable changes in surface level. This is unfortunate since for a considerable proportion of the calculations, this part of the curve has to be used, since the flow number is so small.

Profiles were also calculated with the empirically determined value of 'C', but although the depth at the crest of the first wave was not very much less than that recorded experimentally, the calculated wave length was considerably greater, and the depth at the first valley somewhat less than the recorded result.

From a comparison of the recorded results in the channel with a smooth and rough surface, this result indicated that the calculated energy and momentum losses were smaller than those occurring in these practical cases, (i.e.) the values of C were too large.

An attempt was then made to find some mean value of C which could be used in the calculations. It was discovered that if a mean water surface slope was obtained from the records, by taking the slope of a line joining the mean height between crest and valley of successive indulations, this gave a mean value of 'C' which gave results comparable in accuracy with those calculated using the values of 'C' determined as shown above. This however is only of academic interest, since some of the result is required to calculate the answer. What is interesting however, is that the slope calculated on a mean height basis, is greater than that of a similar flow which has reached equilibrium - (i.e.) when the surface shape remains constant. This would apparently show that the losses at the head of the surge are greater than those nearer to the rear of the wave train. A possible reason for this, is that at the head of the surge the flow is approximately laminar and the velocity distribution is parabolic. Hence momentum and energy losses occur not only in the boundary layer, but throughout the liquid, that is to say the boundary layer is practically non existent. Farther along the wave train however the velocity distribution approaches more nearly the conditions assumed theoretically. That is, that the losses all occur in the boundary layer and the velocity distribution outside this layer is uniform, hence the losses in energy and momentum are less than at the front of the surge. This is probably

analagous to the flow past a plate, with a gradually developing boundary layer.

The results of the calculations employing the variable friction coefficient, determined, by the methods described in this section, are shown in Figs. 22 to 24.

CHAPTER 5.

Practical Details in the Calculation of Undular Surge Wave Profiles.

In practice the known quantities would be, the initial discharge, the friction coefficient, the initial depth, and discharge, and the geometry of the channel. From this the profile of the surge could be determined, as explained in the previous Chapter.

To simplify matters a little, however, in the calculations, arbitary values of y_o and Y_o were chosen. From these two, y_c can be determined and hence $Q_H = (y_c^3 g l^2)^{1/2}$ (84)

Then the velocity of the surge $V = \frac{Q_H}{l y_o}$ (85)

From Fig. 13 (which shows the velocity of the surge at each of three depth gauges, plotted against initial discharge) knowing the gauge at which the surge is to be recorded, the initial discharge can be found corresponding to the velocity V. Several runs are then made at this initial discharge with the chosen initial depth, and the surge is recorded at the desired depth gauge. This record is then reproduced to scale, and the calculated points shown on it as large dots. Thus a comparison of the calculated and recorded profile is obtained. Figs. 22 to 24. A numerical example of the preliminary calculations is included in the Appendix.

(a) Step by Step Calculations.

As already described in Chapter 4, a curve is plotted of $W.A.\frac{g}{c^2}$ against Y for the chosen Y_o and y_o. $W. = \left(1 + \frac{2y}{l}\right)$; $A = \left(\frac{1}{Y_o} - \frac{1}{Y}\right)^2$; and C is obtained from Figs. 4 and 5.

The value of $\frac{(\Delta Y)^2 (1 - Y_o^3)}{2Y_o^2} = B$ and $\frac{(\Delta Y)^3}{2}$ are found for the particular Y_o.

Finally a calculation sheet is drawn up embodying all the steps involved in the approximate step by step solution of Equations (70) (71) and (72). A specimen sheet is included (Fig. 27) and an explanation of the headings is as follows.

Column (1) Y_n and Y_n^2

Column (2), (3) and (4) $(n + 1)$, $(n+1)^2$ and $(n + 1)^3$

Column (5) G - T. $G = B(n + 1)^2$; $T = \frac{(\Delta Y)^3}{2}(n + 1)^3$

Column (6) N - P. $N = (\Sigma \Delta \phi)\ Y_n$

$P = (\Sigma \Delta \Xi)\ Y_n^2$

$\Sigma \Delta S$ and $\Sigma \Delta \Xi$ are calculated in the preceding line.

Column (7) G - T + N - P. These values change sign and when G - T + N - P = 0 it represents a crest or valley.

Column (8) $6(G - T + N - P) = (\frac{dY}{dx})^2$

Column (9) $\sqrt{6(G - T + N - P)} = \frac{dY}{dX}$

Column (10) Mean $\frac{dY}{dX}$ is the mean of the values at Y_n and Y_{n+1}, and used in the calculation of ΔX.

Column (11) $\Sigma \Delta X$ and ΔX. $\Delta X = \frac{\Delta Y}{\text{Mean } \frac{dY}{dX}}$, and $\Sigma \Delta X$ is the sum of ΔX from $Y = Y_o$ to Y_n.

Column (12) Point ΔX. Value of ΔX to be used in the calculation of $\Delta \Xi$ and $\Delta \phi$. which is found by trial and error and is equal to ΔX, of the next line.

Column (13) $\frac{g}{c^2} (\frac{1}{Y} - \frac{1}{Y_o})^2 (1 + \frac{2y}{l}) = W.A.\frac{g}{c^2}$. This has been already calculated, but the value used is the mean of the two values for Y_n and Y_{n+1}.

Column (14) $\Sigma \Delta \phi$ and $\Delta \phi$: $\Delta \phi = \frac{g}{c^2} (\frac{1}{Y} - \frac{1}{Y_o})^2 (1 + \frac{2y}{l})$. Point ΔX $\Sigma \Delta \phi$ is the sum of $\Delta \phi$.

Column (15) $\Sigma\Delta E$ and ΔE: $\Delta E = \dfrac{\Delta S}{\dfrac{Y_o + Y_{on}}{2}}$

$\Sigma\Delta E$ is the sum of ΔE.

Several points arise from this. It was decided that it would be more accurate to use a mean value of $\frac{dY}{dX}$ in the calculation of ΔX, although, this would probably not have a very large effect.

Point ΔX is the value of ΔX reached in the following line for ΔX. Its knowledge necessitates a certain amount of reiteration but with experience a good guess can usually be made, so that two trials are rarely needed. There are several methods of estimating Point ΔX, but these whilst useful are not of sufficient interest to be explained in detail.

Mean values of $\frac{g}{c^2}\cdot\left(\frac{1}{Y} - \frac{1}{Y_o}\right)^2\cdot\left(1 + \frac{2y}{\ell}\right)$ and of $\frac{\Delta S}{Y}$ also used to increase the accuracy of the calculations.

These calculations are then checked by the method of elliptic integrals, and finally checked against the experimental run, with the exact value of Q required.

(b) Elliptic Integrals [1]

From the step by step calculations the values of y_1 and y_2 (depths at the first crest and valley) are obtained. y_c is calculated and hence K. Then 'k' is determined and the value of $\sin^{-1} k$.

$\frac{2}{\sqrt{K+1}}$ and $\dfrac{y_c^{\frac{3}{2}}}{\sqrt{3\left(\frac{y_1 + y_2}{2} - \frac{y_c^3}{y_1 y_2}\right)}}$ are determined.

It should be noted in the last expression that y_c^3 has already been calculated, and that the divisor squared is 1.5 times the divisor in the expression for K.

From a handbook of elliptic integrals, the value of the incomplete integral of the first kind $F = (\varphi, k)$ is found, where φ is 90°, and sin - 1k (which has been determined) gives the cross reference. The value, thus obtained, multiplied by the two expressions determined above gives the half wave length 'L'. For comparison, the value of L is determined by the approximate method

$$L = \frac{\pi y_c^{3/2}}{\left(3\left(\frac{y_1 + y_2}{2} - \frac{y^3}{y_1 y_2}\right)\right)^{1/2}} \left(1 + \frac{3K}{16}^2\right)$$

Thus finally four values of 2L are available, two by the method of elliptic integrals, one from the step by step calculation and one recorded. These are listed in Fig. 26. or

(c) Elliptic Integrals 2.

A worked example is included in the appendix of the above, and also of an attempt to evaluate the crest and valley height, and the wave length approximately by this method.

This is similar to the above, but requires in addition the value of E_o and β_o (from Equations 63 and 64) and the solution of the cubic $EY^2 - \frac{Y^3}{2} + \frac{1}{2} - \beta Y = 0$.

As the method of working will be shown in full, no further details are presumed to be necessary.

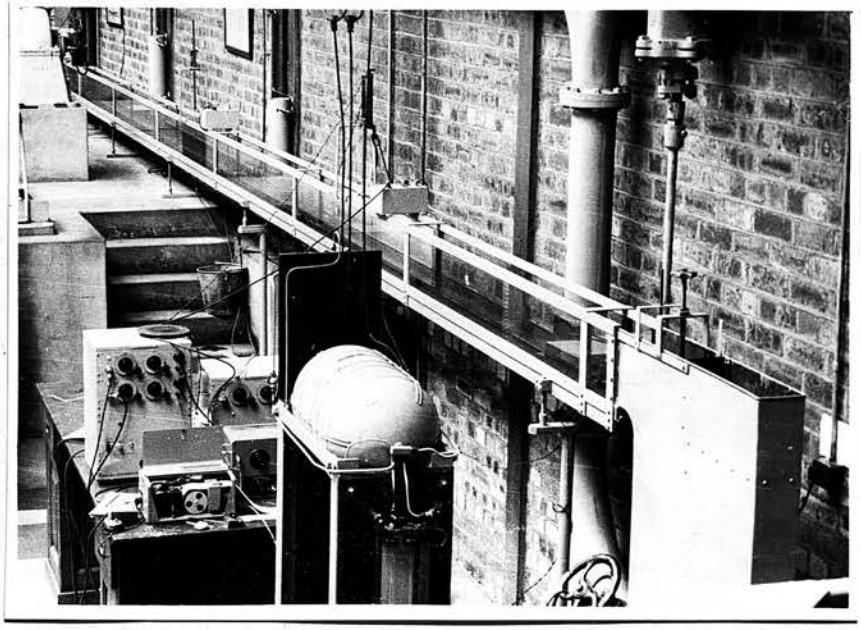

Plate 2. General view of channel and recording apparatus.

CHAPTER 6.

A DESCRIPTION OF THE APPARATUS USED AND THE METHOD OF EMPLOYING IT TO RECORD THE PROFILES OF SURGES IN AN OPEN CHANNEL.

Apparatus. Principle of the depth gauges.
Methods of Calibration of Apparatus. Procedure in Producing and Recording a Surge Profile.
Determination of Wave Lengths of the undulations.
Photographic Comparisons. Check runs. Notes.

(1) Apparatus.

A glass lined channel, forty eight feet long, five inches wide and ten inches deep, was supplied with water from a tower. The water flowed from this channel into a drainage channel, then into a storage tank, and was finally pumped back to the supply tower (Fig. 6)

The water was released into the glass lined channel by means of a slide valve, but first passed into a large tank (A) which helped to ensure that the water entering the channel was not unduly turbulent. In order that the rise in surface level in the channel should be as nearly instantaneous as possible, the water left the tank through a narrow but gradually expanding opening, the size of which could be varied by a screw attachment.

The quantity of water was regulated by a screw valve, and measured by means of a mercury manometer. This manometer was calibrated using a large tank (B) into which the flow of water could be diverted and measured. Tank (B) could then be emptied directly into the storage tanks (Fig. 6)

The channel was constructed with an inner surface of glass, held in place by a steel framework with a mild steel (6 in. x 3 in.)

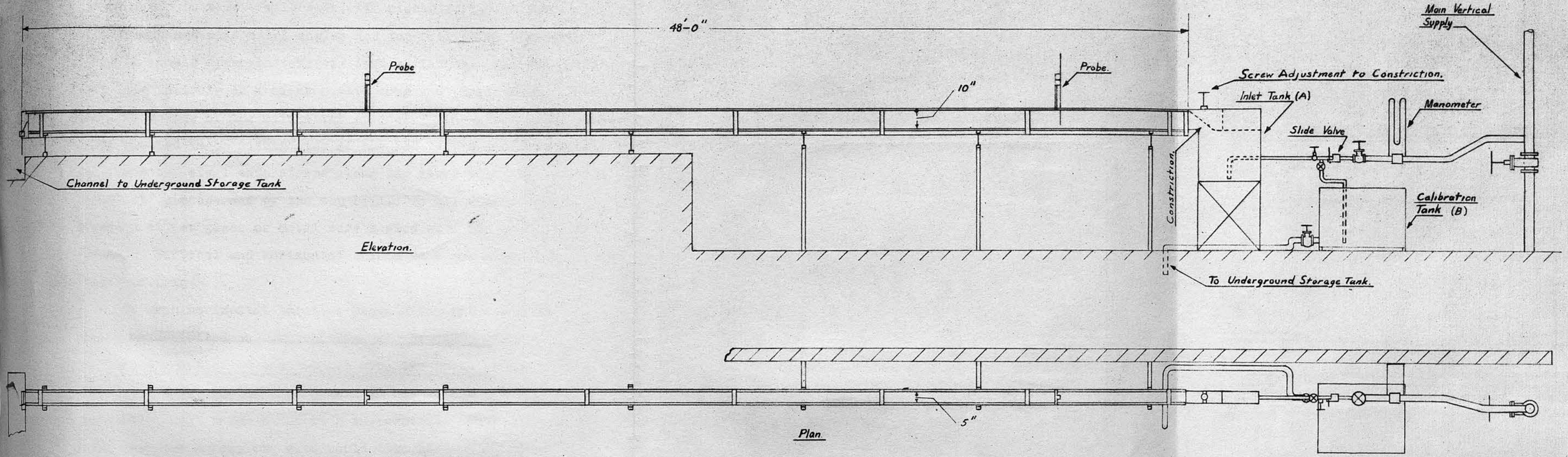

48'— 0" GLASS CHANNEL

(10" x 5")

FIG. 6.

channel as the base. Mild steel "T" pieces formed the sides of the frame, and mild steel angles the top rail. The glass was laid in panels approximately six feet in length. The bed glass was laid entirely on a black mastic compound (Trade Name "Black Magic") on top of the mild steel channel. The glass side panels then slotted in on either side of the bed panels and were held in place by, steel side straps along the lower edge, by the mild steel "T" pieces, and by the top rail. In all cases, joints between either glass or metal were sealed with the mastic compound. Vertical and horizontal joints were not allowed to coincide (Fig. 7).

At each horizontal joint, a brass strip was inserted. These were slotted to take the base of the depth gauges.

At the outlet to the channel were two brass gates. The first was a guillotine type gate. On one face was a brass strip with horizontal holes bored at ½ in. centres. With a metal pin in one of the holes, the gate could then be shut to within a predetermined distance of the bed. To shut the gate completely, the pin was removed; and the shock of closure was cushioned by a thin rubber inset in the bed of the channel.

The second gate was of the usual weir type operating from the bottom of the channel upwards by means of a rack and pinion, and could thus be set to give any required depth of water. A small pointer on the pinion indicated the required position of this gate for various depths of water, at half inch intervals.

Mild steel blocks on the sides of the mild steel channel were drilled and tapped to take ⅝ in. diameter hardened steel threaded rods. Each rod had a large square head, which could

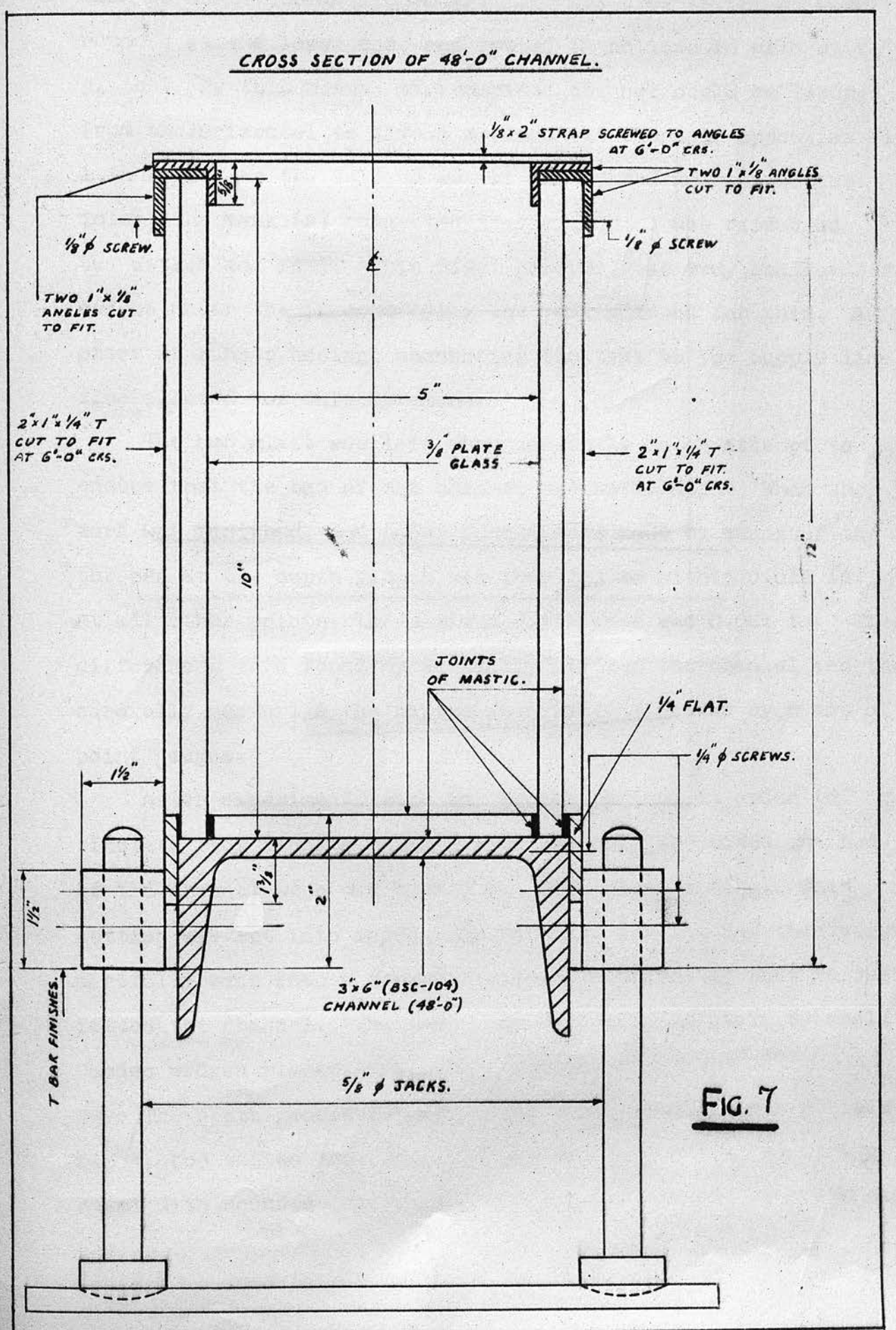
CROSS SECTION OF 48'-0" CHANNEL.
1/8" x 2" STRAP SCREWED TO ANGLES AT 6'-0" CRS.
TWO 1" x 1/8" ANGLES CUT TO FIT.
1/8" ϕ SCREW.
1/8" ϕ SCREW
TWO 1" x 1/8" ANGLES CUT TO FIT.
5/8"
5"
2" x 1" x 1/4" T CUT TO FIT AT 6'-0" CRS.
3/8" PLATE GLASS
2" x 1" x 1/4" T CUT TO FIT AT 6'-0" CRS.
10"
12"
JOINTS OF MASTIC.
1/4" FLAT.
1/4" ϕ SCREWS.
1 1/2"
1 3/8"
2"
1 1/2"
3" x 6" (BSC-104) CHANNEL (48'-0")
T BAR FINISHES.
5/8" ϕ JACKS.

FIG. 7

then be turned using a spanner. The heads of the rods, were rounded at the lower end, and rested in hollows in mild steel plates. By this means, the complete channel could be lowered from the horizontal to give a maximum bed slope of approximately 1 in 100. As the fulcrum was at the "jack" nearest to the inlet, the tank (A) connected to the channel was raised as the outlet end fell. This rise, however, was very small, and small wedges under the frame carrying the tank allowed for this. A piece of rubber hosing, connecting the tank to the supply line, also allowed for this movement.

The bed glass was laid very carefully in an attempt to ensure that the bed of the channel was horizontal. When the work was finished, and minor adjustments made by means of the jacks, the bed at the depth gauges was levelled to within 0.015 in. At all other points, the maximum difference was 0.021 in. These differences were found by partially filling the channel and then carefully measuring the depths at different places by means of point gauges.

After experiments with the smooth channel, in order to simulate flow along a rough walled channel, the sides and bed of the channel were clad with ½ in. mesh wire netting. This netting was cut into approximately 2 ft. lengths and then very carefully bent into a square cornered, U shape; so that it just fitted the channel. The free ends were held in place by small wooden wedges placed across the channel.

The depth gauges (Pl..3) were constructed with a perspex block, top and bottom, connected by two thin pieces of spring steel with rounded edges. The bottom block fitted into the slot

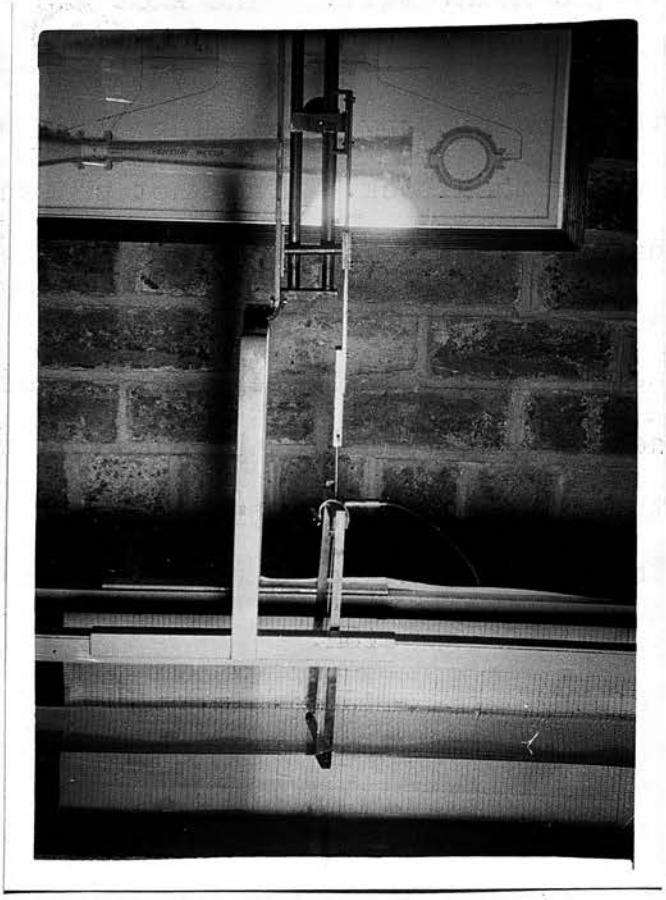

Plate 3. Depth gauge detail.

in one of the brass strips in the bed of the channel. Hence the only obstructions to the flow were these thin pieces of spring steel, and the gauge wire. This wire passed through a hole in the lower perspex block and the end of the wire was knotted, leaving a ¾ in. tail. The knot was fitted into a recess under the perspex block, and the tail after being insulated with a proprietory insulating glue, was fitted into a small slot under the block. The knot prevented the wire from slipping through the block and was found to be preferable to more elaborate systems of screws or clips. The other end of the wire passed through a small perspex cylinder and was again knotted. The perspex cylinder was connected to a threaded brass rod passing through the upper perspex block. A nut on the upper side of this block drew the rod through the block and tightened the wire to a suitable tension.

The end of the threaded rod was held by a small bolt (with a milled head) in a hole drilled longitudinally in a long square sectioned brass rod. The brass rod was divided into inches and tenths of inches along its length. It was raised and lowered by a rack and pinion against a vernier, reading to 0.01 in. directly and by estimation to 0.001 in. By this means, the entire depth gauge could be raised and lowered by a measured amount.

(2) <u>The principle of the depth gauges</u>.

The wire (copper with P.V.C. covering, 0.031 in. overall diameter and manufactured by Henley's Cables Ltd.) and the water form a condenser, with the metal filament of the wire and the water as conductors, and the P.V.C. covering to the wire as a dielectric. As the water level varies, so the capacitance of

OSCILLATOR

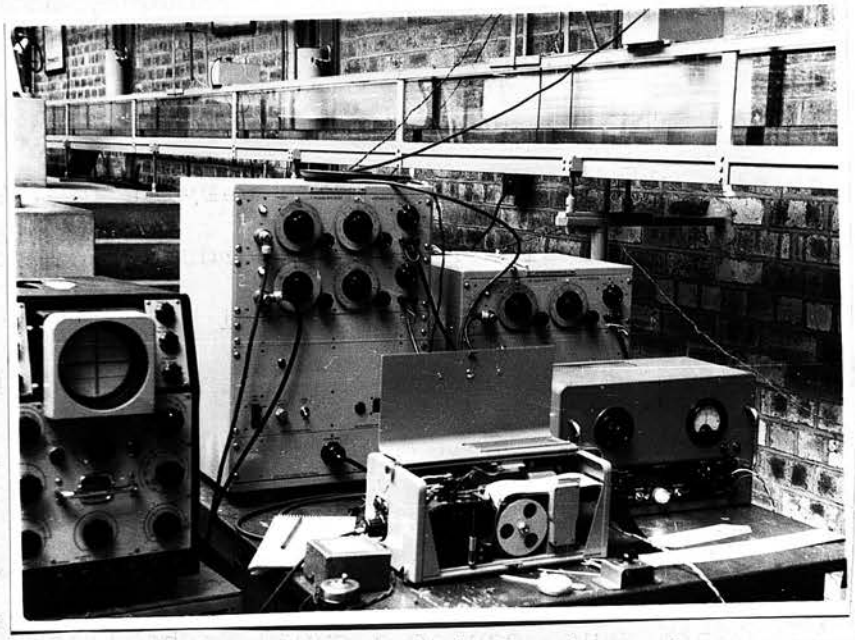

3 SOUTHERN 'MINIRACK' PANELS

C.R.O. TRANSFORMER · PEN RECORDER · AMPLIFIER · ROTARY SWITCH

Plate 4. Recording Equipment.

the condenser varies. The end of the wire is connected to the live terminal of a coaxial socket. A plug and cable then connect this variable condenser into the circuit of a frequency modulated oscillator working at 2 m.c.p.s. As the capacitance varies, so the frequency varies. This changing frequency is then fed into a discriminator circuit, and the resulting varying D.C. signal is then amplified and applied to either a pen recorder or cathode ray oscilloscope. With such a low frequency signal, the pen recorder is preferable and was used throughout the experiments. If the C.R.O. record is used, it must be photographed.

The final D.C. signal varies almost directly in proportion to the varying water level, and for all practical purposes, a calibration of the depth gauge can be assumed to be linear. This, of course, presupposes that the apparatus is worked within the limits specified by the makers. With the maximum initial depth 4 in. and maximum variation in level at this depth approximately 3.5 in., the calibration of the gauges gave a linear result, (i.e. change in depth plotted against millimetres deflection of the pen recorder gave a straight line graph). The oscillator and discriminator circuit were manufactured by Messrs. Southern Instruments, Ltd. The amplifier was designed and made in the Electrical Engineering Department of the Sanderson Laboratories of Edinburgh University. This extremely useful piece of equipment would actually give a full scale recording on the penrecorder for only 10 millivolts input, and with practically no zero drift. This compared very favourably with the best commercial amplifier available which needed 2 volts input for full scale deflection and had a noticeable zero drift. The penrecorder

was manufactured by Messrs. Kelvin & Hughes, Ltd. and used paper divided longitudinally in millimetres and by millimetre arcs transversally at a radius equal to the length of the pen.

Since for some of the experiments three depth gauges were used and otherwise as many as six were in operation, a rotary switch was installed between the various D.C. outputs and the amplifier. Also, to enable the penrecorder to be switched on or off at a distance, as when calibrating the depth gauges, a switch in a long cable was inserted in the mains supply to the pen recorder.

In order that the penrecorder might be calibrated, a frequency meter was employed to give the frequency of the mains electricity supply and a small step down transformer was employed which could also be switched by the rotary switch to the amplifier, and thus to the penrecorder. Thus the mains frequency could be recorded on the penrecorder, and the true frequency noted at the same time. The accuracy of the frequency meter was checked by periodic enquiries at the local power station. It was found that the variation in mains frequency was $\pm$ 0.2 c.p.s. at the maximum. This variation, however, seemed to have little effect on the paper speed of the penrecorder which remained well within the $\pm$ ½% tolerance claimed by the makers.

To ensure that the penrecorder was giving a true record of the phenomena, a number of waves were photographed and compared with simultaneous records obtained by the pen recorder. The camera used was a Kodak 35 mm. with a 3.6 lens. Lighting was provided by a Stroboflood lamp giving a flash of some 10 microseconds' duration. A piece of white paper was securely

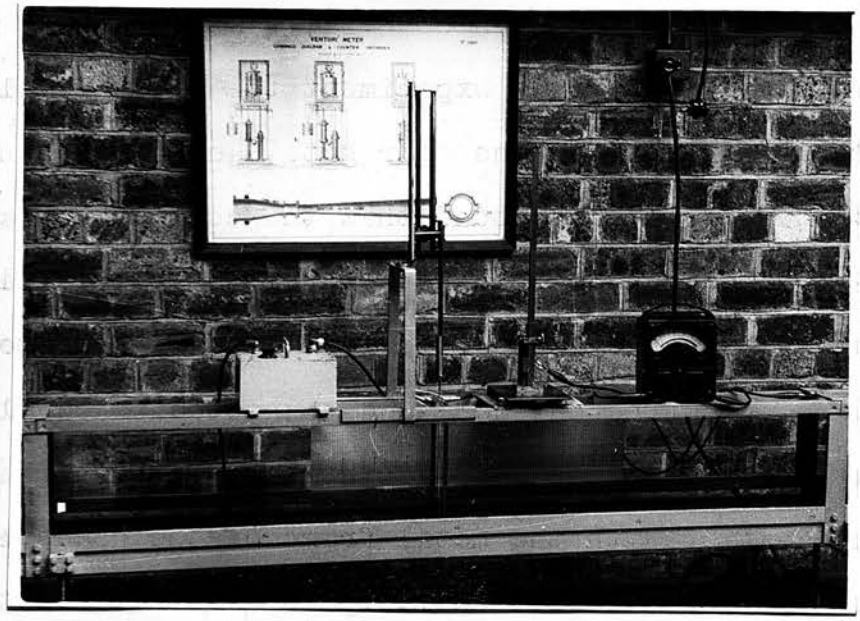

OSCILLATOR · DEPTH GAUGE · POINT GAUGE · AVOMETER

Plate 5. Channel Detail.

fastened to the side of the channel remote from the camera with a fine grid inscribed on it in Indian Ink. Despite Meniscus and parallax effects, the water level could be estimated from the photographs to 0.010 ins.

To measure the depth of still water ordinary point gauges were used. Before each experiment the water level was set to the required depth by the weir gate, and then checked with the point gauges. It was found that the contact between the metal point and the water could be determined very easily and with extreme accuracy by the following method. The point gauge was insulated from the channel, and connected to one lead of an 'Avometer' set to the high resistance position. The other lead was in contact with the metal frame of the channel, and thus with the water. Hence when contact was made between the point gauge and the water, the circuit was complete, and the meter needle swung over.

An ordinary Centigrade thermometer was used to measure the temperature of the water at the inlet to the channel.

The glass channel and the depth gauges were designed specifically for this particular problem, and the circuitry was designed to allow the use of existing equipment. The idea of using a capacitance type depth gauge is not original, but the gauges used in these experiments are believed to be of an original design. A short note on the difficulties encountered in the design is given in the Appendix.

(3) Calibration

(a) Manometer.

With the Mains valve open the slide valve was suddenly

opened and the water was diverted by another screw valve into the measuring tank B. The initial and final levels in the tank were noted, and the flow timed with a stop watch. Since the tank had already been calibrated it was known that a one inch change in level was equivalent to a discharge of 0.818 cubic feet of water, and hence the discharge for the particular valve opening could be determined. The difference in level of the mercury in the two arms of the manometer was also noted. This was repeated for a number of discharges, and the results were plotted as discharge against manometer difference in level. This was repeated later for a larger orifice, since the small orifice was required to give more accurate readings at small discharges, but did not give a sufficiently large discharge to produce breaking waves at large initial depths.

(b) Depth Gauges.

When the electrical equipment had 'warmed up', (i.e.) reached a steady state (this took about five hours), the depth gauges could be calibrated. The long warming up period was presumably due to the fact that as the apparatus eventually became very warm, it was a considerable time before equilibrium was reached between the heat given out by the instrument and the heat losses to the atmosphere.

When the steady state was reached, water was run into the channel until the total depth was approximately twice the initial depth required in the experiments. The gauge was raised by the rack and pinion until the top of the lower perspex block was at the level of the surface of the water. The reading on the scale was noted, and the gauge then lowered by an amount equal

to the initial depth of the experiment. The electrical apparatus was then zeroed for this position, the pen of the recorder being set to one side of the paper. The recorder motor was started, the gauge was raised a little and then lowered to the previous setting, thus ensuring a correct dynamic reading. It was held momentarily at this position, and then lowered in steps of 0.5 ins, with a slight pause at each step (with the recorder still in operation), to approximately a total depth of 1.85 times the initial depth. Again it was lowered slightly and then raised to this level, and then raised by steps of 0.5 ins, until the gauge had reached the initial depth again. Thus a dynamic calibration curve was obtained with the water level rising and falling, in terms of millimetres deflection for each half inch change in depth. Originally the calibration depth intervals were 0.1 ins., but as all the calibration curves were found to be straight lines, the interval was increased to 0.5 ins. One result was to show that the difference in meniscus effect between the water level rising and falling, was negligible, being of the order of 0.010 ins.

As already stated a continuous calibration curve was obtained, as stopping and starting the motor did not give consistent results. Earlier experiments confirmed that raising and lowering the gauges was the equivalent of lowering and raising the water level respectively, and was a much more rapid method of calibration. This was important as the calibration was carried out each day, and for each initial depth.

To ensure a constant depth of water during calibration, the 'guillotine' gate was shut, and the surface given a considerable

time to settle. Each gauge was calibrated in turn, and the record plotted on graph paper as, millimetres deflection to change in depth.

(c) Penrecorder.

The paper speed of the recorder was checked at frequent intervals, but the variations were so minute as to be negligible. The mains frequency was applied to the recorder via the transformer and rotary switch, and the frequency noted on the frequency meter. Thus the paper speed could be calculated.

(4) Experimental procedure in producing and recording a Surge Wave.

With the depth gauges calibrated, the initial depth of water was set to the required level by the weir gate, and checked by the point gauges. The depth gauges were returned to their slots, and the guillotine gate removed. About fifteen minutes interval was necessary between experiments to allow the water level to settle. Then any slight adjustments necessary were made to the zero positions of the electrical apparatus, and the rotary switch was set to the first depth gauge.

The valves were checked to ensure that the water entered the channel and not the measuring tank. The control valve was set to give a relatively small flow, and the slide valve was then opened as rapidly as possible. The surge appeared at the entry to the channel almost instantaneously, and moved downstream. As it approached the first gauge, the penrecorder motor was started, and thus the profile of the wave as it passed the gauge was recorded. As the head of the surge approached the second depth gauge, the output from this was switched to the recorder

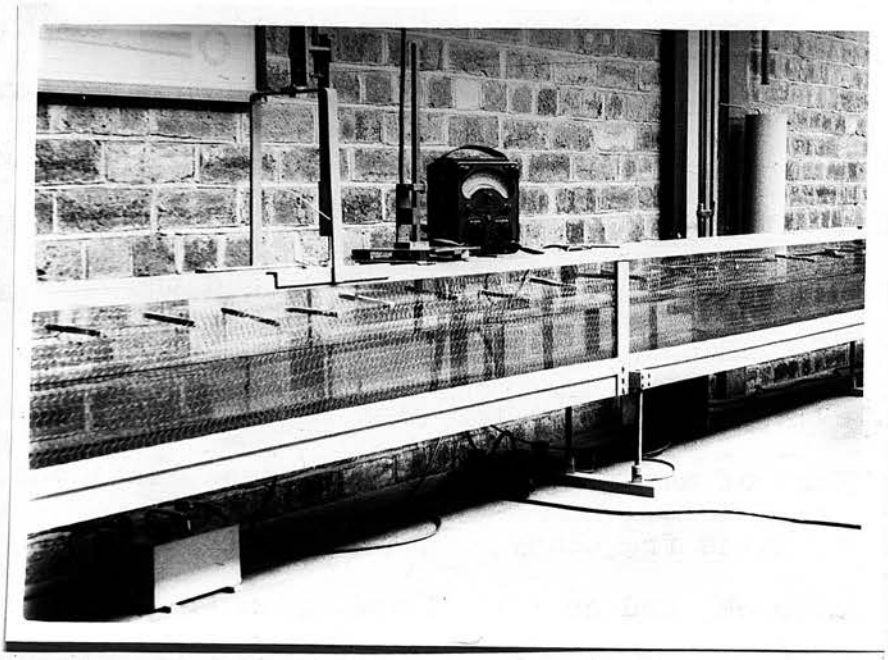

Plate. 6. Channel lined with netting.

by means of the rotary switch, and similarly at the third, fourth, fifth and sixth depth gauges. It was found, however, that to get a reasonably lengthy record at each gauge only three gauges could be employed.

When the surge reached the end of the channel the recorder motor was stopped, and the rotary switch reset to the first gauge in readiness for the next experiment. The manometer difference in level was measured, and then the control valve opened a little more to give a suitable change in the manometer readings. The slide valve was shut, and the water level allowed to settle. Each of these experiments was entitled a 'Run'. The relevant information for each run - day, date, time, number, temperature of water, manometer difference in level, initial depth of water, mains frequency, and the amplification used were recorded in a note book, and on the record taken from the penrecorder.

The discharge was increased for each run, until the first wave was observed to break. Then these runs constituted a series. With the initial depth, and the amplification suitably changed, a further series of runs was made after calibrating the depth gauges. This was accomplished for initial depths of 2, 3, 4, and 6 inches with the smooth channel, and for depths of 2, 3, and 4 inches for the rough,netted channel. The 3 and 4 inch smooth channel runs were also continued for larger discharges after the first wave had broken to ascertain the effect on wave length, crest height, velocity, etc. of waves breaking with increasing force.

Calibration graphs were then plotted for each gauge in each series of runs. Hence the depth at each crest and valley could be determined. This information was then tabulated.

CHAPTER 7.

DETAILS OF EXPERIMENTS.

When the channel, the depth gauges, and the electrical apparatus had been completed and checked, the experimental procedure was as follows.

(1) The calibration of the manometer, which has been already described.

(2) The calibration of the pinion on the weir gate to give settings for predetermined depths.

(3) Checking that raising and lowering the gauges was equivalent to raising and lowering the water level. The water level was allowed either to rise or fall steadily, and at the instant of contact with a point gauge, with the level rising a break was made in the graphical record of the penrecorder by rapidly switching the recorder off and on. With the level falling, the instant of switching was when the pointer just disappeared when observing across the underside of the water surface. Then the gauge was lowered and raised an amount equal to the previous rise and fall in the water level, with a pause at similar intervals. The penrecords of both sets of observations were compared, and were found to be almost identical. Some very slight differences were noted, but further tests showed that this was due to slight drifts in the electrical signals which were naturally more marked when lowering or raising the water level, as this took considerably longer than raising or lowering the gauges. The coincidence of the results was eminently satisfactory.

(4) Determining the friction coefficient (C) for the smooth and rough channel.

Two point gauges were set up at a known distance apart, and at a known distance from the depth gauges. A quantity of water was run into the channel, practically filling it, and when the level had settled to a steady value, the readings on the point gauges were taken for this depth. This gave a fixed level between the two point gauges. The reading at the bed was also taken for both point gauges.

The weir gate was then lowered a little, and a small constant discharge was injected into the channel. When conditions had reached equilibrium the readings on the two point gauges were made. The weir gate was lowered somewhat, and again with the same discharge the levels were read, when the flow had settled to a steady state. This was repeated until the weir gate was fully open. Hence the slope of the water surface for this discharge could be determined at any depth, at any of the depth gauges. This was repeated for different discharges, for both the smooth channel, and when it was lined with netting. Thus for a given depth, discharge, and position in the channel, the surface slope could be calculated, and this value inserted in equation (83) gave the value of the friction coefficient (C) for these conditions. The values could then be inter-polated from one discharge to another. C was then plotted against "r" $(= \frac{Q}{l}_H . m(\frac{1}{y_o} - \frac{1}{y}) = R_N r)$. Fig. 4 In addition Y was plotted against $\frac{Q_H}{l} . m (\frac{1}{y_o} - \frac{1}{y}) = r$. Then for a known Y, r could be determined, and hence C.

One point to be considered was that the point gauges had to be placed so that they were not affected by the initial unstable conditions, or the draw down curve, in the channel.

(5) Determination of the profiles of undular surges.

At each initial depth a number of runs were made, and each of these groups of runs was called a Series. These are tabulated in Fig.8

Series 1 - 4 are at different initial depths in the smooth channel (y_o = 2", 3", 4", and 6"). The surge profiles are recorded at depth gauges 2, 3, and 5.

Series 5 - 7 are runs at various initial depths with the channel lined with wire netting (y_o = 2", 3", and 4"). The profiles were recorded at gauges 2, 3, and 5.

Series 8 - 14 are 'Velocity Runs', used to determine the velocity of the head of the surge at any position in the channel, for the conditions in Series 1 - 7. Hence six depth gauges were employed.

Series 15 is composed of runs used for comparison with the photographic records of the surge profiles in the smooth channel, (y_o = 2", 3", and 4"). These were taken at one particular gauge for each run.

Series 16 - 22 are the runs made for the purpose of checking the calculated profiles, and again were recorded at one particular gauge for each run. A profile was not calculated for an initial depth of 6", as it was seen from Series 4 that the waves in the surge train were far from fully developed even when they had reached gauge 5, and hence no comparison was possible between the pen record and a calculated profile.

Series	y ins.	Runs	Use of Runs	Mean Water Temp. °C	Channel Surface	Remarks
1	2	1 - 19	Determination of surge profiles for varying initial discharges.	11.8	Smooth	Calibrated 3 gauges employed.
2	3	20 - 39		11.1		
3	4	40 - 58		13.2		
4	6	59 - 69		17.2		
5	2	70 - 80		10.9	Rough	
6	3	81 - 92		11.3		
7	4	93 - 104		11.5		
8	2	105 - 116	Determination of velocity of head of surge at any point in the channel.	11.5	Smooth	Not Calibrated 6 gauges employed.
9	3	117 - 128		9.6		
10	4	129 - 142		12.2		
11	6	143 - 154		12.3		
12	2	155 - 165		13.1	Rough	
13	3	166 - 177		13.3		
14	4	178 - 190		12.8		
15	2,3 4	191 - 202	Verify recorder results.	14.3	Smooth	Calibrated
16	2	203 - 206	To check accuracy of calculated surge profiles	17.2	Smooth	Calibrated 3 gauges used.
17	3	207 - 209		17.3		
18	4	209 - 211		16.8		
19	6	212 - 214		17.5		
20	2	215 - 217		18.0	Rough	
21	3	218 - 221		17.2		
22	4	222 - 224		17.4		
23	4	225 - 230	Effect of time of valve opening	17.1	Smooth	Calibrated

FIG. 8

Series 23 comprises 6 runs at an initial depth of 4" and a constant discharge. The time of opening of the inlet valve was varied from instantaneous to approximately 4 secs. to see what effect, if any, this had on the surge profile. The results of these runs are discussed in the next Chapter.

Certain of the results obtained from Series 1 - 7 are tabulated in Figures 17 to 20. Many more values are available, since the crest and, valley depths, and the wave lenghths have been recorded of the first three waves at gauge 2, the first four waves at gauge 3, and the first six waves at gauge 5. These are then available should they be required at a later date.

The final results of the velocity runs in Series 8 - 14 are shown in graphical form in Fig. 13 as velocities at gauges 2, 3, and 5 plotted against initial discharge.

No numerical results are given for any of the Series 15 - 22. Also the series used for photographic comparison if reproduced to the same scale as in Figs. 22-24 , show no discernible difference between the recorded and photographed profiles, and hence are not included. The graphical results of Series 16 - 22 are presented in Figs. 22 to 24 showing the differences between the calculated and recorded profiles.

Only 230 runs are indicated in these records, but many more were made. In each of the Series only a selection of the runs are given, as the results of the full number would occupy an inordinate amount of space. Further Series were also completed with initial depths of 1, 1½, 2½, and 3½ ins, but again it was thought that the runs selected would present sufficient information, although the remainder would always be available.

Finally a number of runs were made, after the graphical results had been started, in order that various points on the curves (i.e. wave lengths at low discharge, or depths after breaking had occurred) might be more definitely ascertained. The total number of calibrated and checked runs was 517.

The work was not carried out in the order shown in Fig. 8, which is presented in this manner for ease of interpretation. The first runs made, were Series 15 to check the accuracy of the recorder with photographs of runs in the smooth channel. The grid did not appear on the photographs when the wire netting was in place, and hence no comparison was available for these runs. Then the determination of the friction coefficient and the various runs to determine the profiles and velocities were made, first with the smooth channel, and then with it lined with wire netting. The netting was retained for the runs made to check the calculations and to check isolated results. Finally with the smooth channel again the remainder of the runs were made.

Fig. 9 shows a recorded run from the penrecorder. This is not a specific run, but is included to show the type of results obtained. It is of little use as a visual record since the amplification of the record at each gauge is different, although it does give an idea of the change of shape of the profile. An attempt was made to make the output of the Southern instrument panels connected to the gauges, equal to each other for the same input, but without success. This would have then given a direct visual impression of the growth or decay of the waves.

The results of these experiments are given in graphical form, and are commented on, in the next Chapter.

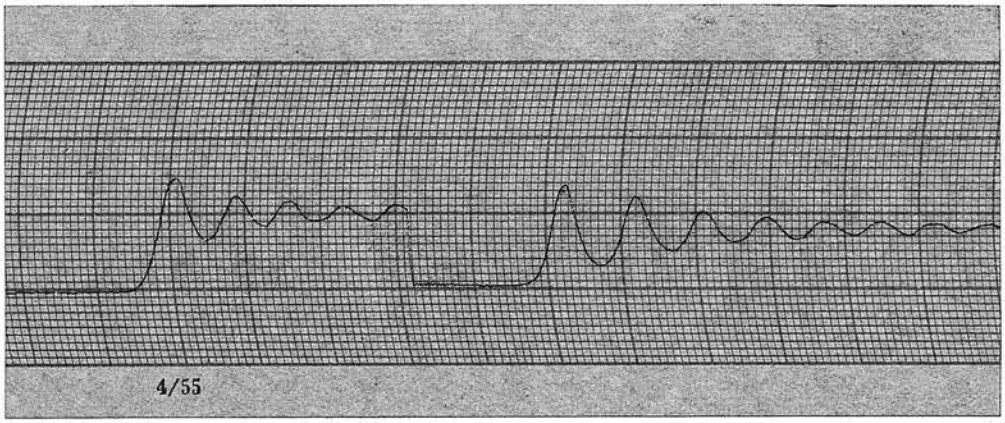

gauge 1 gauge 2

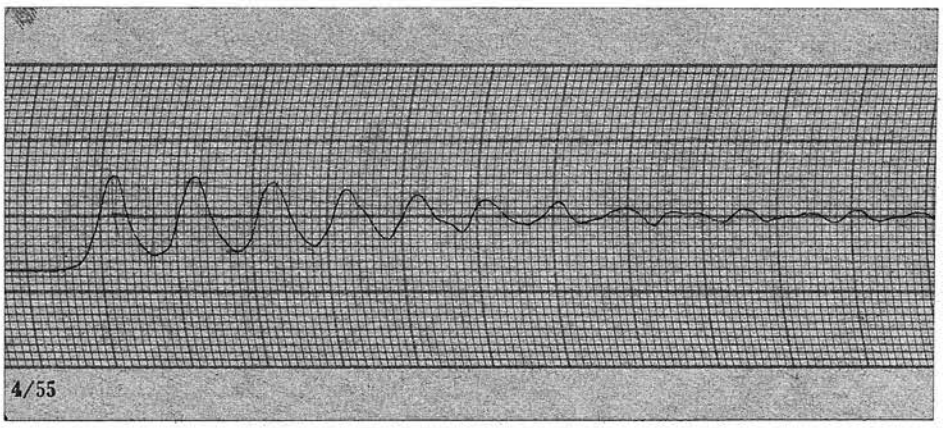

gauge 3

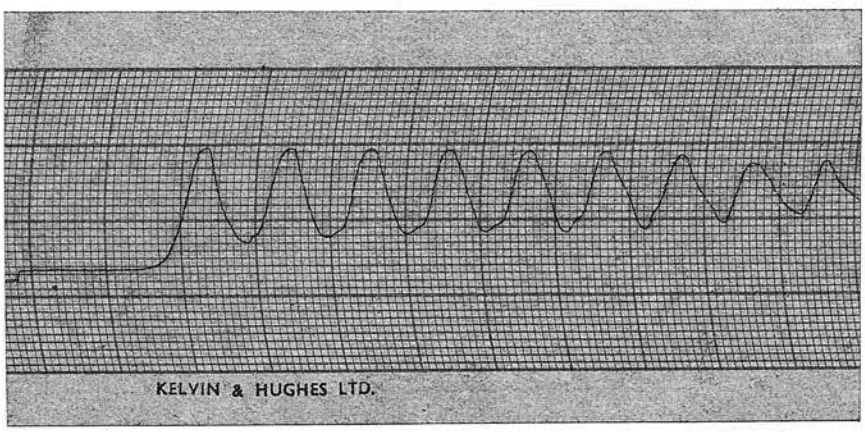

gauge 5

Fig. 9. A recorded Run

(5) Determination of the Wave Lengths of the undulations forming an undular surge.

Having determined the depth of water at the crest and valley of an undulation, the next problem was to determine the wave length. This required an accurate knowledge of the apparent velocity of the undulation at the depth gauge. To determine this velocity, several series of 'Velocity Runs' were carried out. The previous runs were of little value for this purpose, since only three depth gauges had been employed in order that a record of reasonable length could be obtained at each. In the velocity runs, six gauges were employed, and a number of runs made at each depth, and with the smooth and rough surfaces to the channel.

From the record, the distance in millimetres between the first crest at each depth gauge was measured. From this the time taken for the surge to travel from one gauge to the next could be calculated. Knowing the distance between the gauges, the mean velocity could then be found. These velocities were then plotted against distances along the channel at the mid distance between the gauges. From these further graphs could be plotted of the velocity at any gauge against manometer difference in level, or against discharge, for particular initial depths. Fig 13

Therefore, for any particular run, the velocity at a gauge could be found from the curves of velocity against discharge. Then having measured the distance between successive crests on the record in millimetres, the distance between the crests could be calculated. Strictly speaking this would only be accurate for at the most, the first wave length, since the velocity would vary but this variation is sufficiently small to be neglected over the first few undulations.

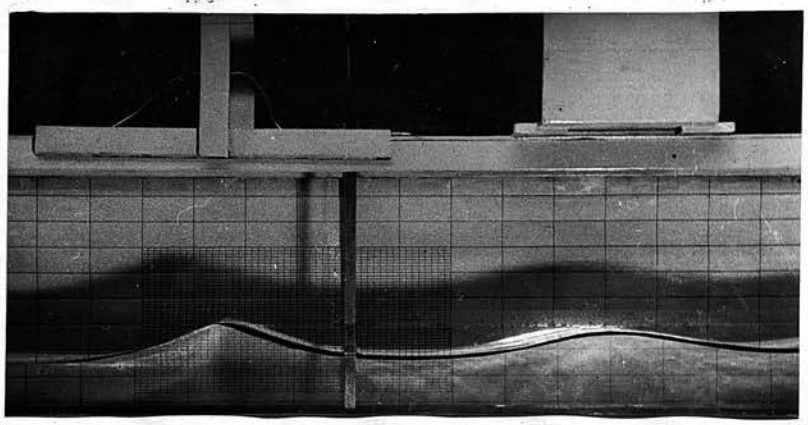

Plate 7. Head of Undular Surge. y_o=2". gauge 2

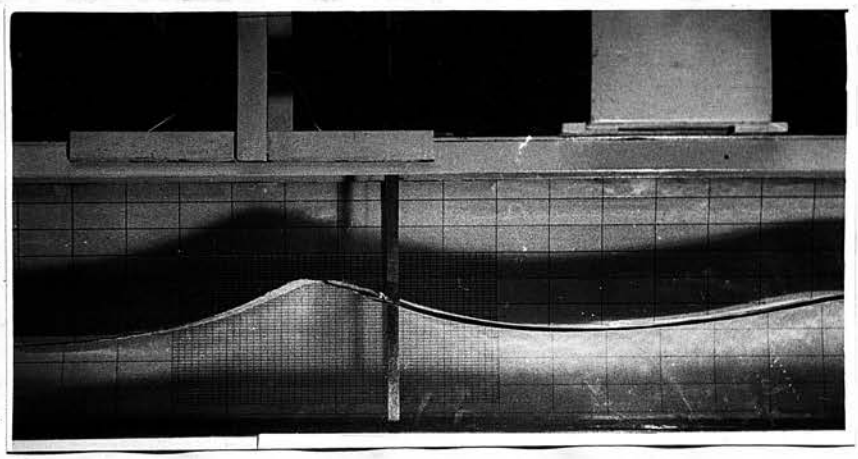

Plate 8. Head of Undular Surge. y_o=3". gauge 2

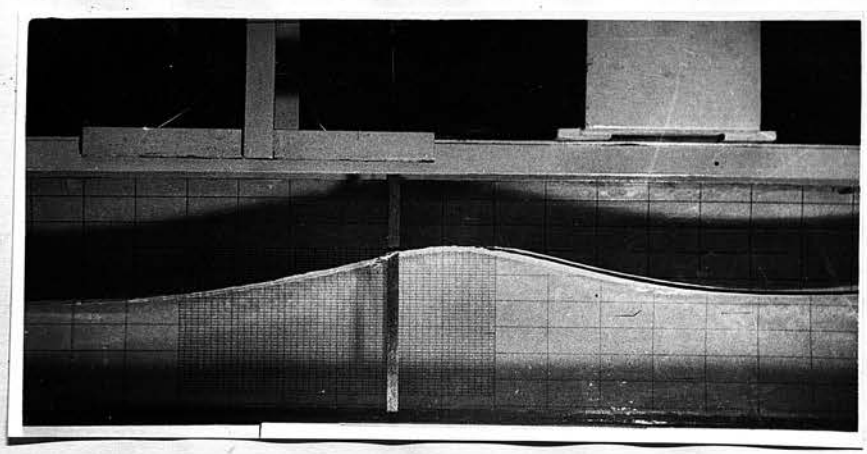

Plate 9. Head of Undular Surge. y_o=4". gauge 2.

(6) Photographic Comparison.

A further series of runs was made at initial depths of 2, 3, and 4 ins. in the smooth channel, and the record was taken at only one gauge. From the calibration curve and the curves of velocity against discharge, the profiles could be reproduced to scale. Further as each surge passed the depth gauge a photograph was taken. From the grid on the paper at the back of the channel a reasonably accurate record of the profile of the surge could be taken from the photograph. The two sets of records were compared, and inall cases were almost identical, showing that the recorder gave a true record of the phenomena.

To obtain the best results the photographs were taken at night. The camera shutter was held open, and with the surge at the probe, the flash was triggered. The shutter was then allowed to close again. From negatives, enlargements were taken (PLATE I.) and the wave profile could be plotted. Alternatively the true to scale profile from the recorder could be plotted on the photograph.

(7) Check runs.

The profiles calculated theoretically were finally checked by a series of carefully controlled runs at the correct discharge. The comparisons are shown in Figs. 22-24. These runs were performed exactly as the previous ones, except that an even longer interval was allowed, to ensure an absolutely horizontal water surface at the correct depth, was obtained. The discharge had also to be set very carefully to that calculated, and this necessitated a careful setting of the difference in level of the manometer readings. The particular gauge at which the

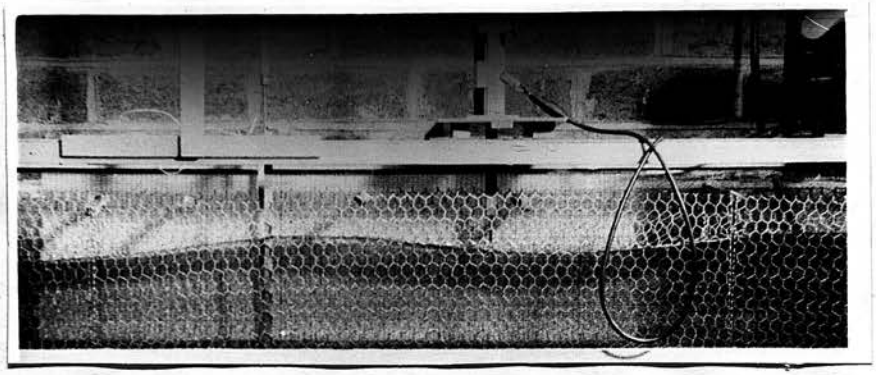

Plate.10. Head of Undular Surge. $y_o = 4''$. gauge 5. channel lined with netting. N.B. compare with plate 1

profile was to be recorded (the one nearest to the outlet) was calibrated, and the run carried out as already described.

(7) Notes.

(a) It should be realised that the profile shown by the pen recorder is in fact not identical with the photographed record, since the depth gauge records a variation with time at one point, whereas the camera record is the variation of water level with distance at one instant. Since the differences are obviously small, however, the two are regarded experimentally as identical, and probably the various errors introduced by the experimental technique are greater than these differences.

(b) The Meniscus effect is very small, but its effect can be seen when recording surges of a small height at a large amplification. The effect is shown exaggeratedly in Fig. 10.. However, the calibrated runs could not be recorded at these large amplifications, since it was found that the penrecorder was not reliable beyond about the middle two fifths of the paper. Hence to obtain the maximum change in depth (even with the lower initial depths) of a series of runs within these limits on the paper, the amplification had to be relatively small. Thus the meniscus effect was found to be of the same order of the errors in measurement of any depth, and could be neglected.

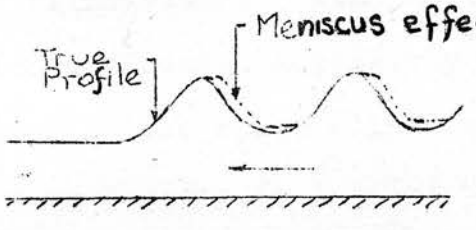

FIG.10.

(c) Distances of gauges from inlet (feet)

gauge	1	2	3	4	5	6
Distance	3.90	9.95	22.15	34.3	40.25	46.00

CHAPTER 8.

Results of the Experiments and Calculations.

Experiments

Figs. 11 to 21 show some of the more important results obtained from the experiments. It was not thought advisable to include any further results, though many more were available, since it was hoped that those presented would provide a sufficiency of information. The results of Series 23 are given at the end of the Chapter. This series was undertaken to ascertain the effect of the time of opening of the main valve on the shape of the wave profile.

Fig. 11 shows the variation in height of the first crest of the surge, as the discharge is increased, until the first wave just breaks at some point in the channel (indicated by 'Br.'). Apart from a slight curve at low discharges, the resulting line is apparently straight under all conditions. This shows that discounting the effects of very low discharges, there exists a linear relationship between crest height and discharge, at any position in the channel, up to the discharge required to cause breaking of the first wave. It would appear further from inspection, that the greater the initial depth, the smaller becomes the effect of low discharges on linearity. Also in the smooth channel the slope of this line decreases, noticeably with increase in initial depth, whilst with the rough (lined with netting) channel the change in slope with changes in initial depth is small. This is to be expected, since it shows that in the smooth channel the surge can build up to breaking more quickly than in the rough channel, since less energy is dissipated in friction. This

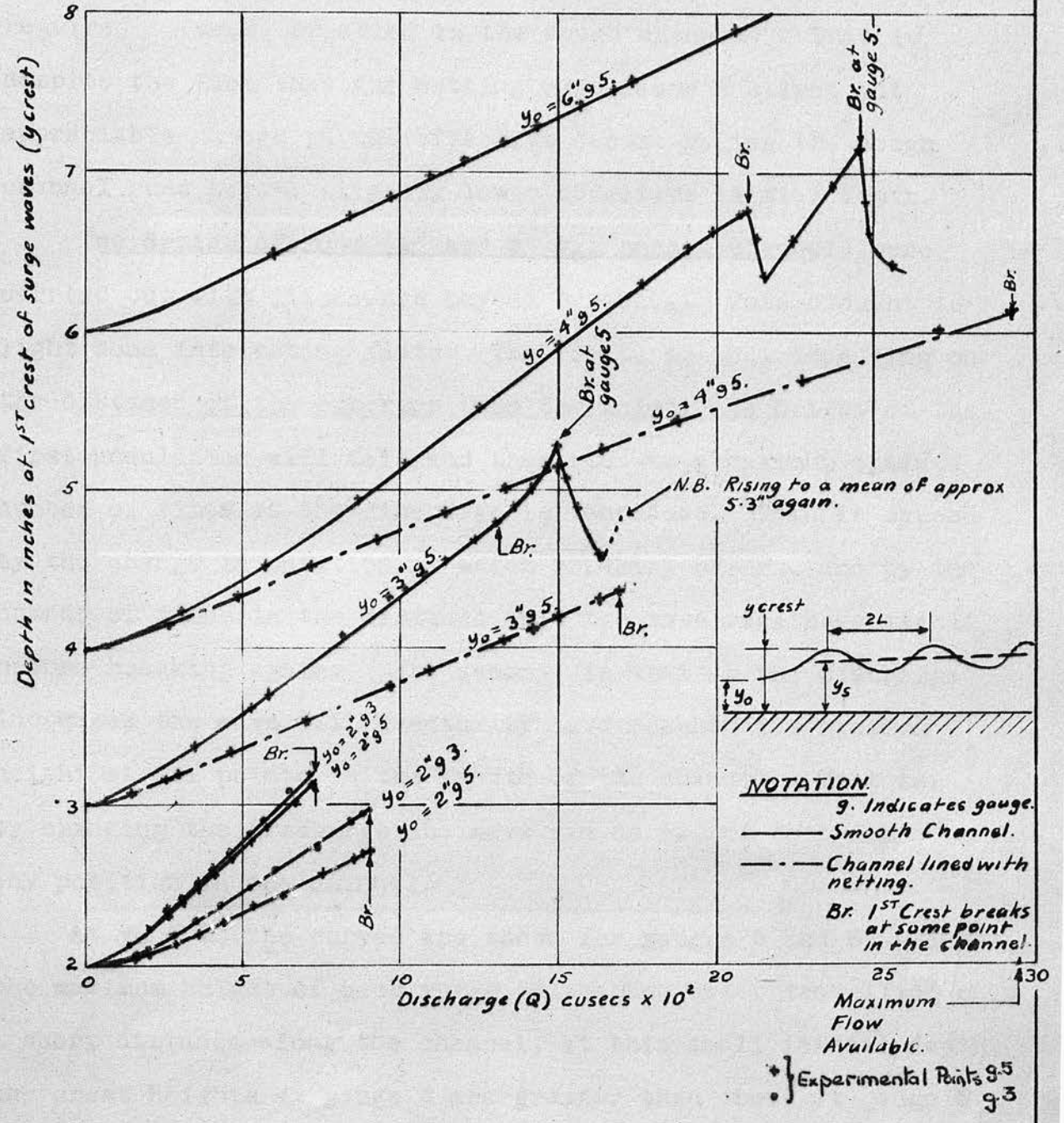

FIG. 11 DISCHARGE (Q) TO DEPTH AT 1ST CREST (y crest) WITH DIFFERENT INITIAL DEPTHS (y_0)

is also evident from the steeper slope of the lines relating to the smooth channel, and from the greatly increased quantity required to cause breaking in the rough channel. This is despite the fact that the netting must cause a slight but appreciable change in the effective depth, making the rough channel runs have a slightly lower effective initial depth.

Two Series of runs (4" and 3" y_o, smooth channel) were carried out with discharges beyond breaking. This brought to light some interesting facts. The first, is that depending on the distance of the observer from the inlet, the height of the first undulation will fall, and then rise to a maximum again a number of times as the discharge is increased. This is caused by the change in position at which breaking occurs, and by the number of times in the distance, that the wave regathers itself before breaking again. The second, is that as the discharge increases the wave will eventually have reached its maximum height at all points in the length of the channel. That is, by changing the discharge the wave can be caused to break at any position in the channel.

At y_o = 2" the curves are shown for gauges 3 and 5. Since the maximum height of each surge is reached after travelling only a short distance along the channel, at this small initial depth, the crest heights at gauge 3 are greater than those at gauge 5.

Fig. 12. These curves show the change in depth of the first valley of the surge wave for different discharges, at one position in the channel. The curve at low discharge is much more pronounced than that of the crest heights, and does not appear to change in shape with increases in initial depth. Beyond this curved part of

NOTATION

——— Smooth channel.

—·— Channel lined with netting.

Br. 1ST Crest break at some point in the channel.

g. Indicates gauge.

• g.3
+ g.5 } Expermental Points.

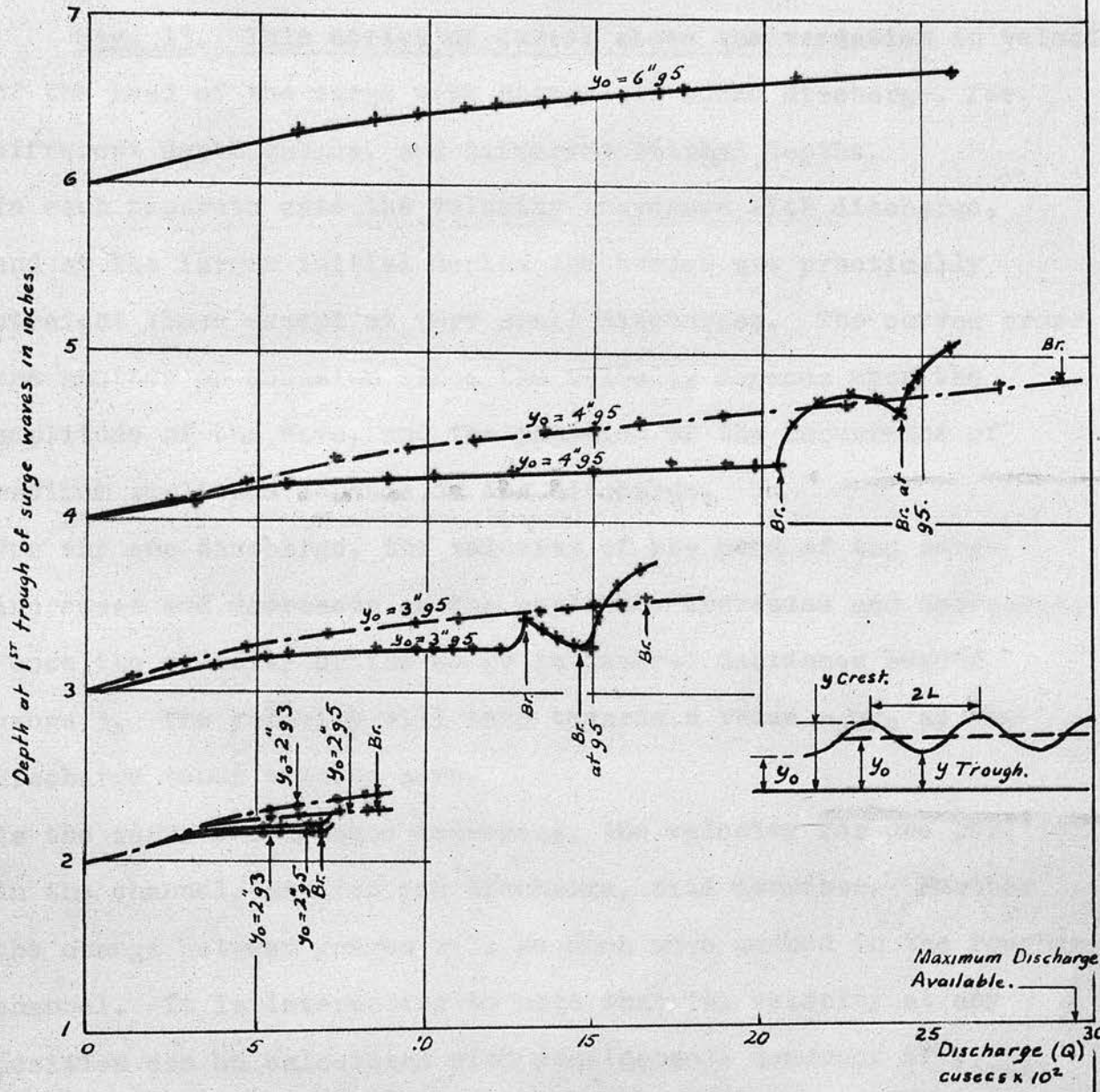

FIG. 12

DISCHARGE (Q) TO DEPTH AT TROUGH 1 WITH DIFFERENT INITIAL DEPTHS (y_0)

the graph, the depth increases very slowly, but steadily with discharge until the first wave breaks. Then again in the intermediate region of the breaking undular surges, the depth changes rapidly with discharge, until finally it approaches the crest height, when the steep fronted surge occurs.

Fig. 13. This series of curves shows the variation in velocity of the head of the surge with changes in added discharge, for different depth gauges, and different initial depths.
In each separate case the velocity increases with discharge, and at the larger initial depths the curves are practically straight lines except at very small discharges. The curves cross one another on occasion since the velocity depends upon the amplitude of the wave, and the position of the occurrence of maximum amplitude depends on the discharge.
For any one discharge, the velocity of the head of the surge increases and decreases as the amplitude increases and decreases. Hence the velocity of the surge in general decreases beyond gauge 3. The velocity will tend towards a value $=\sqrt{gy_o}$ as the discharge tends towards zero.
As the surface roughness increases, the velocity for one position in the channel, and for one discharge, will decrease. Further the change between gauges will be much more marked in the rougher channel. It is interesting to note that the velocity at any position can be calculated with considerable accuracy if y_{crest} is known, from equation 3, due to Scott Russell. $V = \sqrt{gy}_{crest}$

FIG. 13. MEAN VELOCITY (V) OF HEAD OF SURGE PLOTTED AGAINST INITIAL DISCHARGE (Q) AT DEPTH GAUGES 2,3,&5, FOR VARIOUS INITIAL DEPTHS.

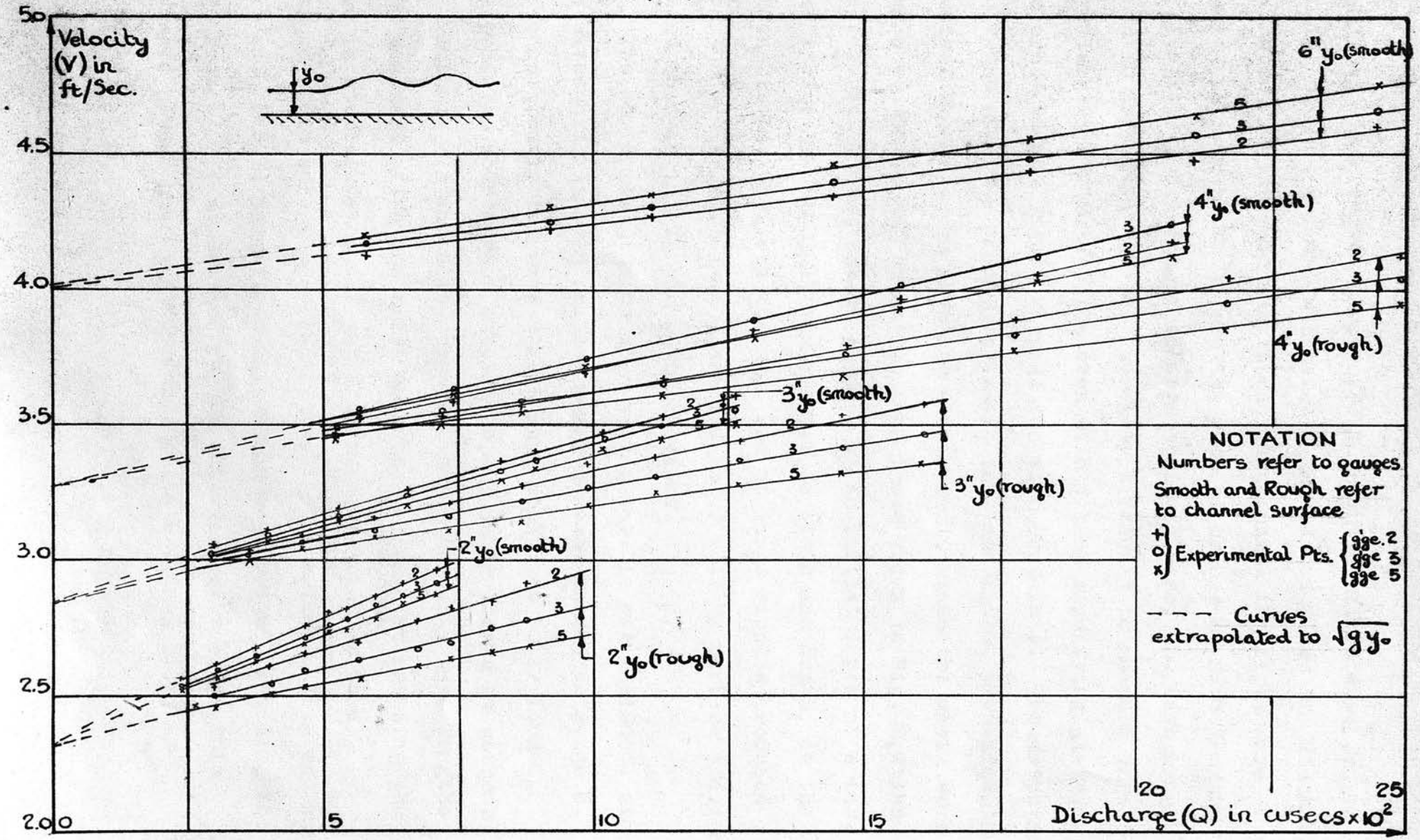

Fig. 14. These curves show the change in the first wave length plotted against initial discharge. In all cases, as the discharge increases, so the wave length decreases until the first wave breaks. At small discharges the rate of change of wave length is greatest, and as the discharge tends to zero, the wave length tends to infinity. It was extremely difficult to measure these wave lengths accurately, as even with a hand magnifying glass, the crest was difficult to position with certainty. The waves in the rough surfaced channel at small initial depths, presented the greatest obstacles to accurate measurement, since the waves were rarely as smooth and symmetrical as those shown in Fig. 9, which are recorded in the smooth channel at an initial depth of 4 ins. This is due to slight irregularities in width and depth, as the netting is not entirely uniform, and to large ripples produced when the water level falls, and the water held by surface tension behind the netting is suddenly released.

The appropriate curve when y_o = 6 ins. is not included, since the waves had not even reached their maximum height at gauge 5, and consequently the wave shapes were still not fully formed. The profiles when y_o = 4 ins. are barely fully formed at gauge 5.

With y_o = 3 and 4 ins. in the smooth channel, wave lengths were measured after the first wave had broken. At breaking the wave length fell abruptly and then rapidly built up to a maximum again before decreasing steadily as before. This sudden fall and rise in the wave length would be repeated each time the wave broke. It would also appear that the curve after this downward plunge and recovery follows its original path, but extended.

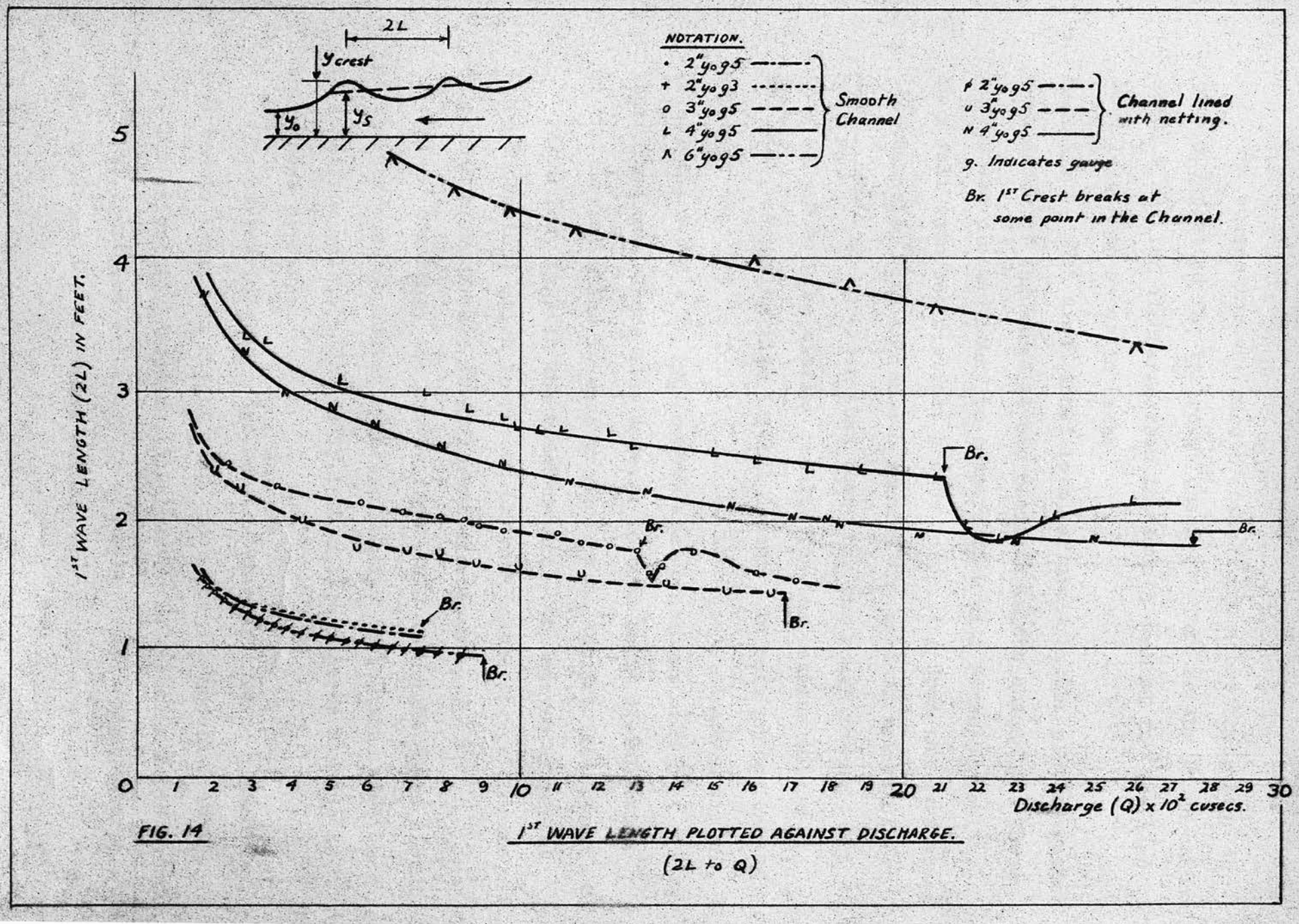

FIG. 14

1st WAVE LENGTH PLOTTED AGAINST DISCHARGE.

(2L to Q)

The curves for the smooth channel are above those (for the same y_o) plotted for the rough channel. That is the rough channel needs a smaller discharge than the smooth channel for the same wave length to occur in each.

Fig. 15. Non dimensional form, of crest height plotted against mean depth of the surge at one position in the channel. These curves are plotted thus, to compare them with Favre's results. They fall into two distinct groups, depending upon the surface of the channel. With the smooth channel the maximum values of $\frac{y_{crest} - y_o}{y_s - y_o}$ are greater than those for the rough channel, but they appear to give similar results for the maximum values of $\frac{y_s - y_o}{y_o}$, comparing like initial depths. In both groups the apparent tendency is for the curves to reach a steady maximum, (i.e.) the 3 and 4 in. (y_o) curves are coincident over part of their lengths. There also appears to be a point of inflexion on the curves, which is more pronounced as the friction increases.

At 2 ins. (y_o) in the rough channel, the curves at gauges 3 and 5 overlap, which is presumably due to the change in rate of growth of amplitude at different discharges.

After breaking, the curves first fall in height - the amount of the decrease depending upon the initial depth, then rise again to a maximum value, and finally fall off to a curve similar to that shown by Favre.

The curves for the rough surface channel tend to a much more constant maximum height than those for the smooth channel.

The value of 'y_s' used in these curves is the mean depth between the first crest and valley up to breaking, and is then interpolated after breaking between these results and the theoretical value of

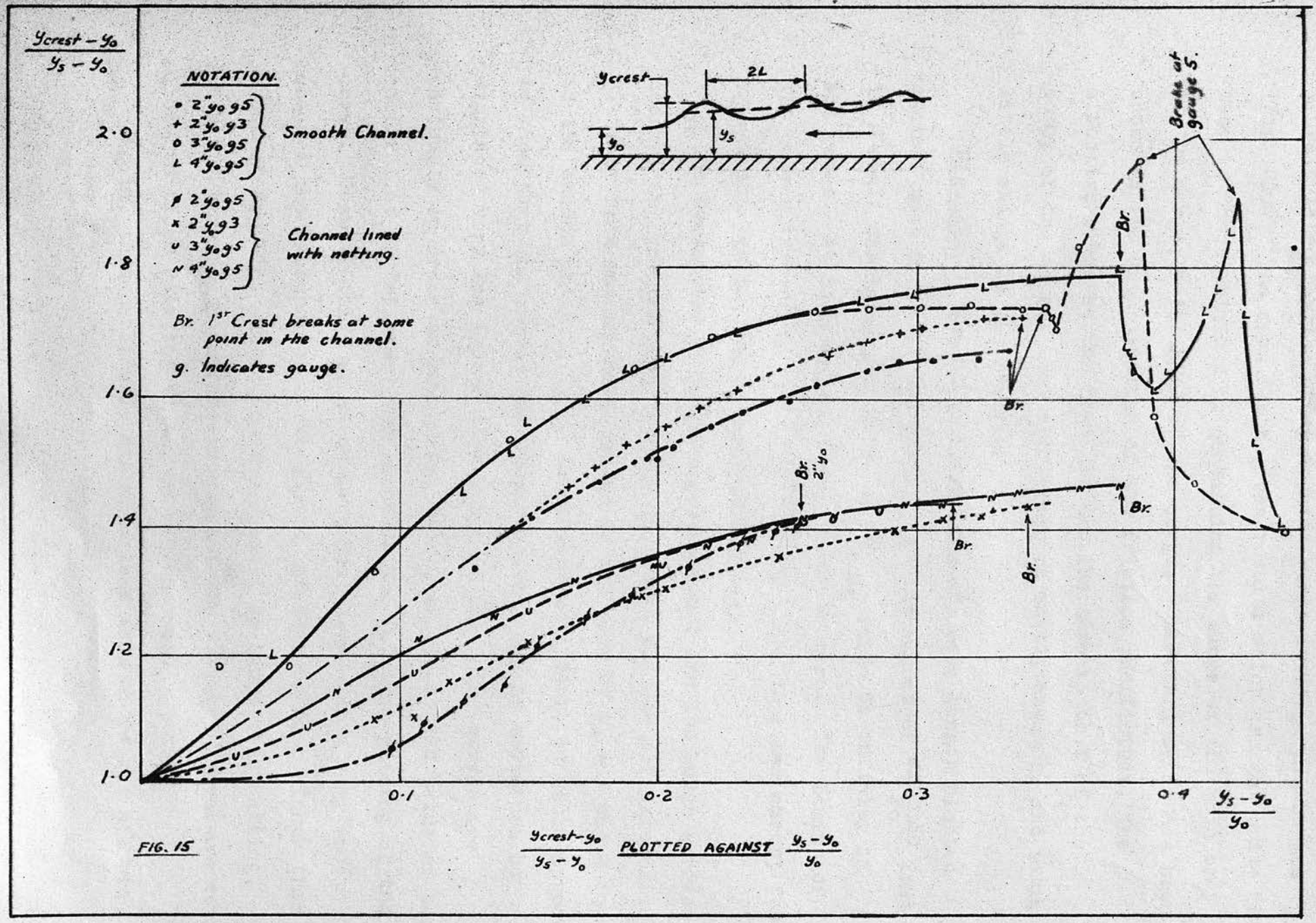

FIG. 15

$\frac{y_{crest} - y_o}{y_s - y_o}$ PLOTTED AGAINST $\frac{y_s - y_o}{y_o}$

y_s calculated for the steep fronted surge at large discharges (Fig. 21). The mean depth gives results which are not quite the same as those obtained by continuing the slope of the main body of the surge, to the head of the surge. However, as it has been shown in the determination of the friction coefficient, the effective slope at the head, is not the same as that of the body of the surge. The difference is small, however, and makes little change in the results.

Fig. 16. Non dimensional form of, wave length plotted against mean depth of the surge. At low values of $\frac{y_s - y_o}{y_o}$ that is at small discharges, the value of $\frac{2L}{y_s - y_o}$ tends to infinity in all cases. At high values, $\frac{2L}{y_s - y_o}$ tends to zero. The limits of the curves, imposed by breaking, are very close together except for y_o = 2 ins. in the rough surfaced channel.

The curves for both the smooth channel and the rough surfaced channel are grouped very closely together, but are definite curves, distinct from one another, except in the case of y_o = 3 and 4 ins. in the smooth channel. This is of interest, since it would appear to show that the curves for deeper initial depths would not be displaced very far beyond this compound one. The curves are obviously in order of roughness, (i.e.) the lower the value of the coefficient of friction, the lower is the relative placing of the curve. Despite this, it is obvious that even with a very smooth channel the appropriate curve should not be very much higher than those of Fig. 16, since when the channel is lined with netting, it has a very rough surface indeed, and yet the relative curves are very close to those relating to the smooth channel.

Again, this particular dimensionless form of result has been

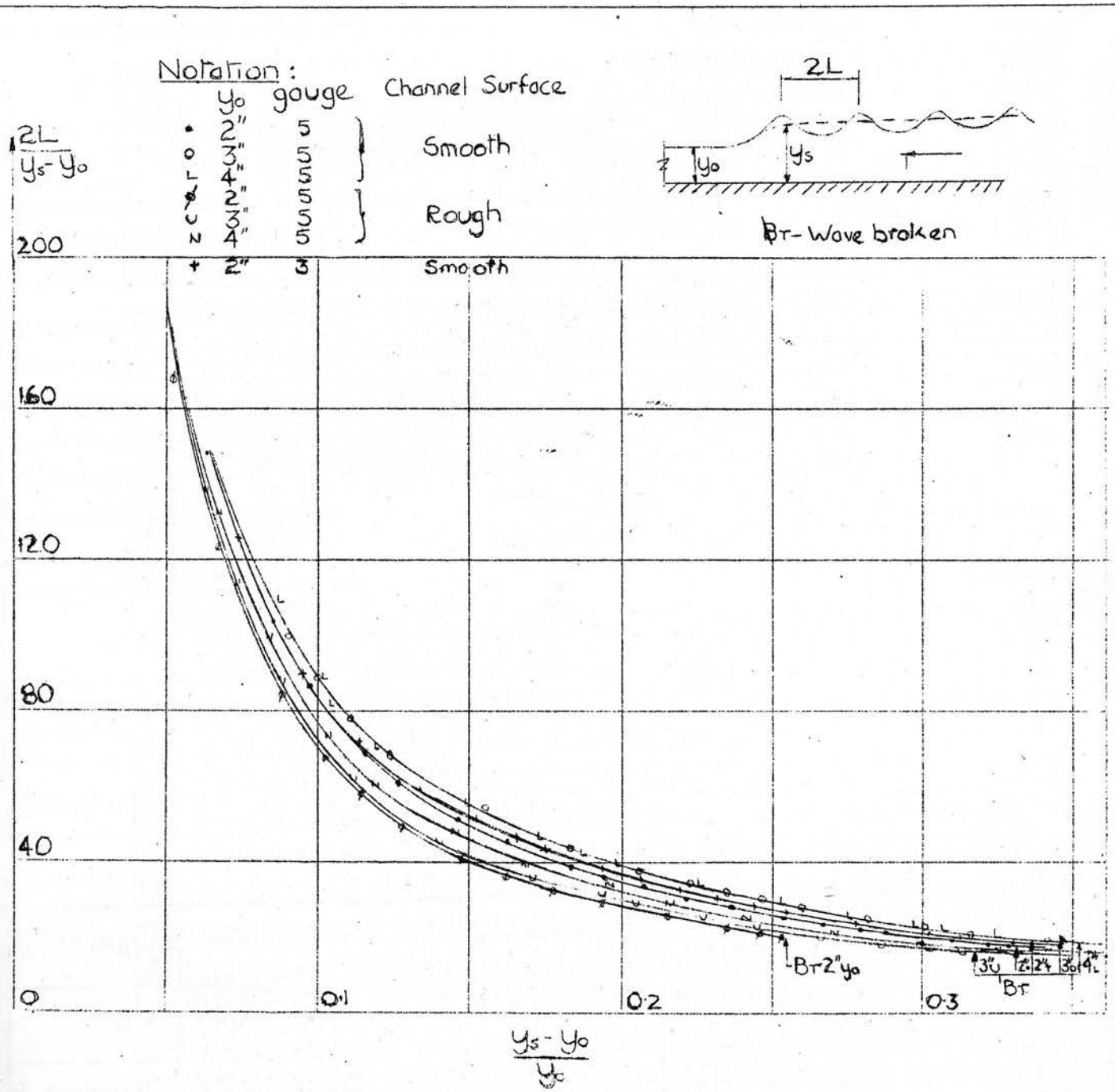

Fig. 16 $\frac{2L}{y_s - y_o}$ plotted against $\frac{y_s - y_o}{y_o}$

	Run	Discharge Q cusecs	Depth Gauge 2				Depth Gauge 3					Depth Gauge 5						Remarks.
			Crest 1	Valley 1		Vel.	Crest 1	Valley 1	Crest 2		Vel	Crest 1	Valley 1	Crest 2	$y_s - y_o$		Vel.	
Series 1 y_{o1} = 2" smooth channel	1	0.0071	0.07	0.06		2.43	0.06	0.05	0.05		2.41	0.05	0.03	0.04	0.04		2.36	
	2	0.0176	0.20	0.13	1.423	2.47	0.19	0.11	0.17	1.560	2.48	0.18	0.08	0.18	0.13	1.575	2.42	
	3	0.0229	0.30	0.16	1.367	2.51	0.28	0.14	0.27	1.430	2.52	0.26	0.14	0.26	0.20	1.420	2.50	
	4	0.0292	0.44	0.19	1.335	2.57	0.40	0.17	0.40	1.360	2.57	0.38	0.17	0.39	0.28	1.346	2.56	
	5	0.0335	0.53	0.20	1.323	2.61	0.49	0.18	0.51	1.330	2.60	0.45	0.18	0.46	0.31	1.320	2.59	
	6	0.0363	0.60	0.20	1.293	2.63	0.55	0.18	0.57	1.317	2.63	0.50	0.18	0.51	0.34	1.300	2.62	
	7	0.0396	0.66	0.20	1.271	2.65	0.61	0.18	0.63	1.300	2.65	0.56	0.19	0.57	0.37	1.280	2.64	
	8	0.0423	0.72	0.21	1.243	2.70	0.66	0.18	0.69	1.287	2.68	0.61	0.19	0.62	0.40	1.260	2.66	
	9	0.0460	0.80	0.21	1.228	2.73	0.75	0.18	0.79	1.270	2.71	0.67	0.19	0.68	0.43	1.240	2.68	
	10	0.0489	0.86	0.21	1.216	2.75	0.79	0.19	0.82	1.257	2.73	0.72	0.20	0.73	0.46	1.220	2.71	
	11	0.0521	0.93	0.22	1.197	2.78	0.85	0.18	0.92	1.240	2.76	0.79	0.20	0.80	0.49	1.200	2.74	
	12	0.0555	1.00	0.22	1.189	2.82	0.92	0.18	0.99	1.220	2.80	0.85	0.20	0.86	0.52	1.185	2.76	
	13	0.0591	1.08	0.22	1.185	2.85	0.99	0.18	1.09	1.205	2.82	0.92	0.20	0.94	0.56	1.165	2.79	
	14	0.0623	1.15	0.23	1.180	2.86	1.05	0.18	1.13	1.190	2.84	0.97	0.20	0.99	0.58	1.150	2.80	
	15	0.065	1.20	0.23	1.176	2.89	1.10	0.18	1.18	1.175	2.85	1.02	0.20	1.04	0.61	1.135	2.81	
	16	0.0662	1.23	0.23	1.171	2.92	1.13	0.18	1.23	1.170	2.88	1.04	0.20	1.06	0.62	1.130	2.83	
	17	0.0707	1.32	0.24	1.165	2.95	1.21	0.18	1.29	1.150	2.91	1.12	0.21	1.14	0.66	1.115	2.85	
	18	0.0734	1.41	0.24	1.159	2.98	1.26	0.19	1.36	1.140	2.94	1.18	0.21	1.20	0.69	1.105	2.88	
	19	0.0751	1.50	0.24	1.158	3.00	1.18	0.23	1.25	0.935	2.88	1.20	0.21	1.25	0.70	1.155	2.89	Breaking between Gauges 2 and 3
Series 2 y_{o1} = 3" smooth channel	20	0.036	0.38	0.18	2.30	2.99	0.43	0.20	0.40	2.30	3.05	0.36	0.17	0.35	0.27	2.28	2.97	
	21	0.055	0.71	0.28	1.96	3.13	0.75	0.21	0.71	2.15	3.18	0.63	0.20	0.62	0.415	2.16	3.12	
	22	0.060	1.20	0.27	1.88	3.17	1.09	0.21	0.99	2.12	3.21	0.92	0.20	0.92	0.56	2.13	3.155	
	23	0.075	1.19	0.35	1.81	3.306	1.26	0.21	1.19	2.03	3.34	1.10	0.21	1.09	0.655	2.02	3.28	
	24	0.092	1.41	0.36	1.71	3.390	1.48	0.21	1.45	1.96	3.42	1.25	0.22	1.26	0.735	1.95	3.34	
	25	0.093	1.49	0.36	1.70	3.391	1.50	0.23	1.47	1.94	3.43	1.27	0.21	1.29	0.74	1.95	3.35	
	26	0.100	1.55	0.36	1.69	3.435	1.65	0.25	1.60	1.92	3.46	1.38	0.22	1.40	0.80	1.92	3.38	
	27	0.107	1.68	0.36	1.67	3.480	1.73	0.23	1.65	1.89	3.50	1.47	0.23	1.48	0.85	1.88	3.41	
	28	0.113	1.79	0.42	1.65	3.508	1.85	0.24	1.80	1.85	3.53	1.55	0.25	1.55	0.90	1.85	3.44	
	29	0.115	1.82	0.39	1.64	3.513	1.88	0.23	1.80	1.84	3.54	1.56	0.25	1.57	0.905	1.83	3.45	
	30	0.120	1.90	0.43	1.63	3.547	2.05	0.23	1.95	1.82	3.56	1.66	0.27	1.67	0.965	1.81	3.47	
	31	0.123	1.98	0.40	1.60	3.560	2.09	0.23	1.96	1.80	3.58	1.67	0.26	1.69	0.965	1.80	3.48	
	32	0.130	2.11	0.40	1.60	3.590	2.17	0.25	2.10	1.77	3.61	1.77	0.28	1.82	1.025	1.78	3.50	Point of breaking
	33	0.133	2.22	0.42	1.58	3.605	1.88	0.41	2.09	1.60	3.55	1.80	0.45	1.61	1.04	1.60	3.51	Broke between 2
	34	0.135	2.24	0.43	1.56	3.610	1.63	0.43	1.68	1.66	3.53	1.86	0.44	1.63	1.05	1.62	3.52	" and 3 "
	35	0.137	2.32	0.50	1.55	3.650	1.73	0.42	1.77	1.70	3.55	1.93	0.42	1.66	1.07	1.65	3.53	Broke after 2
	36	0.140	2.41	0.42	1.58	3.673	1.85	0.46	1.91	1.75	3.56	1.98	0.33	1.70	1.085	1.71	3.56	Good Max.height at 2. Broken
	37	0.148	2.32	0.48	1.58	3.660	2.02	0.56	2.05	1.74	3.59	2.25	0.27	1.88	1.148	1.75	3.58	Broke before 2

Gauges 2, 3 and 5, are 10, 22.2, 39.25 feet respectively from the inlet

All depths at gauges are measured from the initial water level.

Figure 17.

FIG. 18

	Run	Discharge (Q) cusecs	Depth Gauge 2				Depth Gauge 3					Depth Gauge 5						Remarks
			Crest 1	Valley 1	2L	Vel.	Crest 1	Valley 1	Crest 2	2L	Vel.	Crest 1	Valley 1	Crest 2	$y_s - y_o$	2L	Vel.	
Series 2 Cont.	38	0.158	2.02	0.65	1.61	3.66	2.02	0.98	2.06	1.32	3.68	1.79	0.59	1.86	1.22	1.69	3.58	Broke Twice
	39	0.170	2.77	0.91	1.66	3.70	1.99	0.98	1.97	1.34	3.71	1.87	0.75	1.73	1.31	1.41	3.61	Broke continually
Series 3 Initial depth 4" Smooth Channel	40	0.031	0.30	0.18	2.69	3.33	0.24	0.17	0.25	2.94	3.38	0.24	0.19	0.23	0.215	3.80	3.35	Gauges 2, 3 and 5 are 10, 22.2, and 39.25 feet respectively from the inlet.
	41	0.060	0.69	0.34	2.45	3.45	0.59	0.27	0.57	2.92	3.53	0.59	0.22	0.58	0.405	3.00	3.50	
	42	0.084	0.97	0.44	2.30	3.58	0.94	0.32	0.83	2.70	3.66	0.93	0.27	0.90	0.60	2.82	3.63	
	43	0.104	1.23	0.43	2.24	3.68	1.21	0.31	1.06	2.62	3.77	1.22	0.275	1.20	0.75	2.71	3.74	
	44	0.127	1.63	0.51	2.13	3.81	1.62	0.33	1.37	2.49	3.88	1.56	0.28	1.54	0.92	2.61	3.85	
	45	0.151	1.97	0.56	2.05	3.92	2.00	0.36	1.82	2.38	3.99	1.93	0.28	1.91	1.11	2.53	3.95	
	46	0.176	2.29	0.72	1.98	4.03	2.39	0.40	2.14	2.28	4.10	2.30	0.30	2.28	1.30	2.44	4.04	
	47	0.188	2.40	0.72	1.97	4.08	2.50	0.39	2.22	2.26	4.15	2.44	0.305	2.38	1.37	2.42	4.08	
	48	0.198	2.53	0.68	1.95	4.10	2.73	0.40	2.35	2.25	4.18	2.59	0.31	2.51	1.45	2.39	4.12	
	49	0.210	2.71	0.71	1.93	4.17	3.03	0.37	2.50	2.24	4.23	2.72	0.30	2.73	1.50	2.37	4.15	
	50	0.212	2.72	0.71	1.92	4.175	3.05	0.37	2.50	2.24	4.24	2.53	0.53	2.51	1.52	2.20	4.16	Broke after G. 3
	51	0.215	2.71	0.73	1.92	4.19	3.05	0.40	2.50	2.22	4.25	2.35	0.50	2.65	1.53	1.97	4.17	"
	52	0.221	2.86	0.73	1.90	4.21	2.55	0.57	2.60	2.34	4.18	2.48	0.71	2.52	1.57	1.88	4.18	Broke before G. 3
	53	0.235	3.10	0.78	1.89	4.26	2.42	0.93	2.47	2.13	4.00	2.86	0.69	2.35	1.65	2.01	4.21	Broke between 2 and 3
	54	0.240	3.16	0.83	1.88	4.27	2.60	1.00	2.58	2.04	3.91	3.00	0.71	2.43	1.67	2.05	4.27	"
	55	0.243	3.22	0.84	1.88	4.28	2.55	1.09	2.65	1.93	3.83	3.10	0.69	2.45	1.69	2.06	4.32	"
	56	0.247	3.30	0.87	1.90	4.29	2.55	1.05	2.53	1.92	3.85	2.82	0.99	2.37	1.71	2.08	4.20	
	57	0.249	3.40	0.88	1.89	4.30	2.42	1.10	2.45	1.76	3.80	2.50	0.98	2.18	1.72	2.09	4.17	Broke between 2 and 3
	58	0.260	3.39	0.92	1.84	4.32	2.50	1.18	2.52	1.73	3.84	2.42	1.09	2.29	1.77	2.15	4.14	Broke at G. 2

All crest and valley depths in inches above initial depth. Wave Length (2L) in feet.
Velocity (V) in feet/second.

FIG. 19

	Run	Discharge (Q) cusecs	Depth Gauge 2				Depth Gauge 3					Depth Gauge 5						Remarks
			Crest 1	Valley 1	2L	Vel.	Crest 1	Valley 1	Crest 2	2L	Vel.	Crest 1	Valley 1	Crest 2	$y_s - y_o$	2L	Vel.	
Series 4. y_o = 6" smooth channel	59	0.066	0.53	0.32	3.98	4.05	0.55	0.31	0.50	4.12	4.12	0.56	0.33	0.51	0.44	4.81	4.15	The restrictions of the apparatus, limited these runs and a breaking wave could not be obtained. (Runs 59-69)
	60	0.081	0.67	0.40	3.66	4.12	0.70	0.40	0.63	3.82	4.15	0.71	0.37	0.66	0.54	4.55	4.21	
	61	0.096	0.77	0.45	3.46	4.16	0.81	0.44	0.75	3.76	4.20	0.84	0.39	0.76	0.62	4.35	4.26	
	62	0.114	0.95	0.53	3.36	4.21	1.00	0.50	0.91	3.66	4.26	1.01	0.44	0.92	0.73	4.27	4.33	
	63	0.140	1.16	0.63	3.14	4.28	1.24	0.57	1.09	3.62	4.34	1.27	0.48	1.15	0.88	4.13	4.38	
	64	0.161	1.33	0.69	3.02	4.37	1.45	0.62	1.30	3.54	4.41	1.48	0.53	1.35	1.01	4.05	4.47	Gauges 2, 3 and 5 are 10, 22.2, and 39.25 feet respectively from the inlet
	65	0.185	1.50	0.76	2.96	4.42	1.62	0.70	1.48	3.52	4.48	1.70	0.56	1.57	1.13	3.93	4.54	
	66	0.209	1.70	0.85	2.94	4.50	1.82	0.73	1.67	3.48	4.56	1.93	0.59	1.79	1.26	3.80	4.63	
	67	0.233	1.78	0.86	2.92	4.56	1.90	0.74	1.77	3.44	4.62	2.16	0.60	2.04	1.38	3.68	4.68	
	68	0.245	1.85	0.88	2.87	4.59	2.00	0.77	1.85	3.40	4.65	2.27	0.64	2.15	1.46	3.60	4.71	
	69	0.261	1.95	0.95	2.85	4.60	2.15	0.81	2.00	3.34	4.68	2.42	0.65	2.33	1.54	3.54	4.74	
Series 5. y_o = 2" channel lined with netting	70	0.019	0.14	0.12	1.28	2.41	0.09	0.08	0.10	1.43	2.39	0.07	0.06	0.08	0.065	1.50	2.38	
	71	0.026	0.20	0.16	1.19	2.47	0.18	0.14	0.19	1.27	2.44	0.14	0.12	0.19	0.13	1.32	2.41	
	72	0.034	0.35	0.20	1.13	2.54	0.28	0.22	0.30	1.16	2.49	0.20	0.18	0.22	0.19	1.22	2.46	
	73	0.040	0.49	0.23	1.09	2.58	0.37	0.24	0.41	1.06	2.53	0.28	0.22	0.30	0.25	1.17	2.49	
	74	0.053	0.71	0.26	1.06	2.67	0.52	0.28	0.55	1.02	2.61	0.41	0.25	0.43	0.33	1.08	2.55	
	75	0.064	0.92	0.28	1.00	2.75	0.68	0.33	0.71	0.99	2.66	0.49	0.27	0.52	0.38	1.04	2.60	
	76	0.073	1.05	0.31	1.00	2.80	0.80	0.35	0.81	0.97	2.71	0.58	0.29	0.61	0.44	1.00	2.64	
	77	0.081	1.16	0.33	0.98	2.85	0.89	0.37	0.90	0.96	2.75	0.64	0.30	0.67	0.47	0.98	2.67	
	78	0.087	1.24	0.34	0.96	2.88	0.97	0.37	0.95	0.95	2.78	0.69	0.33	0.70	0.51	0.97	2.68	
	79	0.089	1.28	0.34	0.95	2.89	1.00	0.38	0.98	0.95	2.79	0.72	0.30	0.75	0.52	0.97	2.69	Broke just after gauge 2. Broke beforeGauge 2.
	80	0.091	1.19	0.47	0.93	2.90	1.04	0.35	1.01	0.94	2.80	0.74	0.32	0.76	0.54	0.96	2.69	

N.B. Crest and valley depths in inches above initial depth. Wavelength (2L) in feet
Velocity in feet/sec.

FIG. 20

	Run	Discharge (Q) cusecs	Depth Gauge 2				Depth Gauge 3					Depth Gauge 5						Remarks
			Crest 1	Valley 1	2L	Vel.	Crest 1	Valley 1	Crest 2	2L	Vel.	Crest 1	Valley 1	Crest 2	y_s-y_o	2L	Vel.	
Series 6.3" y_o Channel lined with netting.	81	0.016	0.17	0.15	2.01	2.82	0.15	0.13	0.15	2.40	2.85	0.09	0.08	0.11	0.085	2.60	2.80	
	82	0.025	0.29	0.21	1.94	2.87	0.27	0.20	0.29	2.19	2.90	0.18	0.17	0.20	0.175	2.28	2.85	
	83	0.030	0.33	0.20	1.86	2.91	0.30	0.22	0.33	2.06	2.93	0.21	0.18	0.23	0.20	2.20	2.88	
	84	0.047	0.56	0.31	1.82	3.03	0.51	0.32	0.53	1.94	3.03	0.37	0.27	0.39	0.32	1.97	2.96	
	85	0.071	0.88	0.39	1.68	3.16	0.76	0.38	0.85	1.75	3.14	0.57	0.33	0.59	0.45	1.76	3.06	
	86	0.097	1.25	0.47	1.57	3.30	1.06	0.45	1.10	1.58	3.25	0.80	0.40	0.80	0.60	1.60	3.17	
	87	0.109	1.38	0.48	1.52	3.36	1.17	0.48	1.23	1.48	3.29	0.87	0.41	0.86	0.64	1.55	3.21	
	88	0.130	1.58	0.51	1.44	3.45	1.36	0.53	1.45	1.43	3.37	1.07	0.46	1.08	0.77	1.49	3.28	
	89	0.139	1.70	0.56	1.39	3.49	1.44	0.56	1.53	1.40	3.40	1.14	0.47	1.13	0.81	1.46	3.30	
	90	0.150	1.97	0.59	1.37	3.54	1.54	0.62	1.62	1.38	3.43	1.22	0.49	1.23	0.86	1.42	3.33	
	91	0.165	2.22	0.63	1.40	3.58	1.66	0.69	1.71	1.26	3.38	1.33	0.53	1.34	0.93	1.39	3.38	Broke after G.2
	92	0.175	2.10	0.78	1.36	3.55	1.78	0.83	1.76	1.25	3.41	1.47	0.55	1.48	1.01	1.41	3.43	Broke before G.2
Series 7.4" y_o Channel lined with netting	93	0.026	0.21	0.19	2.40	3.13	0.24	0.22	0.23	2.83	3.22	0.17	0.16	0.19	0.165	3.30	3.22	
	94	0.048	0.40	0.24	2.32	3.32	0.45	0.29	0.44	2.76	3.37	0.34	0.26	0.36	0.30	2.79	3.35	
	95	0.070	0.72	0.38	2.26	3.42	0.64	0.37	0.63	2.37	3.49	0.52	0.33	0.53	0.43	2.65	3.46	Gauges 2, 3, and 5
	96	0.088	0.91	0.44	2.11	3.51	0.84	0.41	0.84	2.32	3.57	0.68	0.40	0.69	0.54	2.49	3.53	are 10, 22.2, and
	97	0.114	1.16	0.56	2.07	3.63	1.00	0.45	1.00	2.30	3.67	0.88	0.46	1.90	0.67	2.28	3.61	39.25 feet res-
	98	0.136	1.38	0.60	2.01	3.73	1.21	0.52	1.22	2.20	3.74	1.06	0.53	1.07	0.80	2.18	3.65	pectively from the
	99	0.150	1.56	0.65	1.96	3.78	1.36	0.54	1.37	2.13	3.78	1.19	0.56	1.20	0.88	2.11	3.71	inlet.
	100	0.165	1.74	0.70	1.84	3.84	1.50	0.57	1.49	2.03	3.82	1.29	0.59	1.30	0.94	2.05	3.74	
	101	0.186	1.90	0.74	1.80	3.92	1.67	0.62	1.65	1.94	3.88	1.44	1.60	1.44	1.02	1.98	3.79	
	102	0.226	2.41	0.96	1.71	4.05	2.00	0.70	2.15	1.87	3.98	1.74	0.71	1.73	1.23	1.85	3.87	
	103	0.268	2.86	1.10	1.66	4.17	2.42	0.77	2.35	1.75	4.06	2.01	0.76	1.98	1.39	1.80	3.92	
	104	0.277	3.21	1.22	1.62	4.18	2.90	1.23	2.40	1.76	4.00	2.20	0.81	2.11	1.49	1.80	4.01	Broke on G.2

Crest and valley depths in inches above initial depth. Wave length (2L) in feet.
Velocity in feet/second.

employed in order that these results may be compared with Favre's results. It is interesting to note how very closely the experimental points lie to the smooth curve drawn through them. This indicates that either, the measurements of the wave length have been, by good fortune most accurate, or that little differences in the measured values do not greatly affect the position of the point relative to the curve.

Figs. 17 to 20. Tabular results of information presented graphically in Figs. 11 to 16. Little need be said about these tabular results since the information has been plotted in graphical form. They are included, however, to show the specific results obtained, from which the curves were plotted.

Fig. 21. This shows for one initial depth (4 ins.) the complete diagram of the change in depth of the surges through the three stages, undular, breaking undular, and steep fronted, plotted against initial discharge . The depth at the first crest and valley are plotted from Figs. 11 and 12. Also included are the measured values of y_s , which is the mean height of the first crest and valley. These are shown with a solid line up to the maximum flow available. The calculated values of y_s are also inserted for flows above this, using the standard theory and considering the surge as steep fronted. These values are plotted with a long dotted line. The assumed paths of the three curves, y crest, y valley, and y_s, between the experimental values and the calculated values of y_s are included with point dotted lines.

It is interesting to note, how well these curves run into each other, particularly those relating to y_s . It is a great pity, that sufficiently large flows were not available to

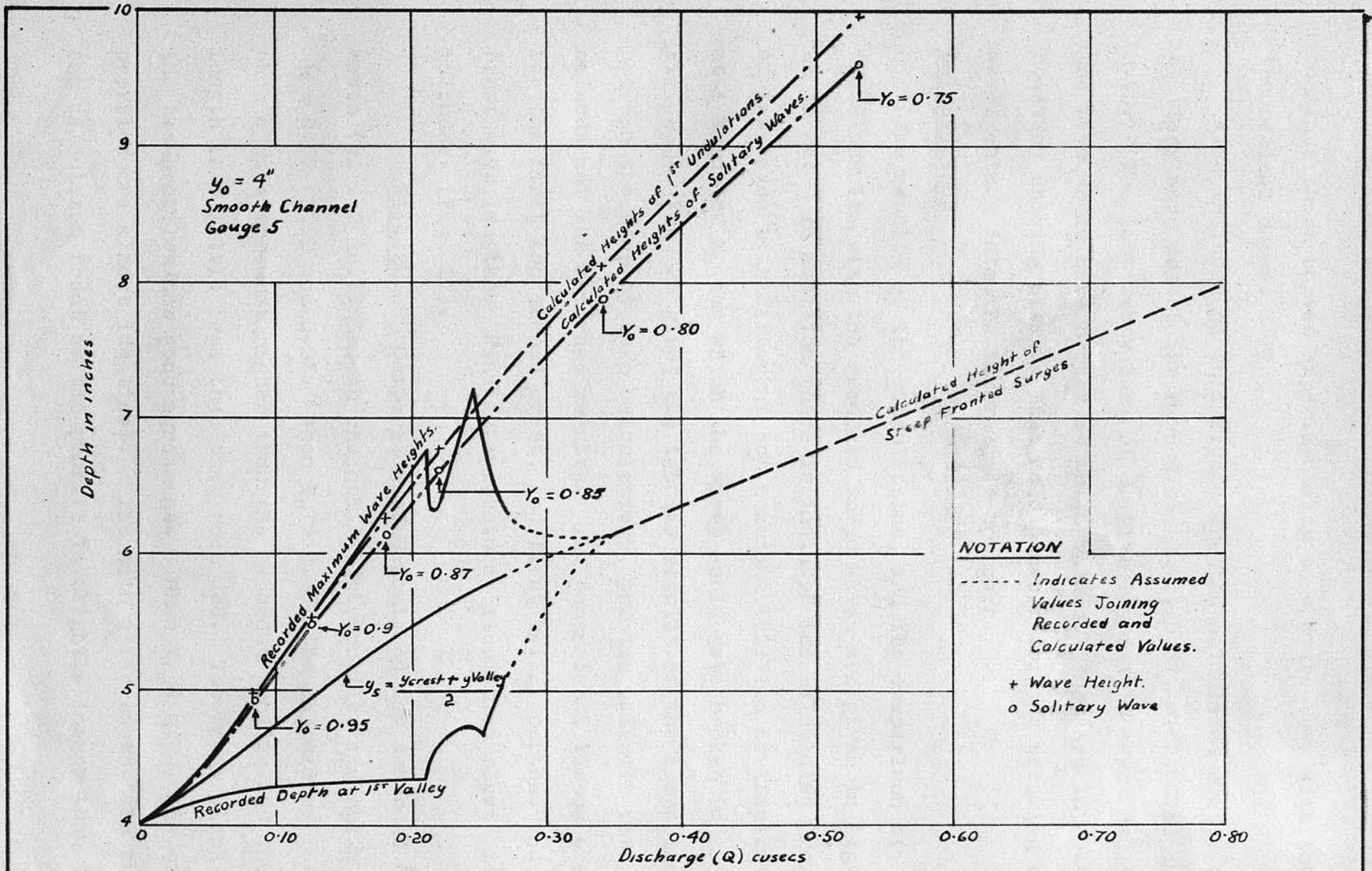

FIG. 21 COMPARISONS OF RECORDED AND CALCULATED VALUES OF SURGE WAVE PROFILES.

continue these curves experimentally to compare them with the theoretical curve.

Also included on this figure are the calculated crest, and solitary wave depths for Y_o = 0.95, 0.90, 0.87, 0.85, 0.80 and 0.75. The last two values of Y_o give impossible crest depths, since the wave would have broken at these values. They are interesting however, showing clearly that no allowance for the breaking of the waves enters into the theoretical approach.

Calculations

The results of the calculations, and the comparison of these results with the recorded surge waves are given in Figs. 22 to 24. In addition there is included the calculated profile of two waves with different but constant friction coefficients, at a value of Y_o for which the waves would have broken in practice (Fig. 25.). Fig. 26 gives the tabular results of the comparisons between the step by step calculations, the two elliptic integral methods and the recorded results. The comparisons listed are for the first and second crest, and first valley depths, and the first wave lengths. Finally a specimen calculation sheet is included. (Fig. 27).

Fig. 22. Comparison of Calculated and Recorded Surge Waves (y_o = 2 in.). Smooth channel. The profiles are shown for Y_o = 0.87, 0.90 and 0.95. When Y_o = 0.95, the calculated results show a wave somewhat higher than the recorded profile and the wave length is a little less than that recorded. The front slope of the two profiles show good agreement. When Y_o = 0.90, the two profiles are almost identical. The main differences, are that the calculated front of the profile is slightly longer than that

recorded, the calculated crest height is slightly higher, and the wave length a little longer than that recorded.

With Y_o = 0.87 the discrepancies between calculated and recorded values are most obvious at the crests. The calculated front is slightly longer, the calculated wave length a little greater, and the valley depth very little deeper than the recorded values.

The first two of these profiles were recorded at gauge 5, and the third at gauge 3 as this value of Y_o could not be obtained at gauge 5 before breaking occurred.

Fig. 23. is a similar record to Fig. 22, but for Y_o = 0.9, and y_o = 3 and 4 ins. Again at this value of Y_o, the agreement between calculated and recorded values is very good. The crest heights are a little lower, the valley depths are a little higher, and the wave lengths slightly longer when calculated than the recorded values. Both records were made at gauge 5.

Fig. 24. The third record of comparison between calculated and recorded profiles. Three profiles have been plotted at Y_o = 0.9, (with y_o = 2, 3 and 4") when the channel was lined with netting. In all three cases the results follow the same pattern. The front of the wave is a little too long, the crest and valley heights slightly less, and the wave lengths somewhat longer, when comparing the calculated results with the recorded profiles. The agreement in all three cases however is moderately good. Profile (a) was recorded at gauge three, because owing to the friction the maximum wave amplitude at gauge 5 was too small. Profiles (b) and (c) were recorded at gauge 5.

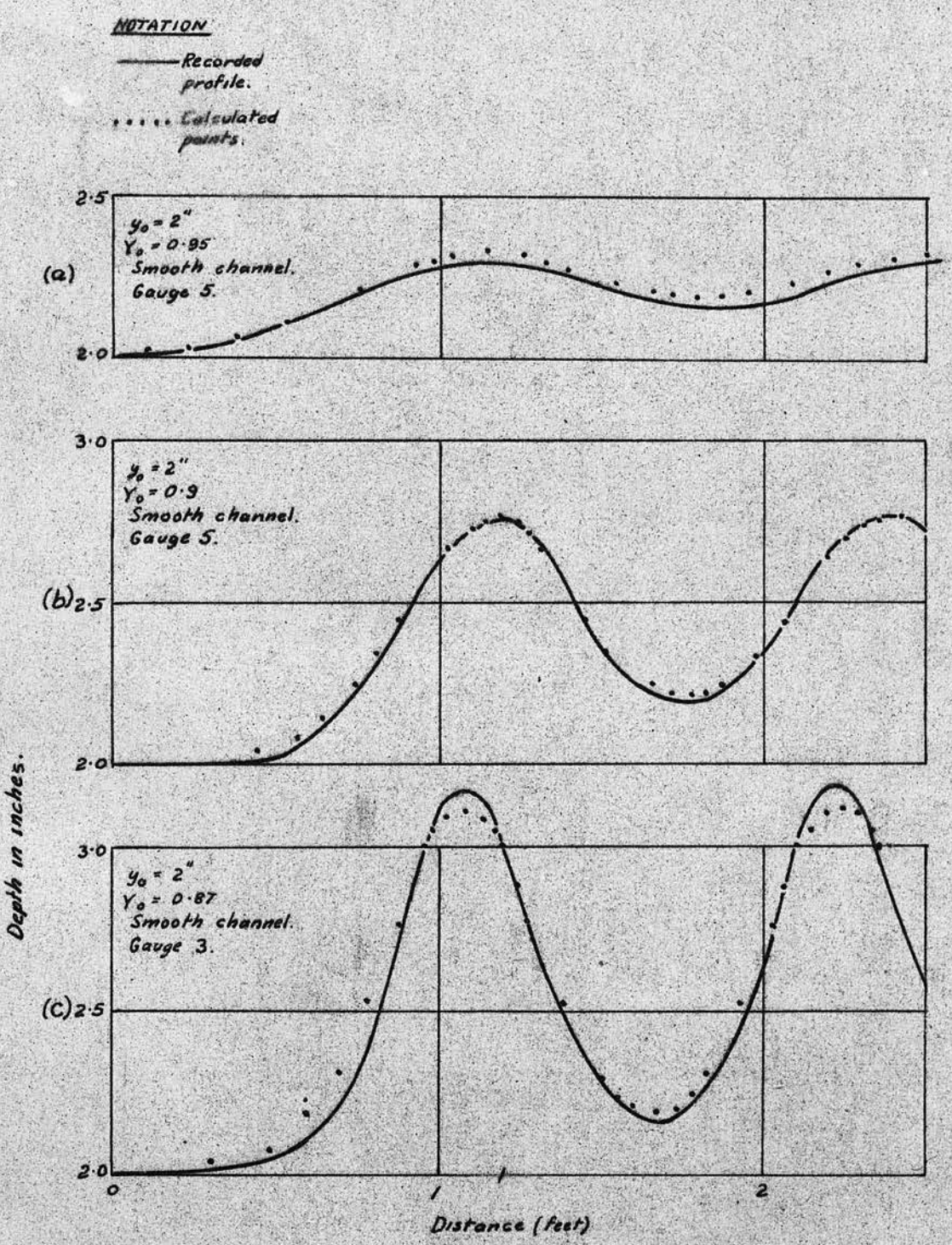

FIG. 22 COMPARISON OF CALCULATED AND RECORDED UNDULAR SURGE PROFILES ON AN INITIAL DEPTH (y_o) OF 2"

Gauges 3 and 5 are approximately 20'-0" and 38'-0" respectively from the inlet.

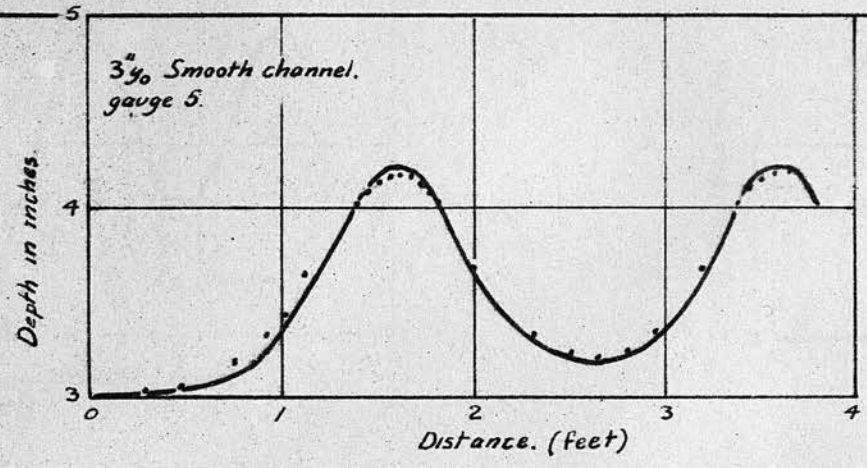

NOTATION

——— Recorded Profile.

• • • • Calculated Points.

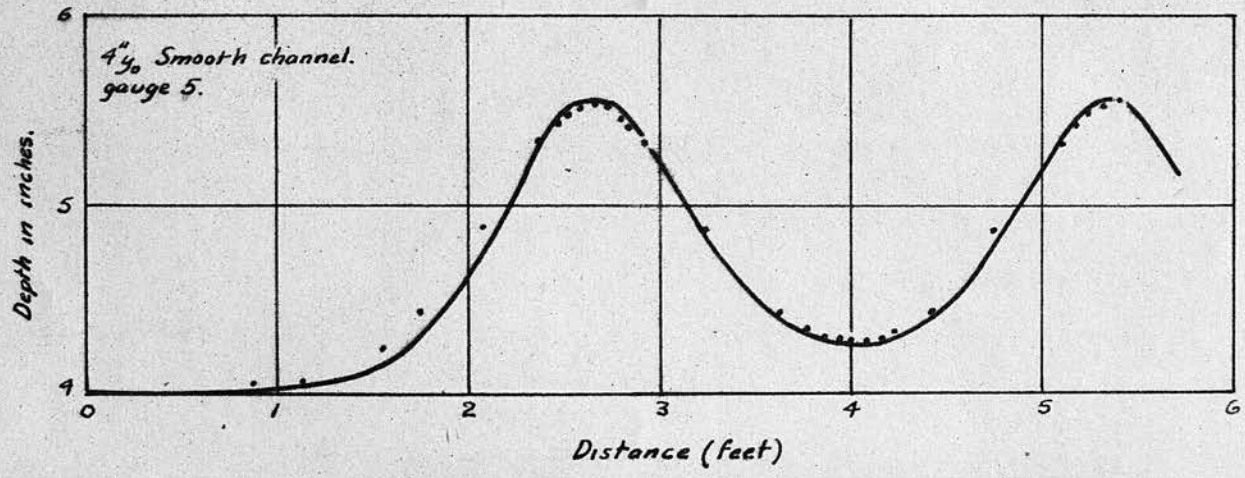

FIG. 23 COMPARISON OF CALCULATED AND RECORDED SURGE WAVE PROFILES.

$Y_o = 0.9$. $y_o = 3"$ and $4"$. Smooth Channel.
Recorded at gauge 5.
Gauge 5 is approximately 38'-0" from the inlet.

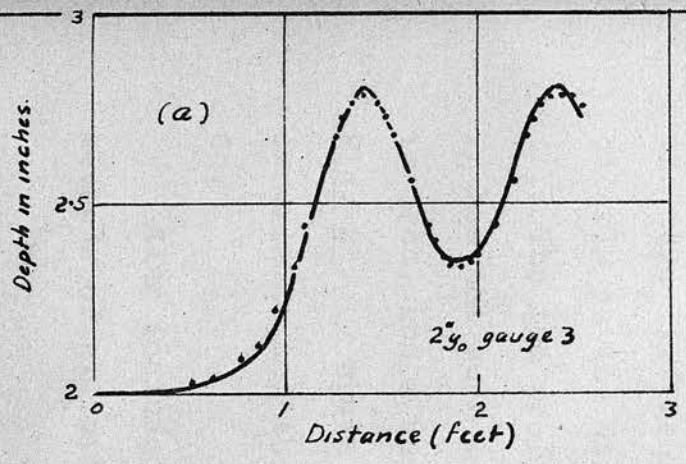

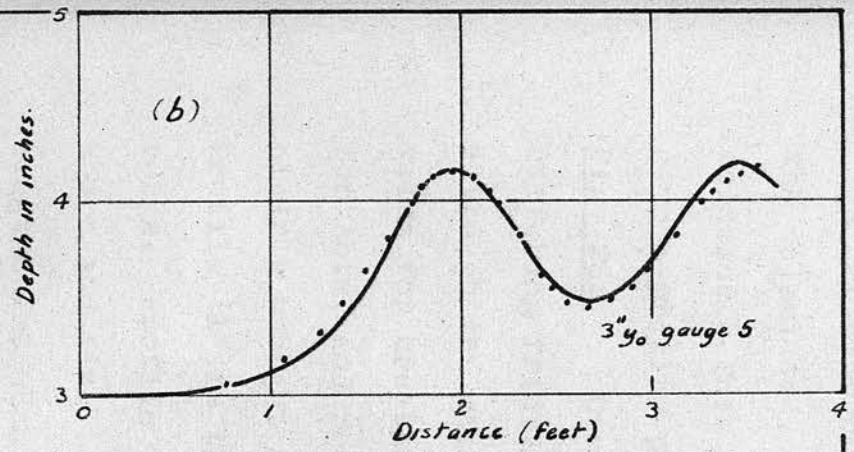

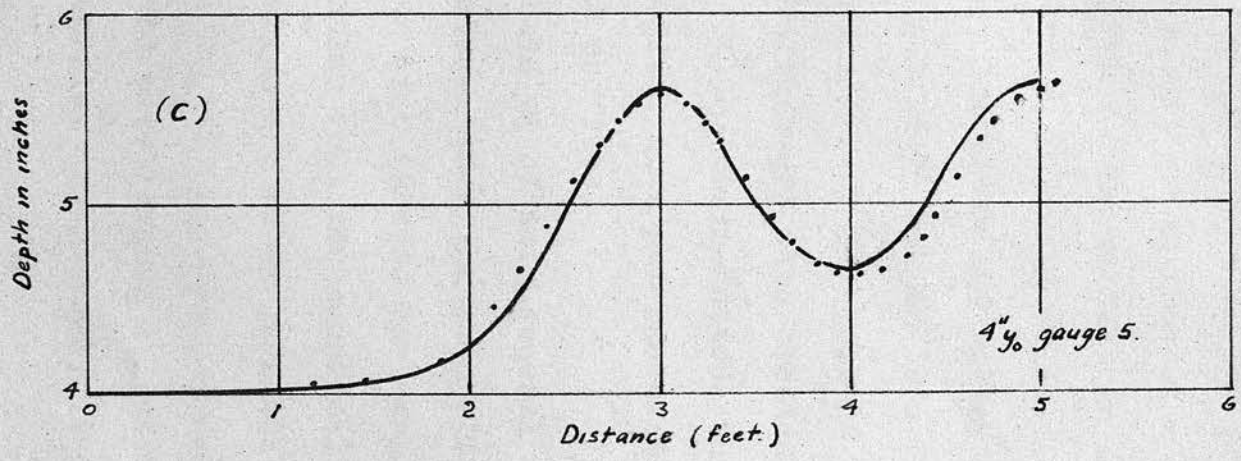

FIG. 24

COMPARISON OF RECORDED AND CALCULATED PROFILES OF UNDULAR SURGES WITH THE CHANNEL LINED WITH NETTING

Gauges 3 and 5 are approximately 20'-0" and 38'-0" from the inlet.

For ease of comparison between these eight sets of profiles, the calculated, and recorded crest in each set, were made to coincide. This was decided upon since it is not possible to give a precise position for the front of the profile.

Fig. 25. Comparison of two calculated profiles, with widely differing friction coefficients. The curves also show that although the value of $Y_o = 0.80$ chosen is lower than the limiting value for breaking (i.e. about 0.83) the calculations do not allow for this, and predict an undular profile again. What is very clearly brought out is the difference in the profiles however. Profile 'A' is that for a very rough channel - almost impossibly rough. Profile 'B' represents the profile in a channel of similar shape and size to 'A', but with smooth walls. In 'A' the wave lengths are much shorter, the crest and valley heights are successively considerably higher than in 'B'. The general shape of the waves is however unaltered, the valleys being much broader than the crests. The profiles are also plotted, with the same horizontal and vertical scale (chain dotted) which whilst showing the true differences in size, does not convey the information so clearly as the distorted profiles.

The two profiles would be of more general application, if Y_o had not such a low value, since the side effects have been ignored, and a mean value of C is used for each profile.

Fig. 26. shows in Tabular form the numerical differences between experiment and theory, which are shown graphically in Figs. 22 to 24.

Also included are the wave lengths calculated by the two methods of elliptic integrals. In general, it can be said that in

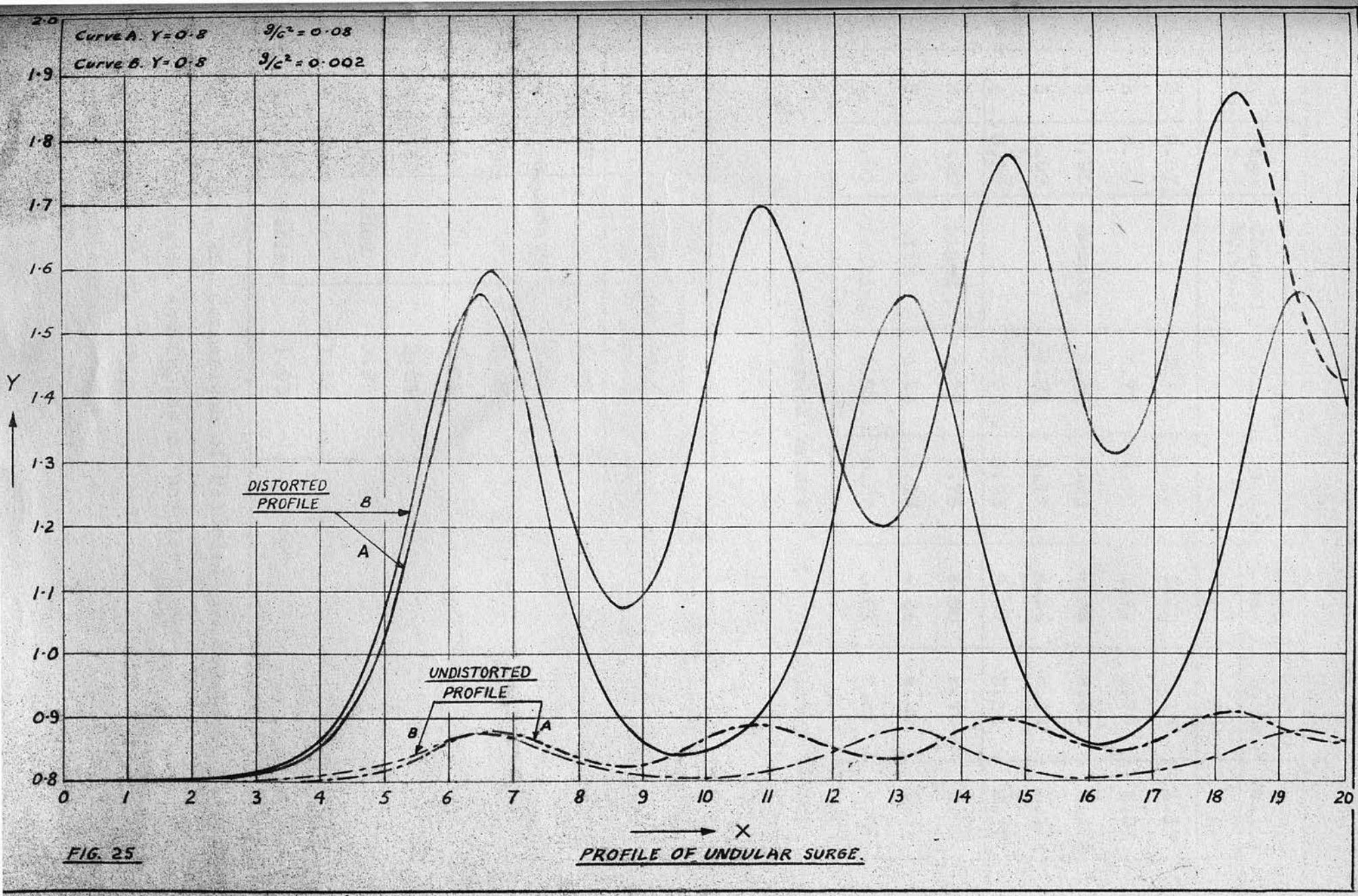

FIG. 25

PROFILE OF UNDULAR SURGE.

y_o ins.	Y_o	Channel Surface	Depth at first crest in inches		Depth of second crest in inches		Depth of first valley in inches	
			A	B	A	B	A	B
2	0.87		3.16	3.12	3.19	3.15	2.17	2.19
2	0.90		2.77	2.78	2.79	2.79	2.21	2.23
2	0.95	Smooth	2.30	2.33	2.32	2.34	2.175	2.20
3	0.90		4.21	4.17	4.22	4.19	3.19	3.20
4	0.90		5.55	5.53	5.57	5.56	4.27	4.30
2	0.90	Lined	2.79	2.76	2.80	2.78	2.35	2.33
3	0.90	with	4.23	4.18	4.24	4.20	3.50	3.47
4	0.90	netting	5.60	5.57	5.61	5.59	4.65	4.60

A - recorded values. B - calculated values.

y_o ins.	Y_o	Channel Surface	First Wave Length			
			Recorded Values (ft.)	Step by Step Calculation (ft.)	Elliptic Integrals Short Method (ft.)	Complete Method (ft.)
2	0.87		1.16	1.18	1.14	1.18
2	0.90	Smooth	1.22	1.25	1.19	1.22
2	0.95		1.36	1.32	1.33	1.34
3	0.90		2.01	2.05	1.95	2.00
4	0.90		2.64	2.69	2.68	2.70
2	0.90	Lined	0.99	1.02	1.06	1.07
3	0.90	with	1.52	1.56	1.61	1.63
4	0.90	netting	1.95	2.09	2.16	2.19

Fig. 26, Comparison of recorded and calculated values of wave lengths and depths of undular surges.

the smooth channel the Complete Elliptic integral method gives the results nearest to the Recorded results, but it must be remembered that these results are obtained from the Step by Step Calculations, and these give the most accurate results when the channel surface is rough.

Fig. 27. This is a specimen calculation sheet for $Y_o = 0.87$, $y_o = 2"$, in the smooth channel. A constant coefficient of friction is used, which was obtained from the mean slope of the appropriate experimental run. It is interesting to compare the results from this, with those plotted in Fig. 22 where a varying friction coefficient has been employed. Apart from this, however, the sheet shows all the steps in the calculation. The symbols in the 'Headings' column have already been explained in Chapter 5.

To obtain the dimensions in inches, the values of Y in the first column, and the values of $\Sigma\Delta X$ in the eleventh column have to be multiplied by $\frac{2}{0.87} = 2.30$.

The Results of Series 23.

A number of runs were made at an initial depth of 4 inches, with a constant discharge. The time of opening of the mains valve was varied from instantaneous to about 5 seconds.

It appeared that with a time of opening of approximately two seconds, there was very little change in the wave profile, taking the run with instantaneous opening as datum. The most evident change was at gauge 2, and was an overall change of maximum value about 4%, showing a decrease in wave height and wave length. The change at gauge 3 was similar but only about 2%, and there was no evident change at all at gauge 5. These percentages are obtained considering the crest height above the initial level,

and the wave length, when the opening was instantaneous, as 100%

With a time of opening of approximately three seconds however, the changes are very much more marked. The wave profile at gauge 2 is very much reduced. The wave height is decreased by approximately 40%, the valley depth increased by about 30%. At gauge 3 the changes are less marked and at gauge 5 are quite small, except for the valley depth which is increased by about 20%.

At 5 seconds opening time, the results are even more marked at gauge 2. The crest height, valley depth, and wave length being changed by - 50%, + 35% and - 17% respectively. Oddly enough at gauge 3 the valley depth has increased by 66%. At gauge 5 the changes are - 5%, + 33%, and - 8% respectively.

It must be emphasised that these values are only approximate, since the valve was opened by hand. The important point is, however, that very little change is experienced until the opening time is about 2 seconds. Between 2 and 3 seconds the effect suddenly becomes very marked at gauge 2. Beyond 3 seconds the effect is markedly noticeable at gauge 3. At gauge 5 however, the changes are small even up to a time of opening of 5 seconds. Favre put this latter time as high as 7 seconds. His channel, however, was much longer - 200 feet approximately and as the results above show, the more distant the observer is from the inlet the less effect, time of opening has on the wave profile.

CALCULATION SHEET

Determination of the Profile of an Undular Surge.

$Y_0 = 0.87$. $y_0 = 2''$ $g/c^2 = 0.01044$. $B = 0.00002256$.

$W = \left(1 + \frac{2y}{c}\right)$ $A = \left(\frac{1}{Y} - \frac{1}{Y_0}\right)^2$ $C = 74$. $\left(\frac{\Delta Y}{2}\right)^3 = 0.0000005$.

Y/Y^2	$n+1$	$(n+1)^2$	$(n+1)^3$	$L-T$	$N-P$	$L-T+N-P$	$G(C-T+N-P)$	dY/dX	$H_{mean}\, dY/dx$	$\Sigma \frac{\Delta x}{\Delta x}$	Point Δx	W.A. g/c^2	$\Sigma \frac{\Delta S}{\Delta S}$	$\Sigma \frac{\Delta E}{\Delta E}$
0.88 0.7744	1	1	1	0.00002256 50 0.00002206		0.00002206	0.00013236	0.0115	0.00575	1.794	0.884	0.000015	0.0000161 760	0.0000185 845
0.9 0.81	3	9	27	0.00020304 1350 0.00018954	0.00001498 1449 0.00000049	0.00019003	0.00114018	0.03377	0.022435	2.678	0.845	0.00009	0.0000921 1457	0.0001030 1523
0.95 0.9025	8	64	512	0.00144 38 2560 0.0011878	0.00009295 7 86495 0.00000 5462	0.0011933	0.0071598	0.08462	0.059195	3.523	0.470	0.00031	0.0000378 4922	0.0002563 4922
1.0	13	169	2197	0.0038126 10970 0.0027156	0.0000563 378 0.0000185	0.0027341	0.016405	0.12808	0.106351	3.993	0.631	0.00078	0.000730 841	0.0007485 764
1.10 1.21	23	529	12167	0.0119342 0.0058509	0.00090568 80100 0.00010468	0.0059556	0.035734	0.18903	0.1581	4.624	0.570	0.00165	0.001571 624	0.001513 520
1.20 1.44	33	1089	35937	0.0245678 179685 0.0065993	0.0021787 18852 0.0002935	0.0068928	0.041357	0.20336	0.19615	5.134	0.259	0.00241	0.002195 965	0.002033 772
1.25 1.5625	38	1444	54872	0.032577 27936 0.005141	0.0021797 17475 0.0004322	0.0055732	0.033439	0.18287	0.193115	5.393	0.325	0.00297	0.003160 291	0.002805 224
1.30 1.69	43	1849	79507	0.041713 39753 0.001960	0.0047404 41080 0.0006324	0.0025924	0.015554	0.12472	0.15379	5.718	0.088	0.00331	0.003451 393	0.003029 300
1.31 1.7161	44	1936	85184	0.043676 2592 0.001084	0.0051981 45208 0.0006773	0.0017613	0.0105678	0.10280	0.11376	5.806	0.115	0.00342	0.003844 850	0.003329 674
1.32 1.7424	45	2025	91125	0.045684 45567 0.000117	0.0058004 50741 0.0007263	0.0008393	0.050358	0.07096	0.08688	5.921	0.240	0.00354	0.004694 546	0.003973 637
1.3285	45.85		963868	0.048193 47426 0.000767				0	0.035486	6.161	0.239	0.00354	0.005540 393	0.004610 298
1.32 1.7424				0.000117	0.0080325 73128 0.0007197	0.0008367	0.0050202	0.07085	0.036635	6.400	0.115	0.00342	0.005933 295	0.004908 225
1.31 1.7161				0.001084	0.0084226 77722 0.0006504	0.0017344	0.0104064	0.10201	0.08664	6.515	0.089	0.00331	0.006228 986	0.005133 758
1.30 1.69				0.001960	0.0086748 80964 0.0005784	0.0025385	0.015231	0.12341	0.11271	6.604	0.332	0.00297	0.007214 643	0.005891 514
1.25 1.5625				0.005141 1872	0.009247 0.0001872	0.00053282	0.031969	0.17881	0.15111	6.936	0.267	0.00241	0.007857 899	0.006405 749
1.20 1.44				0.0065993 2052	0 0092232 0.0002052	0.0063541	0.038365	0.19586	0.1817335	7.203	0.545	0.00165	0.008756 319	0.007154 290
1.10 1.21				0.0058509 9753	0.0096316 86563 0.0009753	0.0048756	0.029254	0.17104	0.18345	7.748	0.326	0.00098	0.009075 282	0.007444 269
1.05 1.025	18	324	5832	0.0073094 29160 0.0043934	0.0095 2875 820701 0.0013 2174	0.0030717	0.0184302	0.13576	0.1534	8.074	0.463	0.00061	0.009357 284	0.007713 254
1.00				0.0027156 16440	0.0093570 77130 0.0016440	0.0010716	0.0064296	0.08019	0.107975	8.537	0.686	0.00037	0.009611	0.007967
0.9725 0.9457	1025	10506	107686	0.0023 7015 53843 0.0018 3172	0.0093467 75351 0.0018116	0.00002012	0.00012072	0	0.040095 $2L = 3.032$	9.193				

CHAPTER 9.

Discussion of the Results.

The purpose of this thesis as propounded in the Introduction, was to develop a theoretical expression for the profile of undular surge waves; to use this expression to calculate a number of profiles, which could then be checked by experiment; and to endeavour to obtain some data from the experiments that would be of practical use. In addition to commenting on the results obtained, and on the measure in which they fulfill the proposed purpose, other facts or theories that have arisen out of this investigation are included in this chapter.

A theoretical expression - or rather a compound of three equations - has been developed which, with certain assumptions and restrictions, can be considered to represent the profile of an undular hydraulic jump. The undular surge which is the main consideration of this thesis is then transformed into this undular hydraulic jump, by superposing on it a velocity equal and opposite to that of the mean velocity of the head of the surge. The resulting expressions are Equations 41, 51 and 52.

These expressions unfortunately do not lend themselves to analytical solution, and consequently they have to be solved by a most laborious step by step process. This process has been carried out for a number of initial conditions and the results have been presented in tabular and graphical form, in the previous Chapter, comparing them with recorded profiles.

The results are moderately good, which is probably all that could be expected, since the final theoretical expressions are arrived at by making a number of assumptions, and the step by step

method of solution is an approximate solution.

The maximum errors in the wave lengths were + 7%, - 3%. Measuring depths above the initial water level, the maximum error in the crest heights was + 9%. This was in only one instance however, and the mean error was + 3%. At the first valley the maximum error was again + 9%. This latter percentage is perhaps a little unjust in presentation, since the depths considered were small compared with the crest heights, and the errors will be much of the same order. Since, however, in practice it will be the crest heights that are of major importance, it is worthwhile noting that the maximum error in these heights was when the wave height was least.

Further it is presumed that should undular surge profiles be calculated for larger channels than that used in these experiments, the results obtained will contain a smaller percentage of error.

The reason for this presumption is as follows. As explained previously the lower values of the graph 'C' to 'r' have had to be estimated, since it was not possible to measure differences in water level at such small discharges. Since the slope of the curve at these values is very steep, small differences in 'r' mean large differences in 'C'. Hence it only requires that 'r' should be slightly inaccurate, or that the path of the curve be wrongly estimated, for quite large differences to occur between the value of 'C' so obtained, and the true value. It has also been determined by calculation that relatively small differences in the value of C have an appreciable effect on the shape of the profile. Hence in the small channel, where the value of 'r' is always

relatively small, it is not surprising that differences occur between the calculated and recorded profiles.

However, with larger channels, the average value of 'r' will be much greater, and consequently as the slope of 'r'/'C' curve is much less at these values the differences between the calculated and recorded results can be expected to be much smaller.

In addition, in larger channels the friction coefficient 'C' more nearly approaches a constant value, and hence it is quite probable that in the type of channel usually met with in practice, (i.e.) lined with concrete, brick, or even earth, the standard value of 'C' obtained from the Bazin or Manning formulae will suffice. It would be interesting to have some comparisons between profiles measured in a large channel and calculated results.

Another point is that in large channels, in general the side effects can be neglected, and consequently the calculations are simplified a little. It would appear from Favre's results, that these remarks are probably justified, since the shape of the surge profiles he obtained, do closely agree with profiles calculated, with high values of 'C' and neglecting side effects.

It is worth noting at this point, considering the curves of 'r' to 'C', the dangers of too facile a comparison between model and prototype, when the model is made to a very small scale.

One point that has not been considered yet, is, what physical reasons can be advanced for the formation of the undular surge. Two reasons are tentatively advanced which approach the problem from different view points.

Let it be supposed first that the surge had no waves on it, and that it is steep fronted. Then if the velocity of travel of

the surge is low enough, the front of it will have the appearance of a wave front, (i.e.) it will be smooth, not turbulent as the front of the normal steep fronted surge. Now somewhere in the body of the surge, the whole mass is moving, if not uniformly, at least it has a constant velocity distribution from point to point. Yet at the head of the surge the velocity distribution varies from zero, to this constant distribution. Then the mean velocity of the body of the surge as experiments have shown, is less than the velocity of the head. Consequently the head tends to move away from the body of the surge, and therefore must leave a depression behind. Then immediately the new head of the surge must do exactly the same thing, (i.e.) move faster than the body, and thus the waves are formed one behind the other. The reason that they do not form solitary waves, is that, before the depression behind any wave can reach the initial level, a second wave is formed, and consequently the valleys intermingle.

This is a somewhat specious argument, since it attempts to explain the phenomena from a 'visual' point of view, but it does at least give an answer. It has always to be remembered however, that the visual impression of the surge, and the paths of the fluid particles are not the same. The path of a surface element in a solitary wave is a half ellipse and the particle after being moved forward a distance equal to the major axis of the ellipse returns to its former level. With the undular surge, the particle has a path much as follows:-

Fig. 28.

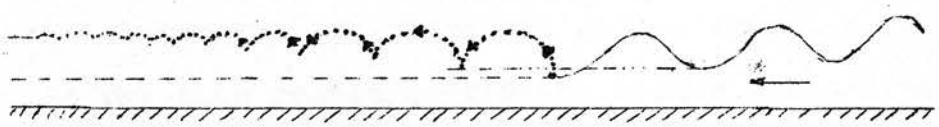

The size of the approximate part ellipse becomes smaller and smaller and the downward motion finishes at a higher level than in the previous part ellipse. Eventually (theoretically at infinity) the ellipse height is zero and the particle moves on the body of the surge with a gradually decreasing velocity, as the height of the surge decreases. The visual impression is obtained from all the paths of the particles added together. The velocity of the surge wave is the mean of the horizontal velocities of the particles when they have reached the highest point in their trajectories.

From a physical consideration of the particle motion, a tentative theory of the cause of these undulations is as follows. There must be some force acting on the particle to cause it to rise and advance. This according to Scott Russell is due to the pressure exerted on the particle by the forward displacement of previous particles caused by the additional flow at the inlet. For the solitary wave Scott Russell shows that the wave can be formed by simply moving a plate forward. Any particle directly in the path of the plate has to rise above particles in front of it, as water is virtually incompressible. A part analogy is the action of a train of railway wagons when a sudden push is applied to one end of the train. Hence considering one particle for the moment, it has to rise and move forward. Then at some point in its trajectory the force must be removed, as the particle rises above the agency of the force. Thus its trajectory must flatten. The particle then possesses a horizontal velocity, and relatively, considerable potential energy. It therefore falls, whilst still moving forward. So far this result applies to either the solitary

wave or any wave in a surge. However the particle in the solitary wave returns to its original level, since all the discharge is contained under the profile of the solitary wave. For a wave in a surge however, more fluid is being injected whilst the particle is following its elliptic path, and consequently the particle cannot return to its original level. In virtue of its potential energy however as it falls, it must displace some of the fluid beneath it. This is happening all the time with different particles and consequently they tend to cause momentarily a massing of water behind them. When the potential energy is destroyed, the pile of water behind, causes the particles, under pressure from the added discharge to perform another elliptic trajectory, but of necessity, a smaller one this time. This continues with ever diminishing height of trajectory, until no further rise or fall is discernible. Then the particle is moving with the surface velocity of the body of the surge. This argument, does appear to advance an explanation a little more in keeping with the fluid behaviour than that originally propounded. In passing it should be mentioned that below the surface the particle path is similar, but the total upward displacement of any particle is proportional to its initial depth above the bed of the channel.

A series of sketches of the paths of particles was undertaken at one point in the investigations and it does elucidate one problem. How is it that the particles move forward in a series of jerks, whereas in surf riding, a planing board will apparently remain at the crest of one visually advancing wave? The solution is, that as each particle rises in its trajectory it strikes the

underside of the board and keeps it moving forward. If the board is horizontal the motive force is friction, and it would appear from purely theoretical considerations that a slight forward tilt to the board would produce a steadier and more reliable propulsive force.

The inception of the phenomenon of breaking is usually associated with the point at which the forward velocity of the particles of fluid at the crest equals or exceeds the translation velocity of the wave. This statement, correct in itself, is substantiated by a methematical analysis based on irrotational motion from which a cusped shape of the crest id deduced. As in such an analysis all effects of surface tension are ignored, it is obvious that the exact height of a breaker will not be arrived at correctly and that a theory taking into account the limiting radius of curvature should be evolved.

These considerations also allow an explanation of the behaviour of the steep fronted surge. The main question would appear to be why, if the particles have previously described an elliptic trajectory will they not continue to do so even after breaking has occurred? The reason is, that for a time the particles do continue to make visual wave forms (breaking undular surge) but eventually, after a wave has broken very violently the turbulent water effectively smothers most of the vertical rise of the particles, leaving it almost entirely with a horizontal motion. This is of course a vast simplification since a great deal of mixing and turbulence occurs at the head of the steep fronted surge. However, before the particle can rise to its full

height, it is overrun by the advancing surge, whereas if there were an unbroken wave behind, there would be no interference with its trajectory.

From the experimental work, a number of interesting facts have emerged, and these are included in note form:-

A surge wave builds relatively rapidly to its maximum height, and then the height decreases slowly as the surge moves along the channel.

The calculations only apply (except to the height of the first wave) when the surge has reached a relatively permanent form.

The rougher the channel, or the smaller the initial depth, the more rapidly the first crest reaches its maximum height.

At a particular gauge, the wave length decreases and the crest height increases until breaking occurs; as the discharge increases. For one run however the wave length will increase at first and then steadily decrease. This sequence of events is much more rapid at the smaller initial depths.

Even if a surge starts its run with a steep front; if the channel is long enough, it will eventually pass through the stages to an undular surge. This is because the friction decreases the discharge at the head. Hence if the available discharge is large enough, a surge wave can be made to attain its maximum height at any position in the channel, by varying the discharge. Also after breaking occurs the maximum wave height at a probe can decrease. As the discharge increases the wave breaks sooner, and has time to rebuild again. Depending on the distance of the probe from the inlet, the crest height can rise and fall several times (each time the wave breaks) as the discharge is increased.

As the discharge increases, so at one gauge the valley depths slowly but steadily increase up to breaking. This experimentally observed fact does not agree with some theoretical conclusions in the literature, that as the discharge increases the waves more nearly approach the solitary wave. On the other hand, as the surge moves along the channel the valley depth does decrease. This is due to the build up of the wave formation, and to the gradually diminishing depth of liquid at the head of the surge, which until steady conditions are reached, does make the effective initial depth greater. The valley depth continues to decrease after the surge profile has reached its stable shape, because the size of the waves decreases, owing to friction effects.

When the surge has reached this stable shape, the crests of the waves are at successively greater depths above the channel bed, but the amplitude decreases from one wave to the next. After reaching this condition it is interesting to note how very accurately the empirical equation (3) due to Scott Russell applies (i.e.) $V = \sqrt{gy_{crest}}$

This can be checked from Figs. 17 - 20.

As the friction increases ('C' decreases), the crest and valley depths are increased, and the wave length decreased.

In practice, to determine the wave height approximately, if the depth of the solitary wave is calculated and an additional 60% of this depth above the initial water level is added, this gives a reasonably good crest height of the first undulation.

The calculations do not give results of the greatest accuracy when Y_o is near to 0.83 (breaking) since the assumption of a uniform velocity distribution is then at considerable variance with actual conditions.

From geometrical considerations alone, if the channel used in these experiments was assumed to be some practical channel, scaled down by about 60:1, then the prototype would be roughly 3,000 ft. long. As however the comparative friction is much greater in the model, than would be met with in any practical channel (except a very rough sided, weed infested, earth one) the prototype to produce comparative results, would have to be much longer. For instance Favre's model channel is about three times the width of the one used in these experiments. Yet with an initial depth of 10.75 cms, which is very similar to our initial depth of 4", Favre's surges reach in 200 ft. the stage in their evolution, that is reached in the small channel in about 40 ft.

A more detailed comparison is given between these results and Favre's in the next chapter.

Another point to be considered, is the effect of the time of opening of the inlet valve. If the time is no more than 2 secs. the effect is negligible at all positions in the channel, and up to about 4 seconds the effects are very small at gauge 5 where most of the surges were recorded.

At low discharges the waves do approximate to a sinusoidal shape. As the discharge increases the profile becomes more nearly cnoidal, up to a certain maximum, and then diverges slightly from this shape when the wave approaches its point of breaking. The ultimate shape just before breaking occurs is almost cusped at the peak.

Finally it is necessary to make some estimate of the accuracy with which the experiments have been carried out.

From the photographic comparison it would appear that the crest heights are accurate to within very small limits, particularly when the record was not allowed to extend beyond the centre two centimetres of the penrecorder paper. After this had been d discovered, all the runs were kepth within these limits. The maximum error would then probably be approximately ± 0.01 inches, that is when the apparatus is used at the maximum amplification employed (i.e. for y_o = 2 ins.), and when y_o = 4 inches this error would be smaller, since the amplification is less. This, however, is counter-balanced by the difference in ease of reading the record, since 1 millimetre of the record represents a greater change in depth as the amplification decreases.

The record can be read direct to the nearest 0.1 millimetres, with the aid of a handglass fitted with a scale, and by estimation to 0.006 inches. However it is estimated that the meniscus and disturbance effect of the wire of the depth gauge have a maximum value in the troughs of the waves of + 0.01 inches. At the crests these effects are much smaller. It would appear from an inspection of Fig. 9 (page 58) that the record itself is subject to irregularities of the order of ± 0.1 mms. However it is believed that these irregularities are caused by surface ripples, and a comparison of the results obtained from these records with photographs, indicates that the maximum errors in the measured crest heights are ± 0.015 inches. The errors in the measurement of depth at the troughs of the waves would appear to have a maximum value of - 0.01 to + 0.02 inches since the meniscus and distrubance effects are positive.

This meniscus error was greatest at small initial depths since the wave length was small.

When measuring wave lengths the error was found to be a little more uncertain. This was due to the difficulty in measuring accurately the distance between crests, as it is difficult to determine their exact position. Eventually however a technique was devised which gave reasonably consistent results, except, as already mentioned with the rough channel and $y_o = 2"$. Even with these however the maximum error was only $\pm$ 0.25 inches (approximately $\pm$ 2%). At greater initial depths the measured error was much the same, $\pm$ 0.25 inches, but the percentage error was considerably less. However when the wave lengths were plotted against discharge, and a probable curve drawn, any values that were suspect, could be checked.

CHAPTER 10.

An appreciation of some of the recent contributions to the literature, relevant to the subject of surge waves in open channels.

The two most important recent additions to the literature dealing with the equations of flow in open channels, with special reference to the undular forms of flow, are those due to Serre, and Benjamin and Lighthill.

Benjamin and Lighthill show that an undular form of surface profile in open channel flow is only possible, because of losses in energy and momentum, due to friction. Serre derives his equations for the flow profile, and the change in energy and momentum, and then shows that under certain conditions the result can only be an undular profile. Both obtain the same equation for the flow profile, although starting from different premises, and this expression readily lends itself to calculation as it contains only known quantities. The equations for the change in energy and momentum due to Serre are however necessary for an undular profile to be obtained. The first equation yields the profile of a solitary wave.

The coincidence of the two results is easily explained. Serre evaluates 'H' and 'M' (Energy and Momentum functions) from first principles by determining 'p' and 'u', (pressure and velocity) and substituting these in the original equations. After assuming temporarily that H and M are constant he integrates, to bring both into one equation.

He finishes by showing that mathematically under certain conditions,

his result will give rise to a periodic solution, when solved for the shape of the profile. On the way he makes a number of simplifying assumptions chief of which is that the velocity distribution is uniform, and that outside the boundary layer the flow is irrotational.

Benjamin and Lighthill on the other hand, assume a harmonic solution for a stream function, thus assuming a periodic solution for the profile, and irrotational flow. Hence the two results should at least be similar. Then it can be seen that Benjamin and Lighthill follow exactly the same steps as Serre, (i.e.) evaluating H and M (which they term R and S respectively), but they rather neatly eliminate a considerable amount of tedious analysis by eliminating 'p' between the two equations for H and M, and thus obtain one equation involving the two. Thus it is not surprising that the two results are identical.

It should be noted that both these methods involve a direct contradiction. Both assume irrotational flow, and then consider the effects of friction. However, simplifications had to be made, in order that the equations might yield some results.

Although it has been stated that our H and M correspond to Benjamin and Lighthill's R and S the relationships are

R = energy per unit mass = H.g.

S = momentum flow rate per unit span = M.g.

Their Q would in our notation be $q = \frac{Q}{L}$ (flow per unit span) and their $\eta = y$.

With these corrections the two expressions

$$\frac{Q^2}{6gl^2}\left(\frac{dy}{dx}\right)^2 = Hy^2 - \frac{y^3}{2} + \frac{Q^2}{gl^2} - My.$$

and

$$q^2\left(\frac{d\eta}{dx}\right)^2 = 2R\eta^2 - g\eta^3 - 2S\eta + q^2. \qquad (86)$$

can be seen to be identical.

The theoretical analysis of this thesis, is based on Serre's method, but Benjamin and Lighthill, whilst not deriving equations for the changes in Energy and Momentum, do make some very interesting observations.

They show that the theory due to Lémoine:, whilst being elegant, is based on false premises. That is, he assumes a sinusoidal wave form. This would then give rise to a constant value for the parameter $\frac{a}{y_s - y_o}$, (where a = wave amplitude) which as can be seen from the results already presented is not correct.

Following this they obtain Equation (86) by the method outlined above. This is then converted into a dimensionless form similar to Equation (41), and a determination of the standard elliptic integral form is made.

One of the most interesting sections of their paper, shows how Equation (86) is analagous to the motion of a particle in a field of zero total energy and whose potential is the cubic in Equation (86). This gives rise to their Fig. 1 (Fig. 29).

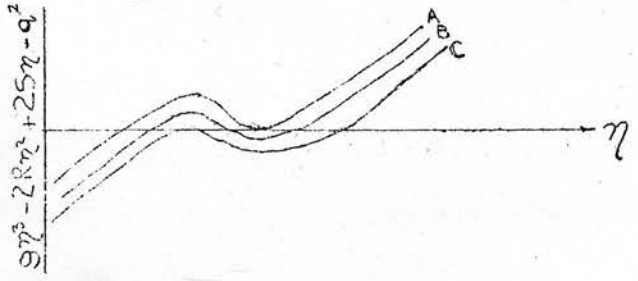

Fig. 29.

Waves appear when the cubic has two zeroes between which it is negative (B). Curve (A) is when the amplitude is zero, and curve (C) when the amplitude is infinite (i.e.) a solitary wave. When $v^2 > gh$, then the cubic corresponds, to curve (C) and Equation (86) becomes Rayleighs Equation for a solitary wave. This emerges from a stream flowing at a depth below the critical depth, without loss of energy or momentum.

Thus, as has already been determined in this thesis, Equation (86) when solved gives rise to a solitary wave, when $y_0 < y_c$. Hence Lemoine's theory can only result in a solitary wave, and not a train of waves.

If, however, some energy is dissipated in friction at the front of the wave train then R decreases, and curve C must be bodily raised to one of type B, where waves are possible. If the energy dissipation is too great then the curve becomes one of type (A), (i.e.) a steep fronted bore with no waves. This latter energy dissipation is then equal to that derived from the standard equations.

Furthermore if momentum is lost at the head of the wave train, the numerical value of the cubic in Equation 86 decreases. Therefore for waves to appear, the energy and momentum losses must be such that when the changes in the values of H and M (or R and S) are included in this cubic, it is represented by a curve of Type B.

Benjamin and Lighthill have also produced another very useful diagram from which the permissible energy and momentum changes can be read directly.

There is one other important treatise on this subject. That is, that part of Favre's thesis 'Ondes de Translation' which deals with the undular surge. He only included it as a part of the experimental results, and obtained his wave profiles by a method similar to that used in aerial surveying. Two cameras take simultaneous photographs of the advancing surge, and then the results (wave lengths and depths) are plotted by means of an ingenious machine, the Wild "Stereoautograph". Favre then plotted two curves from the results. The results of the experimental work in this thesis have also been plotted for the same obscissae and ordinates (Figs. 15 and 16). The comparison of the two sets of curves brings some interesting facts to light.

First, however, there are a few points that merit attention. The depth of the first valley of the surge waves increases as the discharge increases (Fig. 12). This is at variance with Favre's results, which show first an increase, and then a decrease, almost to the original water level. This has been mentioned in the literature as confirmation of the fact that as the discharge increases the waves tend more and more to the shape of a solitary wave. When this discrepancy was noticed, the runs were rescrutinised with even greater care, and additional runs carried out. The result was the same however; the depth increases with discharge until breaking occurs.

Further, an inspection of Fig. 25 shows that even for a very smooth channel ($\frac{g}{c^2} = 0.002$) the depth of the first valley is considerably more than that recorded by Favre in his experiment 24. His result is 3 mms. (valley depth above initial level) whereas the equivalent in Fig. 25 is about 6 mms, and this value

increases at each successive valley.

It would appear therefore, that Favre's results for the depths of the valleys are not very accurate. This is not surprising, since photographs taken from a similar position in the present experiments do not show the profiles very clearly, and secondly since the accuracy depends very much on the skill of the operator of the stereoautograph, this may be a source of error. The operator would be accustomed to dealing with photographs of land areas. In this type of work, there is a very definite visual phenomena when the 'floating spot' descends beneath the ground level. It may well be that water does not give the same response. The crests of course would respond much more readily than the valleys to this method, since they present a much more definite outline.

Reverting to the supposedly greater similarity of the surge waves to solitary waves when the amplitude is large. What does happen, is that at all discharges the waves ressemble solitary waves, except that they are a little steeper at the crest. It is true that as the discharge rises, the surge waves change in shape from near-sinusoidal to near-cnoidal, but the solitary wave also changes in a similar manner.

Referring to Fig . 15 again. This has already been described, but the one important point that stands out, is that (in analogy with Fig. 29), as the friction increases the curves are displaced downwards. Favre's channel was relatively smooth, and consequently his curve is well above those recorded in these experiments. His maximum value of $\frac{y_{crest} - y_o}{y_s - y_o}$ is 2.06. There is a possibility, that as his valley depths are not deep enough

y_s will be increased and the curves raised even a little more.

Hence it would appear that to place reliance on Favre's results, as applying to all cases is not to be recommended. They do give results close to those obtained in the literature from theoretical considerations, but only because the friction losses in Favre's channel are comparatively small. If the practical channel is at all rough, then some intermediate value between Favre's and those of Fig. 15 must be used.

Again the maximum value of $\frac{y_s - y_o}{y_o}$ according to Favre is 0.28, In these experiments the maximum value obtained was 0.38, both when the channel was smooth and had a rough surface; and for an initial depth of 4 ins. which is comparable to his 10.75 cms. It is difficult to perceive how the difference occurs. It cannot be attributed to changes in friction since in the present experiments the maximum value of $\frac{y_s - y_o}{y_o}$ is very much the same for both sets of results. Presumably the difference lies in the two methods of assessing y_s, which is smaller in Favre's experiments.

The final discrepancy between the two results is that in the present experiments it has been found that after breaking, there is a transition period where the curve swoops up and down. Finally it settles to a steady curve, which falls to a value of $\frac{y_{crest} - y_o}{y - y_o} = 1$. As is only to be expected Favre does not include this transition. It is not surprising considering the comparatively few runs that he made for the purpose of determining these profiles.

Comparing the results it can be seen that as the friction decreases, the point of inflexion in the curve (which occurs at low values) disappears.

Fig. 16 on the other hand agrees very well with Favre's plot of $\frac{2L}{y_s - y_o}$ to $\frac{y_s - y_o}{y_o}$. In Fig. 16 as the friction decreases so the curves are raised slightly one above the other. Favre's curve is a little above the family of curves in Fig. 16 at low values of $\frac{y_s - y_o}{y_o}$ (absc. 0.1; ord. 110) but is only fractionally above at high values. This shows that the relationship $\frac{2L}{y_s - y_o}$ is not greatly affected by changes in friction, except at high values (i.e. > 80).

Favre seems to be under the impression that his waves were fully formed by the time the surge had reached the end of the channel. It would appear from the present experiments however that they cannot have been fully formed. His profiles (y_o = 10.75 cms) are very similar to those when y_o = 4 ins, and these, when compared with the profiles at y_o = 2 ins. are seen to be barely fully formed. When the waves have reached this state, the crest heights are successively higher above 'y_o' and consequently it would be more accurate to use the parameter $\frac{a}{y_s - y_o}$, where 'a' is the amplitude of the first undulation and is always the greatest amplitude in a fully formed unbroken surge.

It must be emphasised that this very fine piece of experimental work of Favre's was only a side line to the general work of his thesis. Consequently it is not surprising that some of his conclusions are not very general in application. He was, however, the first to draw attention to the problem of the undular surge, since the time of Korteweg and de Vries.

It is worth noting a quotation of Favre's on P.160. " Il y aurait certainement là une très belle étude expérimentale à faire, consistant à chercher les influences de la rugosité.....

et des rapports $\frac{l}{y_o}$ et $\frac{y_s - y_o}{y_o}$ sur la hauteur relative $\frac{y_{crest} - y_o}{y_s - y_o}$.

Keulegan and Patterson state that Favre's velocities differ only from those calculated on the cnoidal theory (using his values of '2L' and 'a') by 0.1 ± 1.5%. This appears to be rather remarkable considering the scatter in Favre's results as shown by his graphs, and also from the difficulties encountered in the present experiments of accurately and consistently measuring wave lengths. The remainder of Keulegan and Pattersons's work is mainly concerned with compiling and presenting in a more orderly manner, information that was already available.

The final contribution to the literature to be discussed, is a most valuable experimental work due to Binnie and Orkney.

In this, a number of stationary waves were produced in an open channel, by various means. The experimental details make very intersting reading, but the results of the experiments are of immediate concern.

They showed that the stationary undular profile occurs at small discharges, and was succeeded as the discharge increases by the breaking undular and steep fronted hydraulic jumps. Several very informative diagrams are included. Figure 3 shows $\frac{y\ crest}{y_o}$ plotted against F_1 $(= \frac{V}{\sqrt{gy_o}})$ where V is the uniform velocity of approach of the stream. Several interesting points emerge. F_1 is plotted $= (1 + \frac{y_{crest}}{y_o})^{1/2}$, and the experimental points are scattered round this line, much as though this could be taken as a good approximation to the true results. The explanation given for the scatter, is the difficulties in measurement. It is suggested that in fact, however, there exists a family of curves, as already shown in this thesis, differing from one another by the

initial depth difference (i.e.) due to differences in the friction effects. Secondly, the plotted maximum relative height of McCowan's extreme solitary wave is very close to that obtained in this thesis, for the undular surge. This is as expected since the maximum height of the solitary wave is always a little less than the maximum height of the undular jump or surge.

Another interesting point is a comment by Orkney to the effect of the ease of measurement compared with that of a travelling surge. It would appear on the contrary that much smoother waves are experienced with the travelling surge, and that once the technical difficulties of measurement are over come the results should be more accurate, as it would appear that various extraneous effects do detract from the accuracy of measurement of the stationary profile.

Again Binney and Orkney quote the belief (strongly criticized by Benjamin and Lighthill) that energy is radiated in wave form in the undular jump. The opposite contention is not that the waves are created to get rid of excess energy, but that the waves occur because only a small portion of the classical energy is dissipated at the head of the bore and the remainder is dissipated in friction. In the next non dimensional figure, (5) $\frac{y_s}{y_o}$ is plotted against F_1. The scatter in this again would appear to be due to friction effects. Similarly as in our Fig. 16 the results are grouped closely together, but perhaps would have given separate curves, if the hazards of measurement had not been so great.

It is quoted that Favre's maximum value of $\frac{y_s}{y_o}$ is 1.34. This would appear to be a misprint, since it should be approximately

1.28. As pointed out previously Favre's results for $\frac{y_s - y_o}{y_o}$ are rather low compared with those obtained in the present experiments, where the maximum value of $\frac{y_s}{y_o}$ obtained was approximately 1.38.

The final curve of Binney and Orkney is the inverse of our Fig. 16, with modifications, but has been carried through breaking, to the steep fronted surge. Some of their experimental points near breaking,are well away from the mean curve and it is suggested that these might lie in the intermediate region (previously mentioned) that occurs after breaking.

This experimental treatise is of great interest, and does appear to have opened up a a considerable, and profitable field for further research.

CHAPTER 11.

Conclusions.

It is beleived that within limits the stated purpose of this thesis has been accomplished.

A theoretical analysis of the flow problems incurred in the study of undular surge waves has been made, and expressions for the profile, and change in energy and momentum have been derived

These expressions have then been derived in a non dimensional form, and after simplification and rearrangement have been obtained suitable for the purposes of calculation.

A number of numerical examples have been computed from these final expressions, and the results compared with experimental results.

The comparison has shown that despite assumptions and difficulties in the determination of the friction coefficient, the calculations have yielded results that at their worst are within 9% of the recorded results. This maximum error occurs when the wave amplitude is large, and then the original assumption of uniform velocity distribution no longer closely approximates to the actual conditions.

It is believed however, that in larger channels where the Reynolds Number would be considerably larger, that the calculations would yield results of greater accuracy. This is because at these higher values of R , the variation in the value of the friction coefficient 'C' is considerably less.

A method is also indicated whereby in practice the profile of a surge could be calculated (in a rectangular channel) at any

position, if the initial depth, discharge, and geometry of the channel were known.

This method could be applied to a sloping channel, since this is allowed for in the original equations for the change in energy and momentum. It would be necessary to have an initial flow in the channel, and then the undular surge would be formed if there were a sudden limited increase in discharge.

A considerable amount of experimental work has also been accomplished, and the results have been abstracted and presented in both graphical and tabular form. The results have also been expressed in a non dimensional form between the maximum depth and the mean depth, and between the wave length and the mean depth. These figures show that there is a definite relationship between these quantities. With the former, the result is to a great extent dependent on friction, but it is not so apparent in the relationship between wave length and mean depth.

Despite this, there is still a great deal yet to be accomplished on this subject. The effect of friction at higher Reynolds Numbers, the negative undular surge, and the positive downstream surge (formed by suddenly closing the guillotine gate) among other problems have yet to be investigated.

APPENDIX.

(1). Design of Capacitance Depth Gauges.

One of the earlier ideas was to use photography exclusively for the profile determinations. As, however, a quantity of electrical apparatus was available, and photography would have meant the purchase of expensive cameras, the electrical method was chosen.

It had been generally agreed in the literature that capacitance type depth gauges were preferable to the resistance type of gauge, and it was decided, therefore, to use some form of capacitance depth gauge.

At first a length of glass capillary tubing was used with a mercury filling. This, however, offered too much resistance to the water and gave erroneous results. The second method was the most simple and would work very well over large depths. It merely entailed holding a thin strip of metal against the outside of the glass wall, using the glass as a dielectric. At the small depths used, however, the meniscus effects were considerable, especially when the water level fell. Various agents were tried to dispel the meniscus effect, but with no great success, and regretfully the method had to be abandoned. Its great advantage was that it did not interfere with the flow. In large installations this type of gauge could be easily employed let into one of the side walls.

The third idea was to use ordinary enamelled transformer wire. This, however, presented two main difficulties due to the thin enamel coating of the wire. Since the capacity of the condenser

thus formed was proportional to $\log_e \frac{r1}{r2 - r1}$ (where r_1 and r_2 were the radius of the wire filament, and the overall radius respectively) the capacity changes for this type of gauge were very large. For wire with standard thickness enamel, the change was approximately 100 pf. per inch change in depth. Since, however, the maximum range of linearity of the apparatus used was approximately $\pm$ 20 pf, and the maximum change in depth was just over 3 inches this type of wire condenser was useless. The second difficulty was the prevalence of 'pin holes' in the enamel, and this led to breakdowns in the condenser.

Even wires with extra thick enamel coatings failed to give such a small change as 12 pf. per inch. Attempts were made to coat the wires with various proprietary products, but without the help of elaborate equipment these coatings were not sufficiently uniform.

Finally attention was turned to P.V.C. covered wires, and it was found that Messrs. Henley's Cables, Ltd. manufactured the wire with the smallest overall diameter. This cabling turned out to be reasonably adequate for the experimental work. It offered very little resistance to the flow, exhibited small meniscus effects, and most important of all, gave a capacitance change of a very little over 12 pf. per inch change in length. The meniscus effects were rendered even smaller by coating the cable with a very thin film of 'Vaseline'.

Since only one strand of the cable could be employed, the next problem, was adequate insulation of the end under water. A great variety of methods and products were used without success,

until a proprietary insulating cement was tried (Radio Spares Insulating Cement) which was found to be fairly successful. It gave a very high order of insulation over a considerable length of time when totally immersed in water. As, however, when dry, the cement became very brittle, it was necessary to ensure that when tensioning the wire, none of the tension was transmitted to the cement, hence a 'tail' of about ¾" was left below the knot holding the cable to the lower perspex block. This tail was then gently slotted into a small groove cut in the underside of the perspex block.

The frame of the depth gauge was evolved after a period of trial and error, and was designed to allow for the following points. It must; offer minimum resistance to the flow of water; be sufficiently sturdy to survive repeated handling; allow easy and rapid replacement and tensioning of the cable; remain fixed in position when recording, but capable of being easily raised and lowered; must act as an electrical conductor between the water and the earth side of the oscillator cable; and be insulated from the filament of the P.V.C. cable. The requirements are all met in the final design

(2). Water Pollution.

In order that the water should remain clear, it was necessary to stop the formation of rust. This had been accomplished in the Sanderson Engineering Hydraulics Laboratory by adding a quantity of Sodium Nitrite to the water. After even a complete year of continual circulation the water was remarkably clear and free from suspended particles of rust.

(3) Numerical Example

To find y_c, knowing Q, ℓ, and y_o where Q in this case is the discharge at the position concerned and not the initial discharge. This is the practical case. Q initial will be known together with the channel geometry, the Chezy constant for the channel, the initial depth, and the distance of the position in question from the inlet. From Favre's calculations or similar ones, Q at the positon can be calculated. It is then required to find y_c in order that the step by step calculations can be carried out.

Given Q = 0.186 cusecs. ℓ = 5.184 ins.

y_o = 4 ins.

from Equation (76)

$$\frac{Q}{-\frac{3}{2} + \frac{1}{2}(1 + 8\,(\frac{y_c}{y_o})^3)^{1/2}} = y_c^{3/2} \cdot g^{1/2} \cdot \ell$$

and y has to be obtained by a process of trial and error.

A quick check will show that y_c = 4.444 ins.

= 0.3703 ft. is correct.

$\therefore Y_o = \frac{4}{4.444} = 0.9.$

N.B. It is most important in all these calculations to ensure that the same units are used throughout. As Q is usually in cusecs, all the 'y' dimensions must be in feet and not inches.

(4) Numerical Example.

To find the discharge (Q) required in the experiments, if Y_o, and y_o, are given.

Let Y_o = 0.90 and y_o = 4 ins. Smooth channel.

Then $y = \frac{4}{0.9}$ = 4.444 ins.

$Q_H = (y_c^3\ g\ell^2)^{1/2} = \left\{\left(\frac{4.444}{12}\right)^3\ 32.2\ \ 0.432^2\right\}^{1/2} = 0.5524$ cusecs.

This is the discharge for the equivalent Hydraulic jump.

Then $V = \frac{Q}{A} = 3.836$ ft/sec.

From Fig. 13, this gives Q = 0.126 cusecs (the initial discharge) when recording at gauge 5.

(5) Numerical example.

To find the half wave length L given y_1, y_2, y_o and Y_o (y_1 and y_2 are the first crest and valley depths).

Let y_o = 4 ins; Y_o = 0.90; y_1 = 5.55 ins., and y_2 = 4.27ins.

Then $L = \frac{y_c^{3/2}}{\sqrt{3\left(\frac{y_1 + y_2}{2} - \frac{y_c^3}{y_1 y_2}\right)}} \cdot g\ sn^{-1}\ (\varphi, k)$. (put $g\ sn^{-1}\ (\varphi, k) = I$)

$I = \frac{2}{\sqrt{K+1}}\ sn^{-1}\left(90, \sqrt{\frac{2K}{K+1}}\right)$

$K = \frac{y_1 - y_2}{y_1 + y_2} - \frac{2y_c^3}{y\ y} = 0.516$

$\therefore k = \sqrt{\frac{2K}{K+1}} = 0.825$

$\frac{2}{\sqrt{K+1}} = 1.625$

(N.B. as above $y_c = \frac{4}{0.9}$ ins.)

and $\frac{y_c^{3/2}}{\sqrt{3\left(\frac{y_1 + y_2}{2} - \frac{y_c^3}{y_1 y_2}\right)}} = 4.88$

$\therefore I = 1.625\ sn^{-1}\ (90°, \sin^{-1} 0.825) = 3.32.$

$\therefore L = 3.32 \times 4.88 = 16.2$ inches $\therefore 2L = 32.4$ ins. = 2.70 ft.

By the short method $L = \frac{y_c^{3/2}.\pi}{3\left(\frac{y_1 + y_2}{2} - \frac{y_c^3}{y_1 y_2}\right)} \cdot \left(1 + \frac{3K^2}{16}\right) = 2.68$ ft.

(6) Numerical Example.

To find crest and valley depths and wave lengths, knowing only y_o and Y_o.

Given $Y_o = 0.9$, $y_o = 4$ ins.

$E_o = Y_o + \frac{1}{2Y_o^2} = 1.517$ Eqn. 63.

$\mathcal{S}_o = \frac{Y_o^2}{2} + \frac{1}{Y_o} = 1.516$ Eqn. 64.

To find the crest of the solitary wave

$$\frac{(n+1)^2(\Delta Y)^2(1 - Y_o^3)}{2Y_o^2} - \frac{(n+1)^3(\Delta Y)^3}{2} = 0 \qquad \text{Eqn. 70.}$$

$\therefore$ by trial and error $n + 1 = 33.6$

$\therefore$ $Y = 1.236$

and y crest $= 5.49$ ins.

$\therefore$ $y_1 = 5.49$, $y_2 = 4.00$ ins.

From short Elliptic Integral Method -

$$L = \frac{y_c^{3/2} \cdot \pi}{\sqrt{3\left(\frac{y_1 + y_2}{2} - \frac{y_c^3}{y_1 y_2}\right)}} \cdot \left(1 + \frac{3K^2}{16}\right)$$

K is as in Appendix (5)

$$y_c = \frac{y_o}{Y_o}$$

$= 19.7"$ $\therefore$ $2L = 39.4"$ and $\Delta X = \frac{39.40}{4.44} = 8.88$

Take an average value for $y = 4.75$ ins.

$\therefore$ Y average $= 1.07$

$$\frac{dE}{dX} = \frac{g}{YC^2}\left(1 + \frac{2y}{l}\right)\left(\frac{1}{Y_o} - \frac{1}{Y}\right)^2 = 0.000483$$

$$\frac{d\not{S}}{dX} = \frac{g}{C^2}\left(1 + \frac{2y}{l}\right)\left(\frac{1}{Y_o} - \frac{1}{Y}\right)^2 = 0.000517$$

$\therefore$ $\Sigma \Delta E = 0.00483 \times 8.88 = 0.00428$

and $\Sigma \Delta \not{S} = 0.00517 \times 8.88 = 0.00460$

N.B. These values are about twice those calculated by the step by step method.)

$\therefore$ E crest $= 1.52128$

$\not{S}$ crest $= 1.52060$

Then the Equation $EY^2 - \frac{Y^3}{2} + \frac{1}{2} - \not{S}Y = 0$ has to be solved for these values of E and $\not{S}$ to find Y. This yields three roots. The two relevant ones are $Y = 1.25$ and 0.961

whence y crest $= 5.58$ and y valley $= 4.27$ ins.

These two values substituted in the Elliptic Integral Equations of the Short form (as previously) give $2L = \underline{2.665}$ ft.

These three values are seen to compare quite favourably with those recorded (Fig. 26). This can then be repeated ad infinitum to give Wave Lengths and Crest and Valley heights through the train, The major error occurs in the use of an alegbraic mean value of Y in the calculation of E and ϕ. Probably with practice a more appropriate fraction of Y crest would be found.

This method could be employed just as easily, knowing Q at the position, and y_o as in Appendice (3).

7. Addendum

A further contribution to the literature has been brought to the author's notice since the completion of the thesis. A discussion of this follows.

S.C. De (Proc.Camb.Phil.Soc. 51 713, 1955) has made an important contribution to the study of permanent gravity waves. He extends the work of Benjamin and Lighthill, by including the third boundary they mention, in their diagram of r/s. This boundary represents the limits, imposed on wave formations, by the breaking of the waves themselves. Then this complete diagram is presented in a more readily usable form by plotting $S' = 5/2\ (9_s - 11_r + 2)$, against $R' = 3/8\ (11_s - 9_r - 2)$ for constant values of mh and mH, where $m = 2M/\lambda$ (λ is the wave length) h is the mean depth of liquid and H is the height of the wave form trough to crest.

The Stokes theory of permanent waves is extended to the fifth order of approximation for waves in a finite depth. This is because whilst the original work by Stokes (to the third approximation) is best satisfied when the wave length is not large compared with the

mean depth of liquid, and the cnoidal theory (Benjamin and Lighthill) is suited to long waves. Hence it was presumed that both theories should give the same results at some intermediate relationships of wave length to depth, if the relationships of Stokes were carried out to a fifth approximation.

Comparisons of the values of the ratios of h/λ and H/λ obtained from the two theories for values of $\lambda/h > 6$, show that the above supposition is correct since the differences are very small.

For a practical case however some allowance has to be made for the frictional effects. A method of making such allowances has been outlined in this thesis. Combining this with De's work it should be possible to calculate the ratios of mH, and mh in any given case.